UCRL-CR-130729
B334423

BBN Technical Memorandum W1309

Users Guide for the Hydroacoustic Coverage Assessment Model (HydroCAM)

T. Farrell
K. LePage
C. Barclay
J. Angell
M. Barger

May 1998

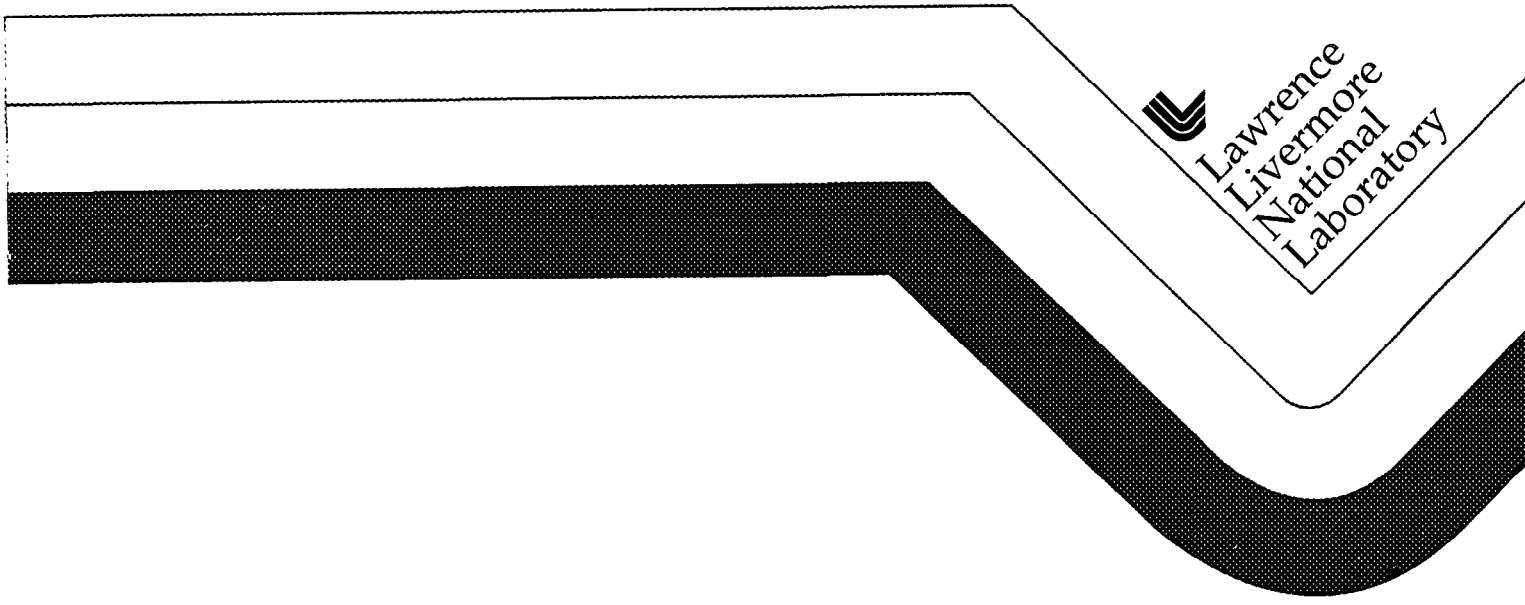

Work performed under the auspices of the U.S. Department of Energy by Lawrence Livermore National Laboratory under Contract W-7405-ENG-48

BBN Technical Memorandum W1309

Users Guide for the Hydroacoustic Coverage Assessment Model (HydroCAM)

Version 2.0

December 1997

Ted Farrell
Kevin LePage
Chris Barclay
Jeff Angell
Mark Barger

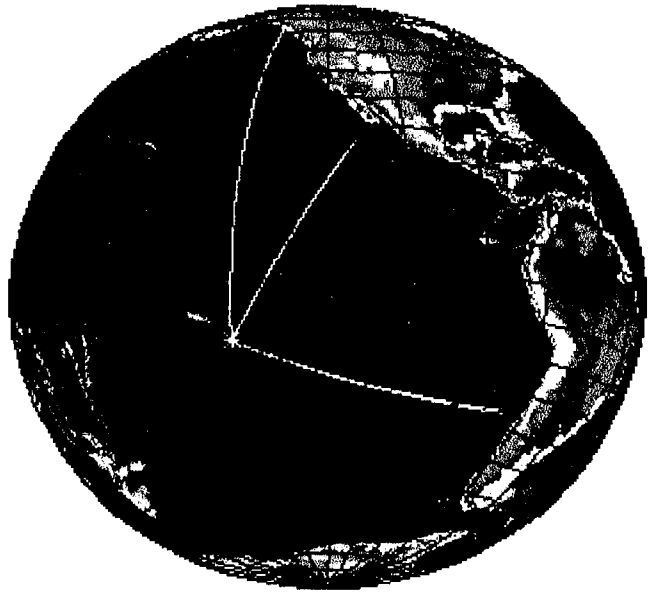

Prepared By: GTE / BBN Technologies
1300 North 17th Street
Arlington, VA 22209

Prepared For: Lawrence Livermore National Laboratory
PO Box 808, L-205
7000 East Avenue
Livermore, CA 94551

Abstract

A model for predicting the detection and localization performance of hydroacoustic monitoring networks has been developed. The model accounts for major factors affecting global-scale acoustic propagation in the ocean, including horizontal refraction, travel time variability due to spatial and temporal fluctuations in the ocean, and detailed characteristics of the source. Graphical user interfaces are provided to setup the models and visualize the results. The model produces maps of network detection coverage and localization area of uncertainty, as well as intermediate results such as predicted path amplitudes, travel time and travel time variance. This Users Guide for the model is organized into three sections. First a summary of functionality available in the model is presented, including example output products. The second section provides detailed descriptions of each of models contained in the system. The last section describes how to run the model, including a summary of each data input form in the user interface.

Funding for the Development of HydroCAM was provided by the U.S. Department of Energy, Office of Nonproliferation and National Security through contracts at the Air Force Phillips Laboratory (1996) and Lawrence Livermore National Laboratory (1997).

Keywords: hydroacoustics, network, localization, oceanography, performance prediction

Acknowledgments

Many people have assisted in the development of HydroCAM, both through general discussions and by providing several of the base modeling capabilities contained in the model. In particular, Dave Harris at Lawrence Livermore National Laboratory has provided many hours of discussion and direction on the model requirements and practical aspects of collected hydroacoustic data from earthquakes and explosions. Greg Orris at the Naval Research Laboratory in Washington, DC provided a copy of the GSOAR horizontal raytrace software and discussed many of the design decisions that went into that model. Mike Collins at NRL provided the Range-Dependent Acoustic Model over the internet. NOAA and WHOI provided the 3-D raytrace software HARPO which was evaluated during the initial stages of this effort. Mike Porter at NJIT provided the Kraken normal mode model and an excellent set of documentation summaring its development and use. Funding for the development of HydroCAM has been provided by the U.S. Department Of Energy.

TABLE OF CONTENTS

APPENDICES

Introduction

Large amplitude underwater acoustic signals, such as those generated by earthquakes, volcanoes and explosions, can be monitored on a global-scale using a relatively small network of hydrophones. At the current time, the design and development of a system for monitoring compliance with a Comprehensive nuclear Test-Ban Treaty (CTBT) is underway. To assure that an effective monitoring capability is developed, a model that can predict the detection and localization performance of the network is required. Many acoustic performance prediction software packages are available. Most of these programs were developed to predict the performance of active and passive SONAR systems for Anti-Submarine Warfare (ASW). These models have been under development for several decades, and have been extensively tested in deep water, open ocean environments over ranges up to hundreds of kilometers.

Unfortunately, there are enough differences between anti-submarine warfare and hydroacoustic nuclear monitoring that the standard models developed for ASW are not sufficient. ASW is primarily a low signal-to-noise (SNR), short range detection problem. Consequently, ASW performance prediction models are focused on the need to accurately predict the transmission loss of propagation paths over relatively short ranges. In this situation, it can usually be assumed that any horizontal refraction of sound is negligible, allowing propagation to be completely modeled in the vertical plane. Over the global length paths (tens of thousands of kilometers) required for nuclear monitoring, the geographic changes in sound speed and bathymetry can cause significant horizontal refraction to occur In addition, the large amplitude of nuclear explosions requires non-linear propagation models to be used for at least the first 10 km of the propagation path. Finally, in order to accurately predict the localization performance of a monitoring network, the travel time and travel time variance must be computed None of the standard ASW models satisfy all of these requirements. None predict travel time variance or include horizontal refraction. Many do not predict travel time and do not include the spherical nature of the earth.

The Hydroacoustic Coverage Assessment Model (HydroCAM) was developed under funding of the U S Department of Energy (DOE) for predicting the detection and localization performance of global hydroacoustic monitoring networks The model accounts for major factors affecting global-scale acoustic propagation in the ocean, such as horizontal refraction from bathymetric features and horizontal changes in sound speed, travel time variability due to spatial and temporal fluctuations in the ocean, and detailed characteristics of the source. Graphical user interfaces are provided to setup the models and visualize the results. The model produces maps of network detection coverage and localization area of uncertainty, as well as intermediate results such as predicted path amplitudes, travel time and travel time variance Although much of the software is recently developed C++ code, existing models and databases developed by the US Navy, NOAA, DOE and other institutions have been integrated when appropriate The result is

a flexible system with the ability to produce quick results, using simple geometric propagation models and low-resolution oceanographic databases, as well as the ability to produce results using research grade propagation models and high-resolution databases. Travel time predictions from the model have been compared to measured data. The model is currently being exercised to resolve issues necessary for the future development of operational monitoring systems.

This *Users Guide* is organized into three sections. First, a functional summary of the model is presented, including example output products. The remaining sections are intended to serve as reference material, not be read as a whole. The second section contains a detailed functional description of each component of the model. The last section describes how to run the model, and includes a summary of each data input form in the user interface

Model Summary

HydroCAM is a hydroacoustic network performance prediction program that runs on UNIX workstations It contains an assortment of oceanographic databases, acoustic propagation models, network performance models, and software for visualizing and interpreting results at each stage in the prediction process. A simplified block diagram of the model is shown as Figure 1. Because we took advantage of the best existing models and databases, the components of HydroCAM are in a variety of data formats and software languages, from FORTRAN-77 to C++ and MATLAB The user interface makes all of this transparent, and provides a capability to perform these functions:

- Access, analyze, and display a variety of oceanographic databases.
- Create geographic databases containing acoustic modes and waveguide parameters.
- Predict global-scale acoustic propagation paths and their characteristics.
- Assess network detection coverage and localization performance.
- Include spatial and signal processing characteristics of acoustic receiver systems
- Predict source effects on acoustic signals received at long ranges.

The following sections describe the functionality in each of these areas.

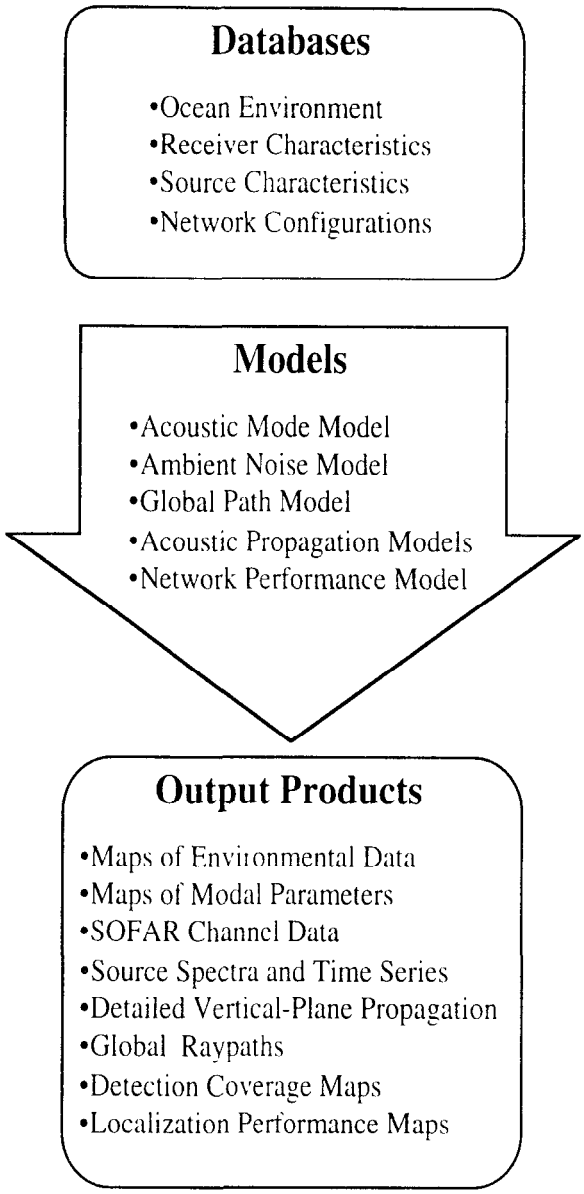

Figure 1: HydroCAM Components

Using Environmental Databases

Compared to seismic propagation, characteristics of the worlds oceans are well known. In a sense, the US Navy, NOAA, and other oceanographic institutions have solved the "regionalization" problem for the worlds oceans. Oceanographic databases are available at a variety of temporal and spatial resolutions, from raw data to analyzed statistics, all in a wide variety of formats. The critical element is the ability to rapidly access, visualize, analyze and incorporate this data into propagation and network performance models. The databases included in HydroCAM are listed in Table 1. They contain information on environmental factors affecting low frequency ambient noise (shipping densities), high frequency ambient noise (ocean surface wind speed and rainfall), and acoustic propagation (sound speed profiles, bathymetry and sediment characteristics).

Table 1 - Environmental databases included in HydroCAM

Database Name	Database Description	Temporal Resolution	Spatial Resolution (min)
ETOPO5	Bathymetry	N/A	5
SIO	Bathymetry	N/A	<2
GDEM	Sound speed profiles	Seasonal	30
WOA94	Temperature and Salinity	Monthly	30 and 300
HWS	Historical Wind Speed	Monthly	60
HITS	Historical Temporal Shipping	Monthly	Variable
GDS	Global Daily Summary (Temp/Precip)	Daily	Variable

HydroCAM allows users to interactively extract, visualize and analyze data for a given region with a graphical user interface. The left side of Figure 2 shows an example display containing bathymetry data for the South Indian Ocean. The small box in the center of the display was selected using a mouse. The locations of sound speed profiles from the WOA database that are available inside the boxed region are overlaid on the bathymetry. The plot on the right hand side of the figure shows the sound speed profiles. HydroCAM also enables predictions of the modal characteristics and acoustic propagation to be performed without regard for the specific database format or the input formats required by the propagation model.

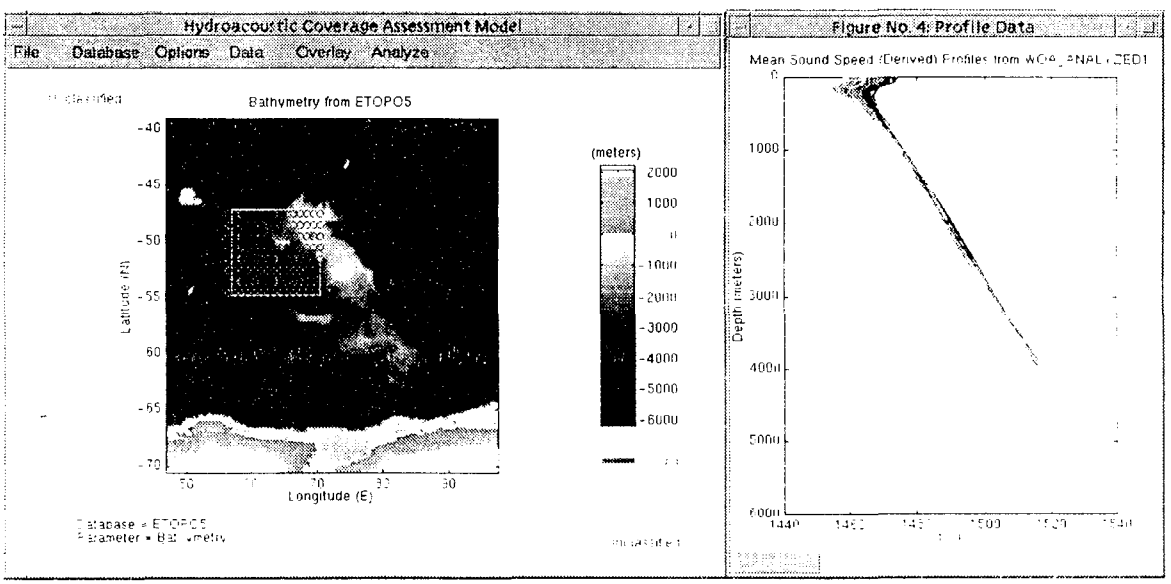

Figure 2. Example Display of Environmental Data

Characterizing the Ocean Waveguide

Two options for characterizing the ocean waveguide are provided The first assumes that all energy propagates in the SOFAR channel. In this case, the oceanographic characteristics at the SOFAR depth (which varies according to geographic location and season) are automatically extracted and provided to the propagation models The second, more accurate, approach is to separate the vertical component of the problem by treating individual geographic locations in the ocean as range independent waveguides

In this approach, the environmental data *at each location on a geographic grid* is used to calculate the mode structure in each of these "cells". Two models are available for computing the mode structure at each point; a well known normal mode code called Kraken from NJIT, and a FD-WKB approximation developed by BBN. Kraken calculates eigenvalues and mode shapes exactly for as many modes as are necessary locally, while the FD-WKB code rapidly calculates approximate eigenvalues and mode shapes for only those modes requested. Since it is expected that received signals will contain energy from the first several modes only, the FD-WKB should result in a significant time savings. After the mode structure has been determined, the local phase speed, group speed, modal attenuation and slowness variance [1] are computed. The results are placed into four geographic grids, which are provided as inputs to the propagation models. Figure 3 shows an example display of a group speed grid at 10 Hz. To produce these "derived databases" involves extracting environmental data from a diverse set of databases and running a set of software packages on tens of thousands of geographic locations, a task that previously required manual intervention at many intermediate steps. With the new software interfaces, thousands of model runs and management of the data has been automated. New environmental databases that include seasonal fluctuations and new data collected in the Southern Hemisphere have also been integrated, resulting in the ability to produce better knowledge grids of the ocean characteristics with significantly less effort.

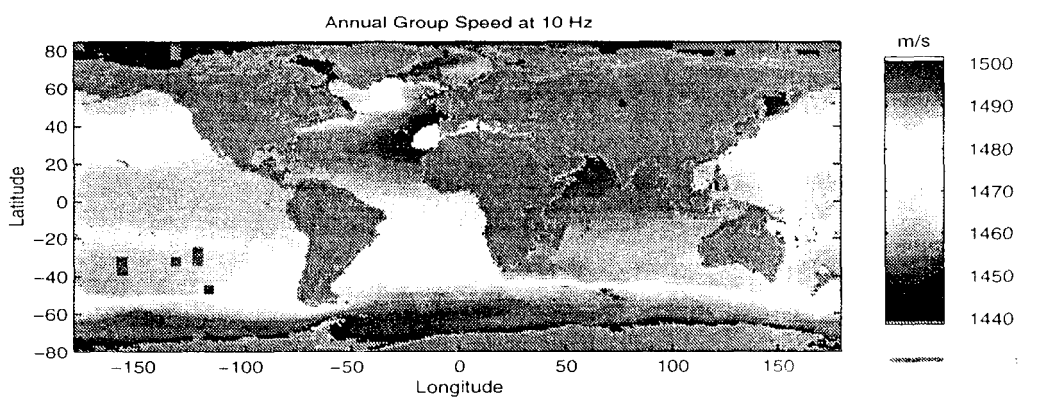

Figure 3 Calculated group speeds at 10 Hz for the worlds oceans These calculations were produced using annual average sound speed profiles from the WOA94 database and running the Kraken normal mode program at each of 36705 geographic locations

Predicting Propagation Paths

Acoustic paths are calculated in 2 steps; first the path itself is calculated, then the travel time, travel time variance and amplitude along the path are obtained. We evaluated five candidate path models: (1) a geometric path model on a spherical earth model for reference, (2) an ellipsoid (geodesic) model, (3) the horizontal ray/vertical mode model developed by NRL, (4) a bender model, and (5) the 3-D raytrace program HARPO [2]. Studies early in the year comparing predicted travel times using spherical paths and ellipsoid paths to measured travel times from the September 1995 French nuclear tests resulted in the elimination of the spherical model. The 3-D raytrace model was also eliminated after we obtained acceptable travel time predictions using the other models with significantly less computational load. The remaining models are part of the baseline capability of HydroCAM. Once raypaths are calculated, the travel time, amplitude and travel time variance along each path are calculated by performing path integrals of the appropriate grid database quantity along the path. For example, travel times are calculated by integrating the group speed database along the predicted path

Output products at this stage include plots of the paths and their characteristics If the predictions are run to a grid of sources (eigenray mode), plots of the path data at the endpoints on the grid are produced. These grids are used to determine network performance as described in "Evaluating Network Performance" below The grids are also used to investigate the ray stability and the sensitivity of predicted travel times, amplitudes, modal content and horizontal multi-path to environmental variability and database interpolation.

The option for extracting sound speed profiles and bathymetry in a vertical plane along the path is often used to investigate blockage. In addition, this environmental information can be passed on to "standard" vertical plane propagation models such as the Range-dependent Acoustic Model (RAM) developed by NRL. This capability is used for determining detailed propagation characteristics along the paths, effects of bathymetric features on loss mechanisms and mode structure, and the detailed structure of the arrival from a specified source Figure 4 shows examples of some of the data products produced by the path model The output products illustrated include (a) trajectories of the acoustic paths from a receiver at Ascension Island, (b) travel time along these paths, (c) sound speed and bathymetry along one of the paths in (a) ending near Australia, and (d) transmission loss in a vertical plane along the path used in (c).

Evaluating Network Performance

The performance of a network is described in terms of the ability to detect and locate sources. The detection performance of a single sensor is measured by the signal to noise ratio observed at the sensor output SNR is usually defined as the peak value of the receiver output relative to the background level, and may be calculated for a complete

event, or for a single component phase. It can be related to a number of other performance metrics, such as detection probability and arrival time accuracy. However, transformation into detection probability requires a model for the receiver output statistics and specification of a detection threshold. Since these are usually determined empirically, we have opted to produce SNR only.

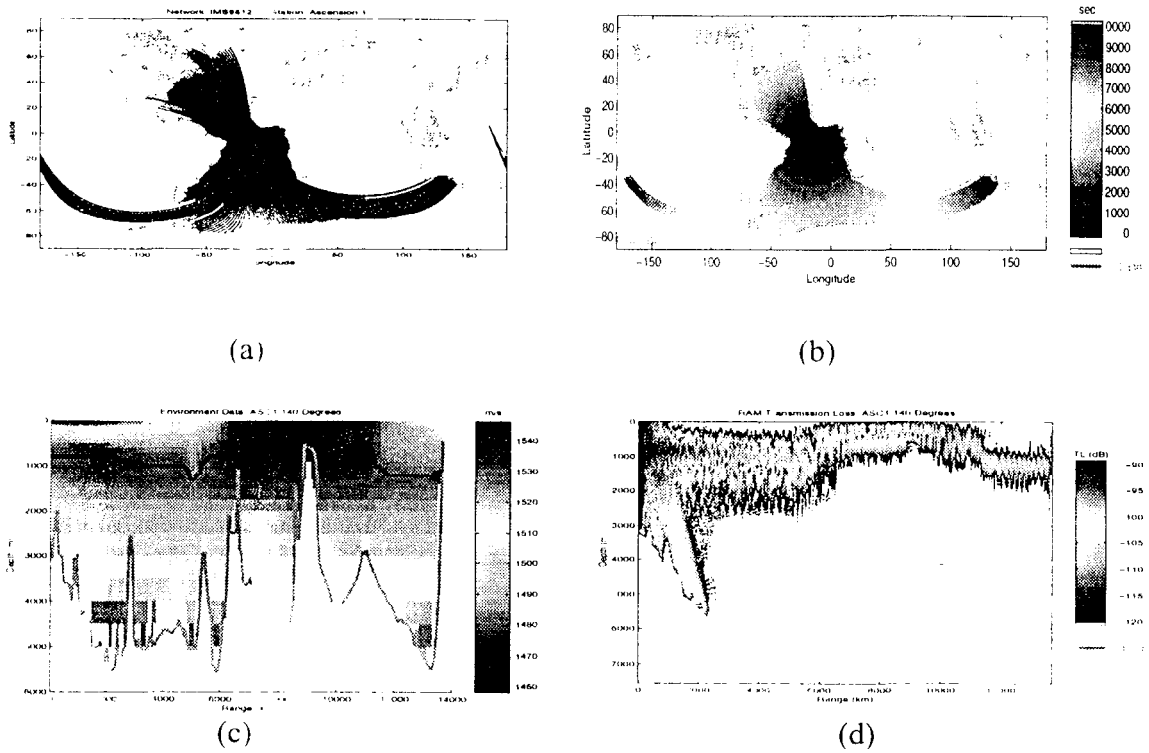

Figure 4. Example output products of the path model . (a) paths, (b) travel time, (c) sound speed and bathymetry, (d) propagation loss

Single-receiver SNR may be used to display the detection coverage or combined with SNR estimates for receivers at other locations to compute the performance of the hydroacoustic network as a whole. Many related data products are available, including geographic plots of:

- SNR for a specific receiver, corresponding to different event locations (for evaluation of existing assets)
- Difference in SNR between two Networks or two receivers
- SNR for a specific event location, yield and depth/height for various receiver locations (for evaluation of alternative locations for new sensors)
- The minimum SNR seen by all receivers in the network
- The Mth largest SNR value seen by the network
- The number of receivers receiving the event above a specified SNR threshold This plot is particularly useful for interpreting localization solutions

The metric for localization coverage is area of uncertainty (AOU), which summarizes the effect of all the uncertainties in the localization calculation, including model uncertainties, e.g., uncertainties in the assumed propagation speeds. At the current time, the AOU model is based on localization using arrival time of one specific phase at multiple receivers. Additional measurements, such as bearing, can be readily added to the algorithms. The size of the AOU is a function of the accuracy of the travel time model, the ability to correctly measure the arrival time of the modeled phase, and the sensor-event geometry. This year, the effort focused on modeling the effects of sensor geometry and the travel time model. Uncertainties in propagation speeds are included in the travel time variance calculations of the path model, using world-wide statistics of the sound speed derived from WOA94 and a sophisticated model for the slowness variance of propagating modes [1] . Measurement uncertainties, which depend on signal-to-noise ratio and the specific signal shape are currently modeled parametrically, as an independent "picking" error added to the travel time error. Measurement uncertainties and the biases due to horizontal refraction will be investigated in the coming year. The primary output products of the localization model are geographic plots of the AOU and specialized display formats showing contributing receivers and path characteristics for a particular source location. Figure 5 shows an example AOU prediction for the IMS network.

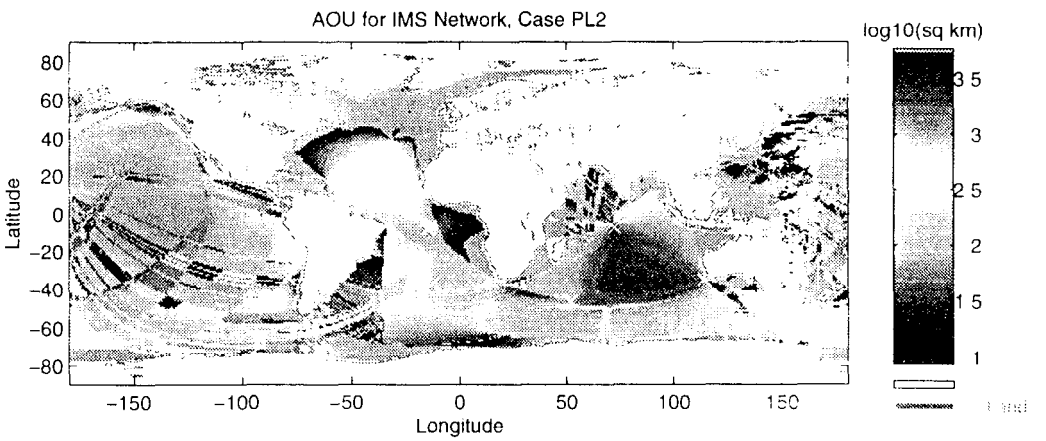

Figure 5: Example output product from the network performance model Localization Area of Uncertainty calculated for the candidate IMS hydroacoustic network. Sources were placed at every location on a 1 degree by 1 degree grid. This example includes the travel time variances using historical statistics of the ocean sound speed, but ignores the effects of horizontal refraction

Investigating the Effects of Different Sources

The performance of the network and the details of the arrival structure depend on the characteristics of the source. DOE funded research at LLNL and NRL has produced a combined hydrodynamic and non-linear acoustic model of the pressure signature from underwater and low-atmosphere nuclear bursts called CALE/NPE [3] The principal development effort for the source portion of HydroCAM was to couple the source

functions produced by this model to the linear acoustic propagation models contained in HydroCAM. Standard models that predict the pressure signature of low-level conventional explosions are also being integrated. [4]

The source function is provided as pressure time series vs depth at a range where the acoustic propagation becomes linear (typically about 10 km from the burst). HydroCAM reads these files and calculates the complex pressure and the ESL over a cylindrical surface in the water column as a function of depth and frequency. This data is used as a "starter field" for the linear propagation model; i.e. the complex pressure is the input to a range dependent propagation model which estimates the complex propagation transfer function, and hence transmission loss (TL) at multiple frequencies along selected bearings from the event position. The result is the estimated received spectral level, for each frequency, to any selected range and depth along these radials.

Output products include displays of the source time series, spectral characteristics and ESL. Figure 6 shows some examples. In addition, plots of the received energy in a vertical plane along any geographic path can be produced. There are many uses for these products, including investigation of potential evasion scenarios, and potential discrimination methods. As an example, the pressure signatures calculated by CALE/NPE contain the most important physical characteristics of underwater and atmospheric explosions. When coupled with the long-range models provided in HydroCAM, the predicted spectral characteristics of the received waveforms may provide important discrimination/estimation clues In addition, the effects of different environmental conditions at the source, such as bursts on a continental shelf, can be investigated.

Including Receiver Characteristics

The primary receiver characteristics that affect network performance are the ambient noise background at the sensor location, the transfer function of the sensors, and the characteristics of any spatial and/or temporal processing Ocean ambient noise over most of the frequency range of concern, 1-200 Hz, is principally due to distant shipping, resulting in a noise field concentrated near the horizontal which varies in both azimuth and frequency. HydroCAM accounts for ambient noise using a table of noise level vs frequency and azimuth for each station in the network. These tables can be produced from measured data at the location if available, otherwise standard underwater noise models, such as the Wenz model [5] are used

Some stations may have different sensor capabilities. For example, the island seismic stations in the proposed IMS are likely be on the order of 40 dB less sensitive than hydrophones placed directly in the SOFAR channel [6]. These effects, along with additional losses due to hydrophone sensitivity, scalloping loss, any other system SNR losses are accounted for in a loss table vs frequency "Picking errors" are characterized by

an arrival time variance term for each station, which is added to the travel time variance calculated by the path model. Typical values are 5 seconds for island seismic stations and 1 second for hydroacoustic stations [6].

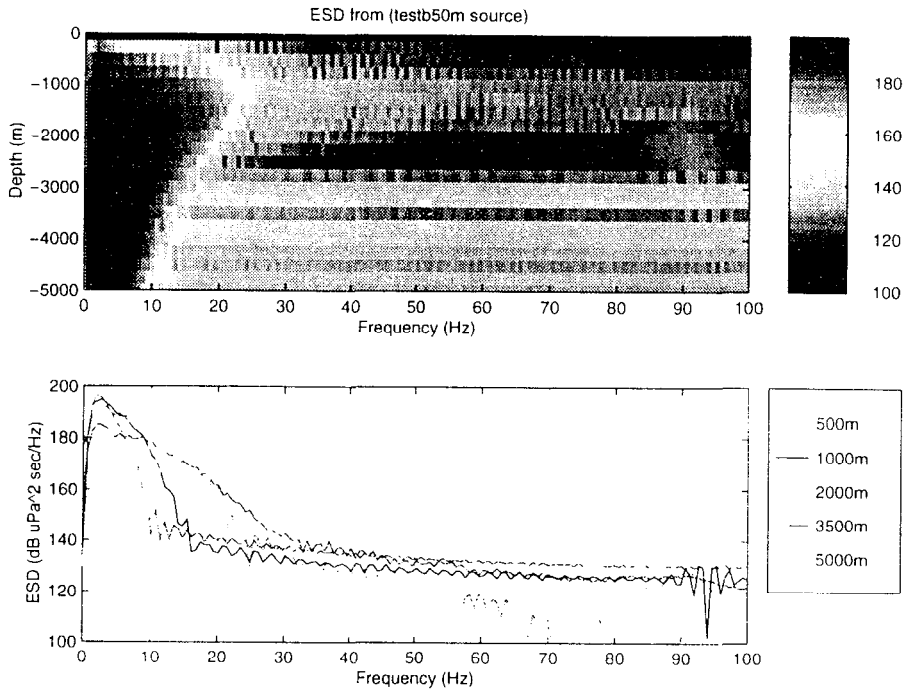

(a)

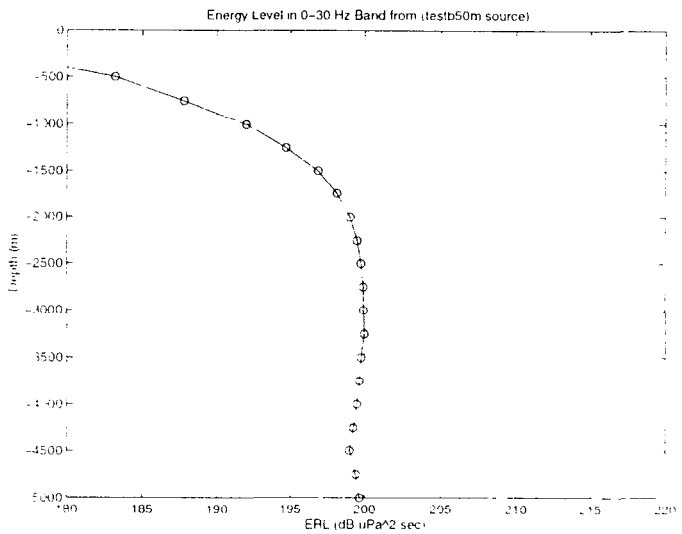

(b)

Figure 6. Example Source Displays: (a) Energy Spectral Density of 1kT explosion predicted by CALE/NPE Model, (b) Energy Level in 1-30 Hz Band

In general, acoustic receivers can range in complexity from single omnidirectional hydrophones to arrays of hydrophones in various configurations. The spatial processing advantage produced by an array is measured by its array gain, which is the noise level of a beam output relative to an omniphone. In other situations where single hydrophones are located close to bathymetric features, it may be more convenient to model the effect of the feature as a directionality inherent in the sensor. In HydroCAM, the spatial characteristics of the receiver in both of these cases are specified either by a table of noise level versus azimuth and frequency, which represents the beam output in each direction, or by a table of array gains vs frequency and azimuth, which is applied onto the omnidirectional noise table described above. Array gains must be calculated offline using the location and orientation of the array and the beamforming parameters, such as spatial shading functions, number of beams formed, and pointing directions

New Features in Version 2.0

HydroCAM version 2.0 includes two new environmental databases, several additional models, improvements to the existing models, an improved user interface and compatibility with MATLAB 5.1

New Databases

Two new databases were added to HydroCAM; the ice cover databases provided by the Defense Meteorological Satellite Program (DMSP) [26] and a new bathymetry database provided by the Scripps Institution of Oceanography [27] which is derived from satellite gravity measurements. The ice cover database contains information on the average monthly extent of the ice cover in the Northern and Southern Hemispheres from January 1992 to December 1996. It is used by the horizontal refraction code GlobeRay to add ice cover attenuation to paths traversing high-latitude waters. The new bathymetry database provides higher resolution bathymetry (at 2 minutes or better) than ETOPO5, and should also be more accurate in areas where ETOPO5 was based on sparse ship measurements. This database has been integrated into both the database access and display software and the modal grid generation software, but not the software to generate transmission loss predictions along a vertical plane using RAM. Since version 4.2 of this database has artifacts in some areas such as Crozet Island, Easter Island and coastal areas of Antarctica [28] it should be used with caution

Model Improvements

New capabilities provided in version 2.0 include:

1. An approximation for the modal bottom attenuation included in the WKB model. (See Appendix A)

2 An ice cover loss model based on empirical measurements of mode 1 attenuation in the Central Arctic [29]. (See the Path Characteristics/Transmission Loss section)

3. A C++ version of the "Bender" boundary value eigenray algorithm.

4. Path to grid interpolation to allow the computation of travel time and attenuation on uniform latitude/longitude grids from a set of refracted raypaths.

5. A first order model which reflects raypaths from bathymetric features based on the incident angle with the local topography.

6. Separation of the transmission loss into path range and attenuation correction components. This allows multiple transmission loss models to be used *after* the computationally intensive raypath predictions are performed.

Software Improvements

A number of improvements have been incorporated into the software These include *compatibility with MATLAB 5.1, improvements to the user interface* enabled by MATLAB 5.1 and/or requested by users at AFTAC and Sandia National Laboratories, and *faster execution time* through approximations in the modal slowness integration and the incorporation of modal attenuation into the WKB model

HydroCAM Validation and Applications

One of the objectives in both the 1995-96 Phillips Laboratory contract and this years effort was to validate the baseline model using measured data Comparisons between travel time measurements taken during the Heard Island Feasibility Test [7], the French nuclear tests in 1995 and an explosion off the coast of Australia in 1960 [8] have been performed Additional travel time comparisons as well as validation of the amplitude and travel time variance models are planned as data becomes available [9, 29]

A number of issues which affect the design of the network and the ability to produce an accurate knowledge database have been studied using the model A short list of these studies include:

- Travel time biases
- Conditions when waveguide parameters (ie phase speed) are needed vs channel sound speed
- Sensitivity of travel time variance predictions to several models of slowness fluctuations.
- Predicted performance of the IMS and other monitoring networks under a variety of conditions.
- Comparisons of the HydroCAM network predictions with those from the Integrated Verification System Evaluation Model developed by SNL.

Deatils of these studies are available in other reports [9, 29] In addition, HydroCAM was used to develop detailed grids of travel time and attenuation corrections for the operational community These grids were delivered in August of 1997. Details on the use of HydroCAM to generate these grids are provided in the summary report [29]

Detailed Model Descriptions

HydroCAM includes a variety of environmental databases, propagation models and network performance models. This section of the Users Guide describes the functional details of each component of the model For newly developed portions of the model, the specific equations implemented are included. For models that we obtained from public sources, such as RAM [10] and Kraken [11], we briefly describe the interface to HydroCAM and applications of the model. Details of these public models can be found in the referenced reports. The programs included in HydroCAM that are discussed throughout this section are listed in Table 2.

Table 2: Software programs contained in HydroCAM

Program Name	Language	Description	Availability
HydroCAM	Many	The entire collection of programs and the MATLAB interface software	HydroCAM
DBTool	MATLAB	Environmental database access software now incorporated in HydroCAM	HydroCAM
WaveGuide	C++	Calculates derived databases	HydroCAM
Kraken [11]	Fortran	Calculates modal eigenvalues and mode functions	Public (NJIT)
WKB	C/C++	Calculates modal eigenvalues and mode functions	HydroCAM
MakeGridDB	C++	Collects waveguide outputs and produces geographic grids of phase, group, atten and slowness variance	HydroCAM
GlobeRay	C++	Calculates refracted and geodesic paths, travel time, travel time variance and attenuation.	HydroCAM
HydroNET	C++	Network performance model, calculates SNR and AOU	HydroCAM
RAM [10]	Fortran	Calculates transmission loss versus range and depth along a path	Public (NRL)
PathToGrid	C++	Interpolates data along raypaths onto a uniform lat/lon grid	HydroCAM

Figure 7 shows a block diagram of the functional components of HydroCAM The variables listed in the rightmost column are each available as output products for display or as data files for additional manipulation The text below each box indicates the toolbar option that is used to calculate and/or display the data contained in the box. A description of each of these "forms" is provided in the Using HydroCAM section of this report

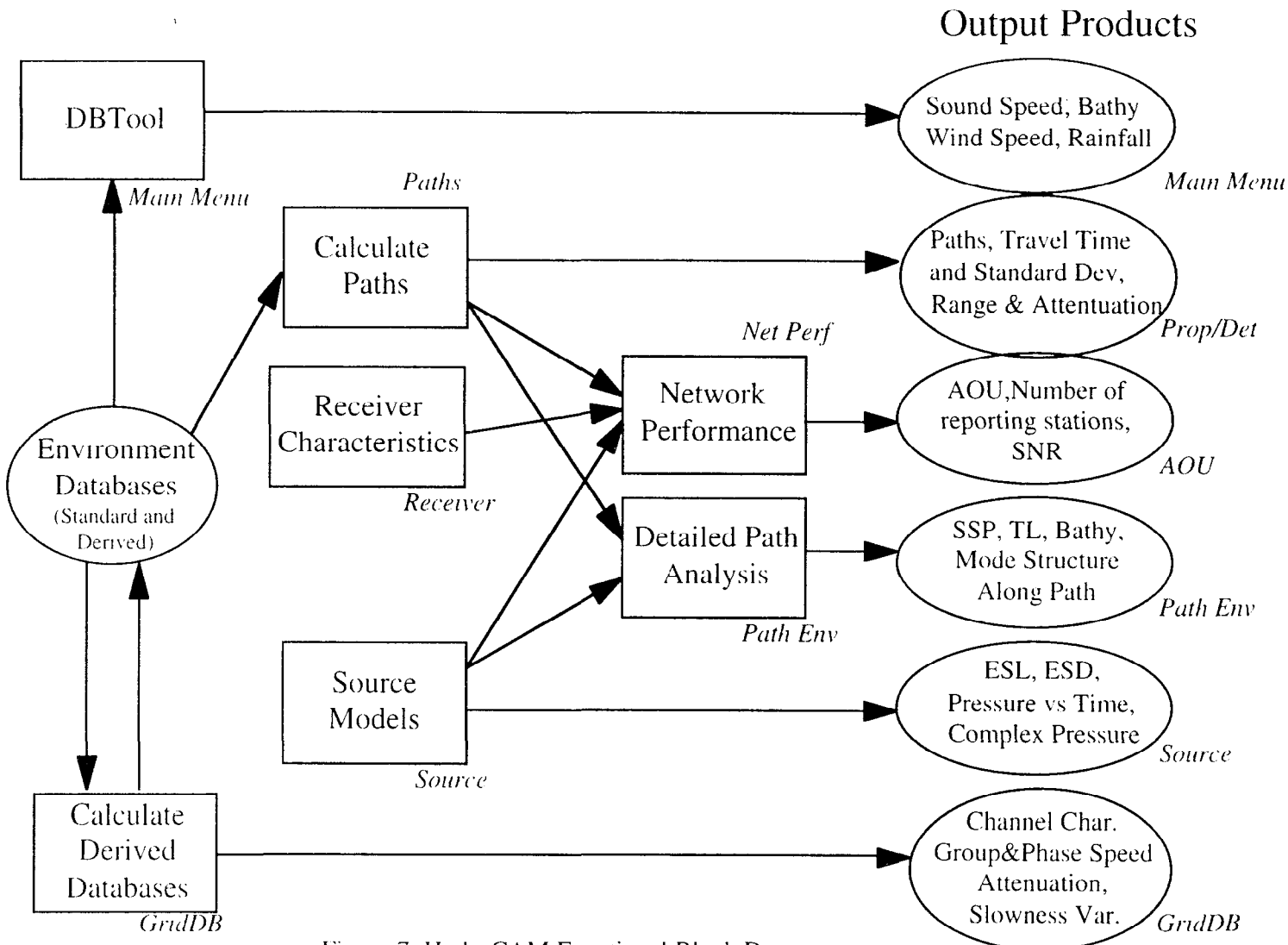

Figure 7: HydroCAM Functional Block Diagram

Source Models

HydroCAM has several options for modeling source characteristics. The first is to use data files containing pressure time series vs depth at a range where the propagation becomes linear (typically 10 km from the burst). These data files are created by other programs, and stored in a special directory structure. HydroCAM allows users to use these files by selecting the characteristics of the desired source (i.e. depth of burst, yield, type of source). After the files are read in the time series data is available in MATLAB for manipulation and display The primary output is the complex pressure as a function of frequency and depth This function is used as the "starter field" for the linear acoustic propagation models. If the pressure time series produced by the source at a fixed range r_0 is given by $p(t,z,r_0)$, then the complex pressure at frequency f is computed by taking the FFT of the time series at each depth, and linearly interpolating the complex pressure at the frequency of interest. The corresponding Energy Spectral Densities (ESD) are calculated using

$$ESD = 10\log\left\{\frac{2}{f_s^2}\left|FFT(p)\right|^2\right\} \quad \text{dB re } (\mu\text{Pa}^2\text{-sec}) \tag{1}$$

where f_s is the sample frequency in Hz and the factor of two is included since only the positive frequency portion of the spectrum is usually displayed. An additional metric, the received energy level in a band (ERL), is calculated using

$$ERL_{f_1 f_2} = 10\log\left\{\Delta f \sum_{k=i_1}^{i_2} 10^{\left(\frac{ESD(k)}{10}\right)}\right\}, \tag{2}$$

where Δf is the frequency resolution of the FFT and i_1, i_2 are the indices of the FFT cells where the band edges f_1, f_2 are located. For atmospheric and underwater nuclear sources, the pressure time-series files can be created using the CALE/NPE software at LLNL [3]. For underwater chemical sources, HydroCAM uses the Wakeley [4] model to calculate the pressure time-series. In either case, graphical plots of the time series, ESD, ERL and complex pressure vs depth can be produced.

When network performance calculations are desired, the ESDs generated by the above procedure can be used as the source level component of the Sonar equation When this option is specified, an additional term must be supplied to convert the ESD, which is calculated 10 km from the burst, to an equivalent ESD 1m from the burst for use in the Sonar equation. Two additional options are available. Users can enter any desired source level referenced to 1 meter. The second option is to specify a height depth of burst for a 1kt explosion. Scientists at LLNL have used the CALE/NPE model to predict pressure time-series for a set of height/depths of burst [3] The total energy level from these

predictions is available as a function of the height/depth of burst The source levels used when the this height/depth option is chosen are determined by linear interpolation of the function shown in Figure 8.

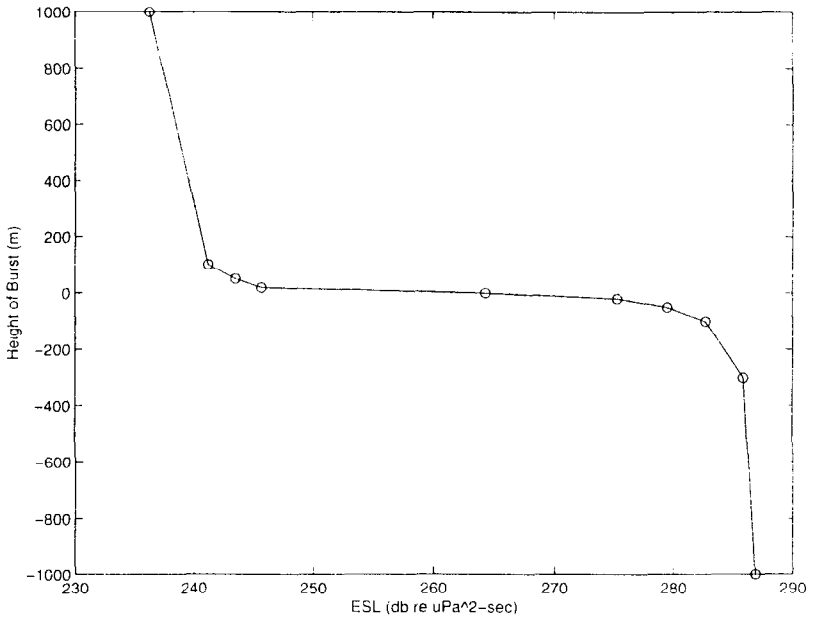

Figure 8: Source Levels vs HOB/DOB for 1 kt explosion.

Receiver Models

Receiver characteristics include the spatial location (lat/lon and depth), the type of station (e.g. simple acoustic, acoustic array, simple seismic, seismic array), the arrival time measurement error ("picking error"), the ambient noise, receiver directionality, and system gains/losses to use for the station. This data is saved as a set of ASCII files for each receiver. Several example data files are provided in the software distribution for each parameter. The receiver location can be overlaid on geographic plots, and plots of the ambient noise, system losses, and receiver directionality can be generated Details of the receiver files are provided below.

System Loss Table.
This file contains SNR gains and losses versus frequency for the receiver These values can include the effects of the gains and losses in the analog electronics, normalization, filtering, scalloping loss and other gains/losses not accounted for elsewhere Logarithmic interpolation is used to obtain values at any desired frequency This file is typically used to include the SNR loss associated with island seismic stations [6]

Directionality Table
This file contains a table of gain versus direction and frequency for the receiver. For stations using array processing, this file contains the array gain for frequencies of interest.

For all receivers, the file can include the effects of blocking from features very close to the sensor, which are too local to be accommodated by the propagation models Logarithmic interpolation is used in frequency, linear interpolation in azimuth.

Ambient Noise Table.
This file contains the ambient noise at the receiver location versus frequency, and where necessary and available, versus azimuth. For receivers north of the equator, the data could be obtained offline from the Navy Wind and Residual Noise (WRN) and Shipping Noise (SN) databases. These databases are not currently integrated into HydroCAM. For other locations, the data can be provided from measurements, or estimated using the Wenz ambient noise model [5]. This model was developed from a large number of observed deep-water ambient noise spectra The model is implemented as sum of four terms [12]

$$AN(f) = AN_0(f) \oplus AN_1(f) \oplus AN_2(f) \oplus AN_3(f) \tag{3}$$

where all terms are power spectral densities expressed in $db//1\mu Pa/\sqrt{Hz}$ and $\oplus$ indicates power addition. Each term is dominant in a different frequency band. Below 10 Hz, the primary contribution is due to turbulence

$$AN_0(f) = 107 - 30\log(f). \tag{3a}$$

Until about 200 Hz, shipping noise dominates

$$AN_1(f) = 76 - 20(\log f - \log 30)^2 + 5(S-4), \tag{3b}$$

where S is the shipping level between 1 and 7 Typical shipping conditions are level 3. Above 200 Hz, the wind-related surface noise is the primary factor,

$$AN_2(f) = \begin{cases} 44 + \sqrt{21W} + 17(3 - \log f)(\log f - 2) & f < 1kHz \\ 95 + \sqrt{21W} - 17\log f & f \geq 1kHz \end{cases} \tag{3c}$$

where W is the local wind speed in knots. For completeness (not necessary for our application) thermal noise is included above 100 kHz,

$$AN_3(f) = -75 + 20\log f \tag{3d}$$

Figure 9 shows the noise spectrum predicted using the Wenz model for shipping level of 3 and a local wind speed of 10 knots

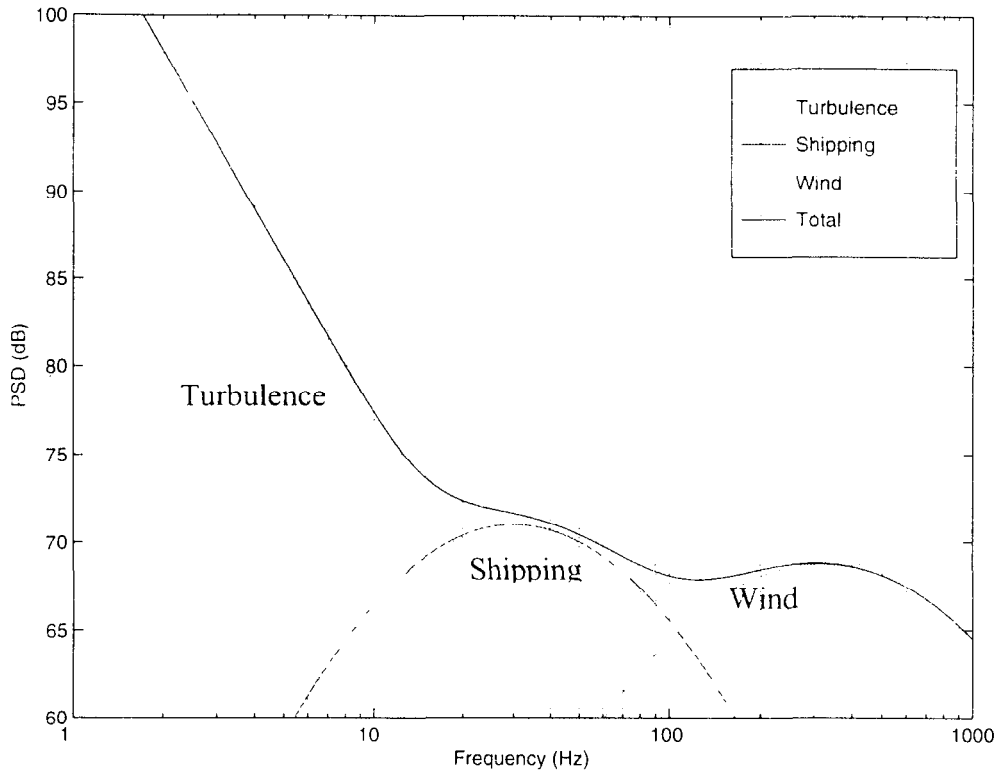

Figure 9. Wenz ambient noise model for 10 knot wind speed, shipping level 3

Network Models

Networks are a list of receiver names. Networks can contain multiple receiver types (SH, SS, etc) The user interface allows displays of the network locations on a geographic figure, and the selection of which receivers are "on-line" during a given prediction

Scenarios

Scenarios are sets of geographic locations to be used for extracting environmental data and propagation predictions There are four types of scenarios in HydroCAM grid, star, point and list. Grid scenarios are evenly spaced set of locations in a rectangular region of lat/lon space. Star scenarios are defined by a set of azimuth (bearing) angles, a maximum range and a range increment. Point scenarios are single locations, usually used for known source locations (such as the HIFT test, or the French Nuclear tests) List scenarios are a set of unconstrained locations contained in a file. This option is can be used for evaluating received acoustic signals from earthquake locations that are estimated by the seismic network Any scenario can be used to predict paths from the scenario locations to a selected set of source or receiver locations. Scenarios be graphically displayed as overlays on other data sets (such as bathymetry), or saved for use by the database extraction and/or propagation modules

Figure 10: Star scenario for two receivers

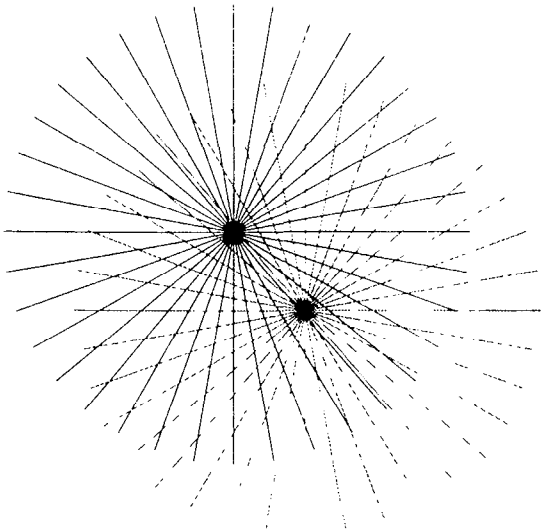

The star scenario is used in two situations, where single sensor coverage is desired, and when detailed characteristics of the propagation path in particular directions are desired. Predictions are computed along radials at a set of fixed ranges from the center point. As the figure shows, network calculations require interpolation from the locations on the radials onto locations which are common to all receivers in the network. This interpolation is described in the Path Section of this report.

Figure 11: Grid scenario for two receivers

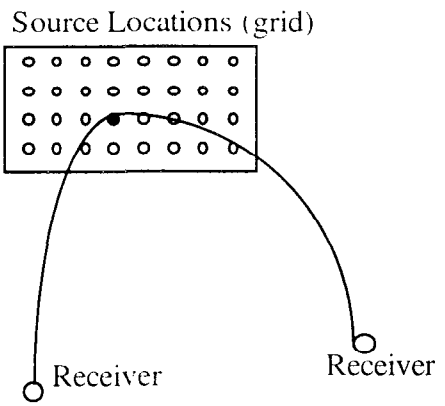

The grid scenario is primarily used when network performance is needed. The paths between each of the receiver locations and every point in the source grid are determined. This requires a path calculation method that fixes the endpoints of the path (such as the *Bender* alorithm), or a non-linear search over a set of rays "shot" from the receiver in the direction of the source location. Grid scenarios require significantly more computation than star scenarios, but don't need to be interpolated when network performance is desired. Path characteristics can be saved along each path, or in a matrix associated with the source locations.

Figure 12. Point scenario for two receivers

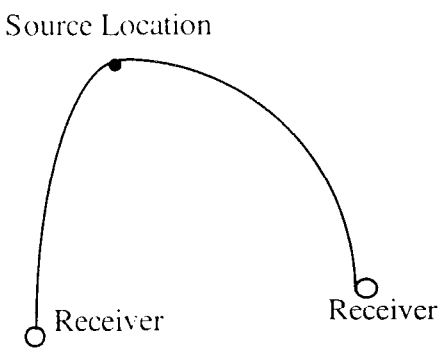

Point scenarios are used for predicting paths between a specific location and a set of receivers These scenarios are most useful when analyzing data from a specific experiment. Examples include analysis of travel times measured during the Heard Island Feasibility Test or data collected after the recent French nuclear tests in the South Pacific.

Figure 13: List scenario for two receivers

List scenarios consist of a set of source locations in a data file. They are used primarily for predictions supporting the analysis of data from clusters of earthquakes which are received by a network.

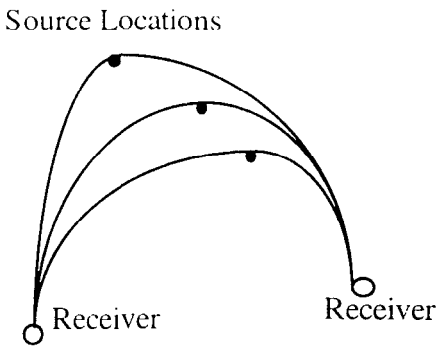

Environmental Databases

Three types of environmental databases are used. "Standard Databases" are databases produced by other organizations, ie the Naval Oceanographic office or NOAA. These databases include bathymetry, temperature, salinity, sound speed and bottom characteristics. The databases are termed "standard" since the quantity and format of the data is fixed once the database is installed in HydroCAM. The remaining two types of databases, channel databases and modal databases contain parameters calculated using HydroCAM. They include channel sound speed, channel depth, phase speed, group speed, modal attenuation and modal slowness variance databases This section describes the characteristics and calculations used for all database types

Standard Databases

Bathymetry

Although many bathymetry databases are available, few contain the world-wide coverage required for predicting the performance of global monitoring networks. The primary bathymetry database used in HydroCAM is ETOPO5 (Earth TOPOgraphy 5 minute), which contains both bathymetry from DBDB5 and topography from a variety of other databases In addition, DBDB for the southern hemisphere, another 5-minute resolution database, is provided since it is in the same format as classified, higher resolution Navy databases. This allows the software for accessing DBDB format databases to be tested. Finally, ETOPO30, which is a version of ETOPO5 decimated to 30 minute resolution, is used for the main figure window and for ray tracing in open ocean regions

Bathymetry data can be accessed by reading in blocks of data, reading single points, or using bilinear interpolation. The detailed methods used for accessing and interpolating bathymetry are provided in the sections where the data is used, ie. "Modal Databases", "Path location", "TL along a path "

Bottom Characteristics

Bottom characteristics are described using a single data file containing sound speed, density, and attenuation versus depth. The default values listed in Figure 14 were provided by NRL. Other modeling efforts at BBN have used bottom characteristics from classified databases (such as LFBL) to produce the same information contained in this table. The software infrastructure in HydroCAM is set up to allow integration of these classified bottom databases, and allowing the bottom characteristics to change geographically. As most significant paths are not bottom interacting, and there was a desire to keep the whole system unclassified, this option was not implemented at the current time.

Figure 14: Summary of Default Bottom Model

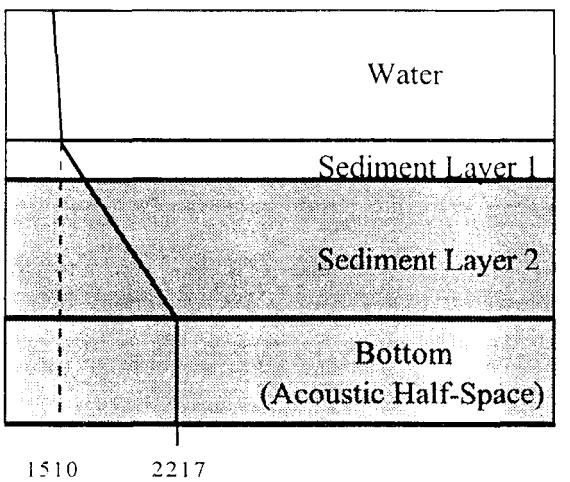

Depth (m)	Sound Speed (m/s)	Density (gm/cm^3)	Atten (dB/λ)
Layer 1			
0	1510	3 02	0.58
50	1567	3 02	0.11
Layer 2			
50	1567	3 02	0 11
700	2217	3 02	0.23
Bottom			
700-inf	2217	3 02	0.13

Sound Speed

Databases of salinity, temperature and sound speed are available in several levels of detail. For prediction of acoustic propagation on global scales, the databases of interest are those which have global coverage, include at seasonal or monthly aspects, and have been interpolated onto a regularly space grid A regular grid reduces the need to smooth and remove bad profiles, and eliminates the need to interpolate using non-uniformly spaced data The two primary sound speed databases included in HydroCAM are the Generalized Digital Environmental Model (GDEM) [13] provided by the Naval Oceanographic Office, and the World Ocean Atlas (WOA) Analyzed database purchased from NOAA [14] Table 3 summarizes the characteristics of these databases The data are provided at the standard depths listed in Table 4

Table 3: GDEM and WOA Characteristics

	WOA Analyzed 1	WOA Analyzed 5	GDEM
Spatial Resolution (degrees)	1	5	0.5 *
Temporal Resolution	Monthly & Annual	Season & Annual	Season
Coverage	Global	Global	†
PROFILE DATA			
Mean Temperature	√	√	√
Mean Salinity	√	√	√
Mean Sound Speed			√
Temp Std Dev		√	
Salin Std Dev		√	
Number of Observations	√	√	

* GDEM has higher resolution data available in some shallow water locations

† No Data is available south of 40 S in the Indian Ocean, south of 60S elsewhere

These tables indicate that although GDEM has better spatial resolution and includes sound speed in the database, WOA has a number of other advantages and is the primary oceanographic database used in HydroCAM. WOA includes monthly variability, mean and standard deviation of the temperature and salinity profiles and is global in coverage. (The standard deviation profiles are particularly useful for predicting the standard deviation of the travel time along a path, see sections "Slowness Variance" and "Travel Time Variance" for details). The statistics of the sound speed profiles can be readily calculated from the temperature and salinity statistics An empirically derived function relating temperature T (degrees Celsius), salinity S (parts per thousand) and depth D (meters) to sound speed is given by [15]

$$C = C_0 + a_1 T + a_2 T^2 + a_3 T^3 + a_4 (S-35) + a_5 D + a_6 D^2 + a_7 T(S-35) + a_8 T D^3, \quad (4)$$

where C_0 is a reference sound speed in m/s the a's are constants listed in Table 5 This equation was shown to provide zero-mean estimates with a standard error of 0.070 m/s on 14,135 samples analyzed [15] The mean sound speed is therefore calculated by substituting the mean temperature and mean salinity into equation (4)

Table 4: Standard Depths in meters for GDEM and WOA

Level	WOA (Monthly)	WOA (Season and Annual)	GDEM
1	0	0	0
2	10	10	10
3	20	20	20
4	30	30	30
5	50	50	50
6	75	75	75
7	100	100	100
8	125	125	125
9	150	150	150
10	200	200	200
11	250	250	250
12	300	300	300
13	400	400	400
14	500	500	500
15	600	600	600
16	700	700	700
17	800	800	800
18	900	900	900
19	1000	1000	1000
20		1100	1100
21		1200	1200
22		1300	1300
23		1400	1400
24		1500	1500
25		1750	1750
26		2000	2000
27		2500	2500
28		3000	3000
29		3500	4000
30		4000	5000
31		4500	6000
32		5000	7000
33		5500	8000
34			9000
35			*Bottom

*GDEM includes a profile point at the bottom after the last standard depth

Table 5: Empirical Constants in Mackenzie's Equation [15]

C_0	1448.96	a_3	2.374e-4	a_6	1.675e-7
a_1	4.591	a_4	1.340	a_7	-1 025e-2
a_2	-5 304e-2	a_5	1.630e-2	a_8	-7 139e-13

An equation for the sound speed variance is derived using general approximation for the variance of a random variable, Y, that is a function of another set of random variables (X_1 , X_2 , . . X_n) [16]:

$$\sigma_Y^2 = \left[\left.\frac{\partial g}{\partial X_1}\right|_{(\mu_1,\mu_2 \quad \mu_n)}\right]^2 \sigma_{X_1}^2 + \left[\left.\frac{\partial g}{\partial X_2}\right|_{(\mu_1\ \mu_2 \quad \mu_n)}\right]^2 \sigma_{X_2}^2 + \cdot \left[\left.\frac{\partial g}{\partial X_n}\right|_{(\mu_1\ \mu_2 \quad \mu_n)}\right]^2 \sigma_{X_n}^2 \qquad (5)$$

where $Y = g(X_1, X_2, \ldots, X_n)$ is the relating function and $\mu_1, \mu_2, \ldots \mu_n$ are the means of X. The partial derivatives of equation (4) are readily computed and substituted into (5) to produce the equation for the standard deviation of the sound speed. The resulting equations are:

$$\frac{\partial c}{\partial T} = a_1 + 2a_2 T + 3a_3 T^2 + a_7 (S - 35) + a_8 D^3. \qquad (6a)$$

$$\frac{\partial c}{\partial S} = a_4 + a_7 T, \qquad (6b)$$

$$\frac{\partial c}{\partial D} = a_5 + 2a_6 D + 3a_8 T D^2, \qquad (6c)$$

and

$$\sigma_c \approx \sqrt{\left[\frac{\partial c}{\partial T}\right]^2 \sigma_T^2 + \left[\frac{\partial c}{\partial S}\right]^2 \sigma_S^2 + \left[\frac{\partial c}{\partial D}\right]^2 \sigma_D^2} \qquad (6d)$$

The depth variance term in (6d) can be ignored, since both the constants in (6c) and the depth variance are small.

To conserve disk space and allow other empirical relations to be substituted for (4), these equations are executed in the database access routines whenever sound speed information is requested from the WOA database

Channel Databases

SOFAR propagation depends on the formation of a sound channel in the water column. This channel is typically formed in mid-latitudes at a depth where the temperature stops decreasing and the increase in pressure causes the sound speed to increase. Figure 15 shows a plot of a typical mid-latitude deep water sound speed profile (10S, 26.5W), and a typical high-latitude sound speed profile (60S, 26.5W). Since many simple models of global propagation depend on the sound speed at the channel axis, these values are extracted and a new database is formed. Channel databases contain environmental parameters at the sound channel depth, and are created offline by a set of MATLAB scripts. This operation takes a modest amount of disk space, with the benefit of not needing to search for the sound speed minimum each time the sound channel data is needed. At the current time, the sound channel minimum is taken to be the minimum of the sound speed using the depths provided in the database (ie no interpolation is used). Versions of the channel database with linear and cubic interpolation may be provided in the future. Two channel databases have been derived, GDEM_Channel and WOA_Channel. GDEM_Channel contains the temperature, salinity, sound speed and channel depth where the sound speed minimum occurs. WOA_Channel contains the same data with the additional sound speed standard deviation. The temporal distribution of the channel databases is identical to that of the raw databases. For the construction of the monthly WOA_Channel database, the sound speed data at depths below 1000 meters was appended using the appropriate seasonal database before the sound speed minimum was determined (See Table 4 for a list of the depths where data is provided).

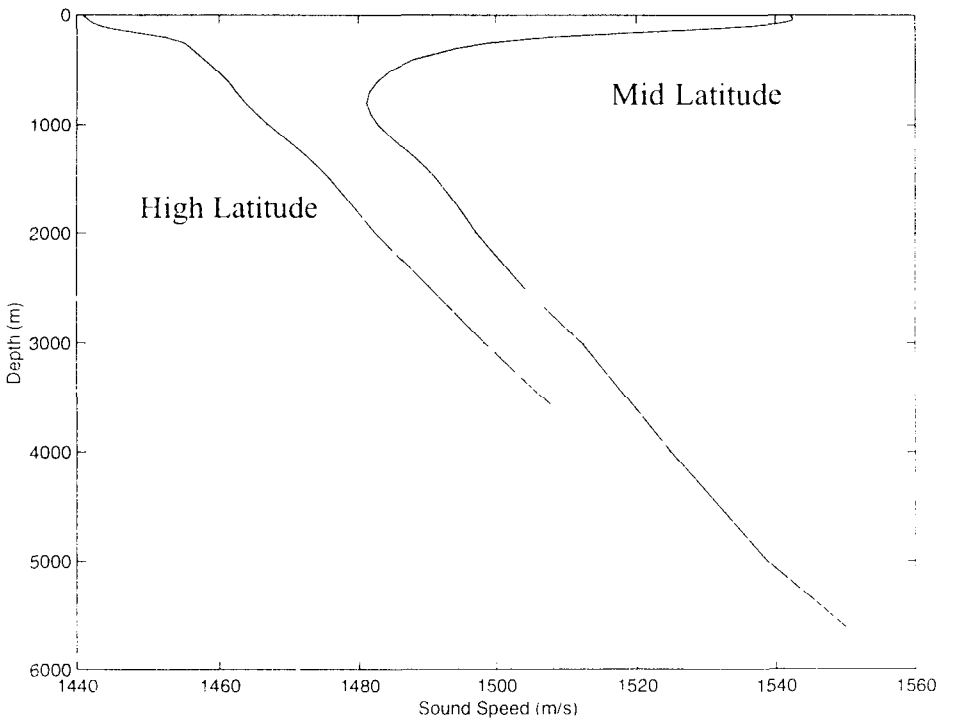

Figure 15: Sound Speed Profile with SOFAR Channel

Modal Databases

The production of modal databases requires a significant amount of computation. A block diagram of the procedure is shown in Figure 16. Modal databases contain a set of parameters describing modal propagation at a each of a set of grid points in a rectangular lat/lon region. After environmental data is extracted and processed, the mode structure is calculated by either Kraken or FD-WKB, resulting in a database of the modal eigenvalues k_n and eigenfunctions. The program WaveGuide uses this database along with the sound speed and sound standard deviation profiles to calculate the modal propagation parameters. Finally, these parameters are collected into single-parameter geographic grids. More than one mode can be included in the same grid file Grid files can be produced at different resolutions where the bathymetry and/or sound speed are expected to vary rapidly

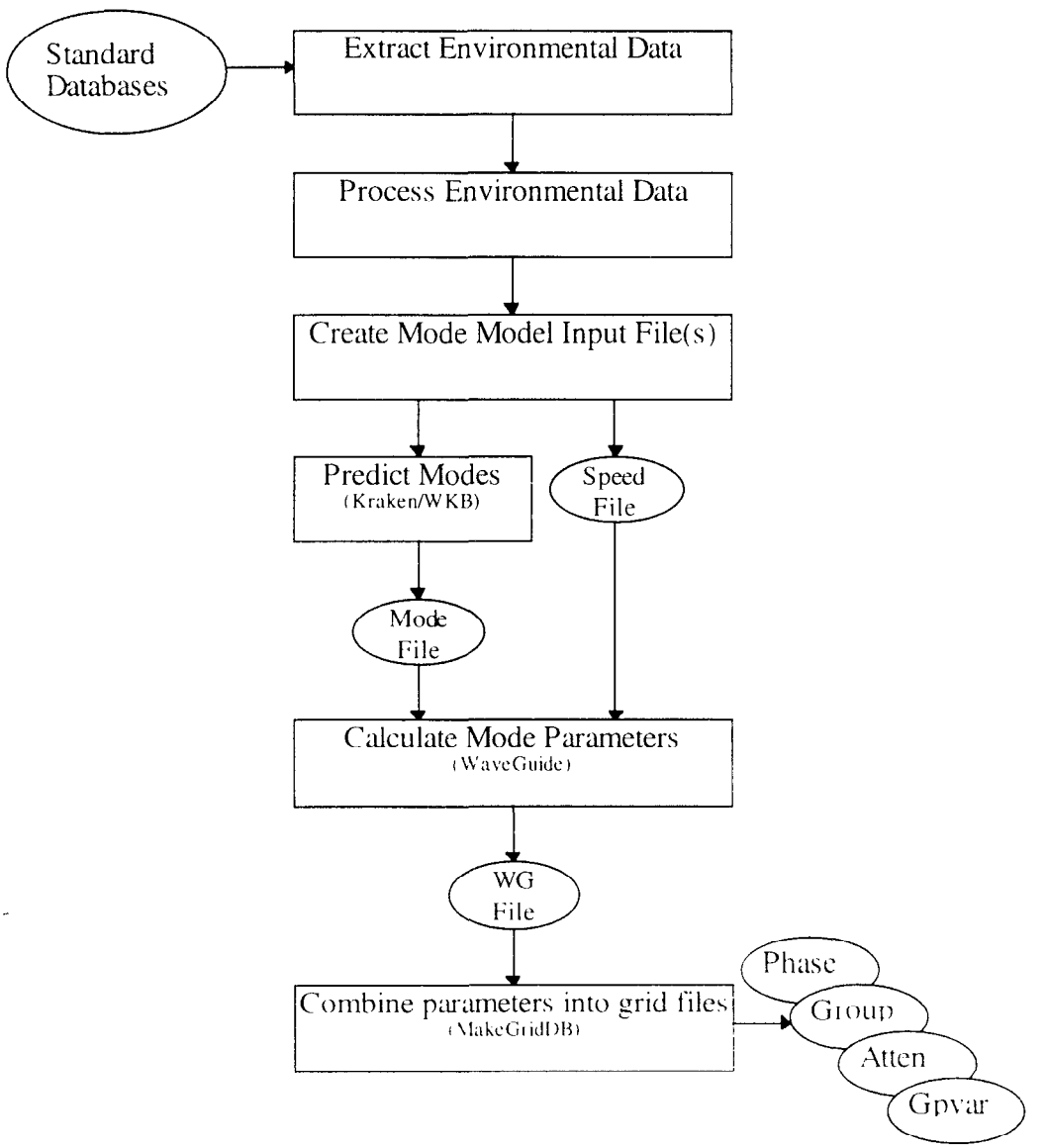

Figure 16. Procedure for creating modal databases

Processing of Environmental Data

In order for modes to be calculated at each point in the desired grid, sound speed and bathymetry data must provided at the grid points. The calculation of modal slowness variance requires the standard deviation of the sound speed at each point in the profile. The extraction and interpolation of these environmental data are performed by the MATLAB function *create_grid_env.m* The procedure is shown in the block diagram of Figure 17.

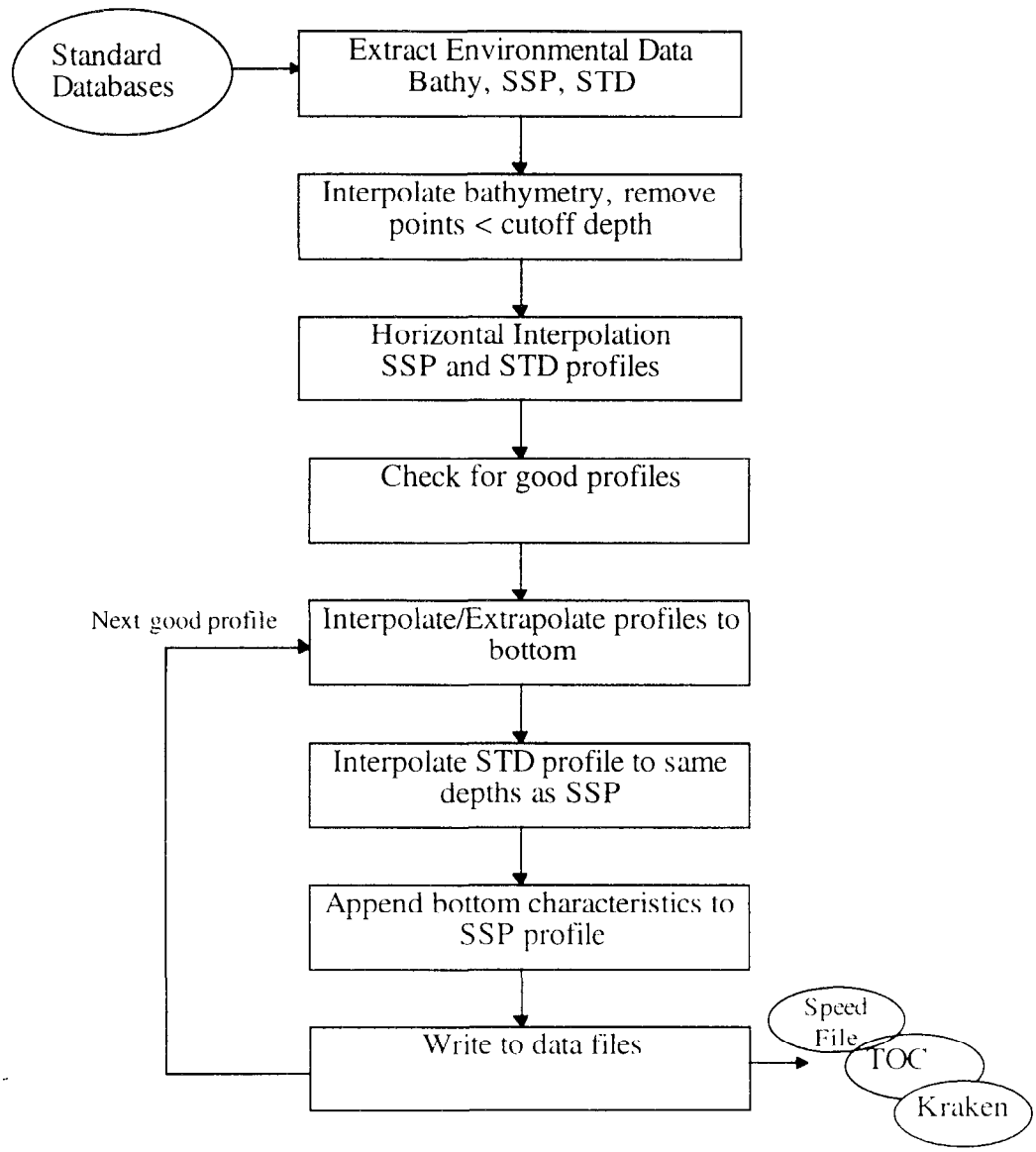

Figure 17. Procedure for Processing Environmental Data and Creating Input Files for the Prediction of Modes using Kraken and WKB

The first step is to read the sound speed profiles, bathymetry data, and sound speed standard deviation profiles for a geographic region at least as large as the desired grid. Bathymetry data is then interpolated using bilinear interpolation to estimate the bottom depth at each point in the desired grid. Since modes are "cutoff" as the bottom depth decreases, grid points with bottom depth shallower than a user specified cutoff depth are not included in the remaining calculations. A recommended cutoff is provided on the user interface to assist users unfamiliar with normal mode predictions. This value is calculated for a Pekeris waveguide, a range-independent environment with an isovelocity water column and isovelocity bottom, using

$$cutoff = \frac{(n-\frac{1}{2})c_w c_s}{f\sqrt{c_s^2 - c_w^2}},$$

where n is the mode number, and the subscripts w and s indicate water and sediment respectively. The suggested cutoff is calculated for the lowest mode number and the highest frequency requested, using $c_w = 1500$ m/s and $c_s = 2200$ m/s.

The sound speed and standard deviation profiles (SSP and STD respectively) are now horizontally interpolated to the remaining grid points. Several interpolation options are provided. "Table lookup" uses data in the SSP or STD resolution cell where the grid point is located. "Nearest" finds the closest profile in the database to the grid point. "Linear" replaces all *No-Data* points with the average of the other points, then does bilinear interpolation. "Linearn" performs the same calculation without the replacement of *No-Data* points. When a reasonably small geographic grid is chosen, the recommended option is "Linear", since the average of the sound speed points contained in the grid will be close to the missing data. This option is not recommended for large grids since the average sound speed may be markedly different from the values near the *No-Data* points, resulting in non-physical changes in the interpolated sound speed field near these points. Figure 18 graphically illustrates the profile interpolation methods.

Figure 18(a) shows 4 cells of data from the standard database, with the values in the cells annotated on the outside of the rectangles. *N* indicates a *No-Data* cell The data values are considered to be located a the center of the cells The circles are at the desired grid points. The resulting values for both "Table" and "Nearest" are shown in Figure 18(b) "Linearn" results in a larger *No-Data* region since the N points are used in the 2d interpolation (c). *I* indicates the values are the result of bilinear interpolation. "Linear" with replacement shows that the *No-Data* cell has been replaced by the average of the other cells before interpolation, resulting in a completely filled in grid illustrated in Figure 18(d).

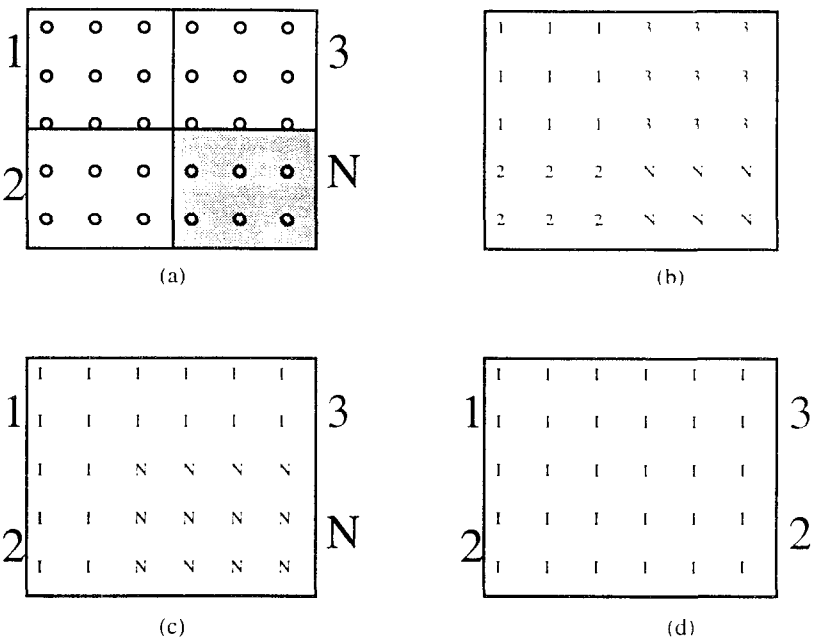

Figure 18: Examples of Horizontal Profile Interpolation: (a) input data, (b) "Table" and "Nearest", (c) "Linearn", (d) "Linear". *N* indicates *No-Data. I* indicates *interpolated.*

After the interpolation is performed at each depth, each grid point is searched to determine whether there are enough points in the profile to do vertical interpolation This decision is made by *good_profiles m* and is currently set to 5 points. Since the resolution of the profile databases and the bathymetry databases are likely to be different, the profiles must now be forced to end at the bottom specified in the bathymetry database. *Force_profiles.m* either interpolates or extrapolates the profiles to the bottom depth, and then truncates any remaining datapoints in the profile.

The bottom profile (see Bottom Characterization section above) is now appended to the water column profiles, and the data files are written. A single "Speed" file contains the sound speed, sound speed standard deviation, density and attenuation profiles for each grid point. If Kraken has been selected, then a separate Kraken environment file is written for each grid point In addition, several index files (table of contents) are written to allow rapid access to the profile or mode datafiles Example profiles are shown along with the resulting mode structure in Figure 19.

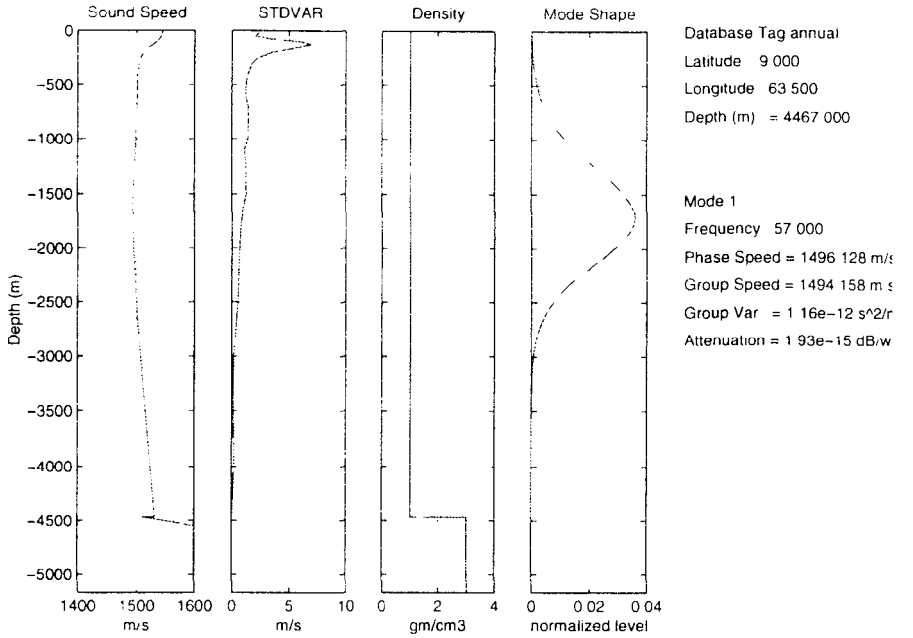

Figure 19: Example profiles, mode structure and modal propagation parameters

Calculation of Modes

Many models have used normal mode methods to predict the transmission characteristics in the ocean. Mike Porter, the developer of the Kraken normal mode model, uses the following analogy to describe normal modes:

> *The normal mode problem involves solving a one-dimensional equation which is very similar to that of a vibrating string. In this analogy, the "frequencies" of vibration give the horizontal wavenumbers associated with modal propagation and a varying string thickness corresponds to a change in sound speed with depth. The relative excitation of the ocean modes depends on the source depth just as the harmonic balance of a note is affected by the position where the string is plucked. [11]*

Kraken has been refined and extended since its initial development in 1980. It is included in a number of standard transmission loss models such as the SNAP model at SACLANTCEN and the Wide-Area Rapid Acoustic Prediction (WRAP) system at NRL. Kraken uses a finite differences approach to solve the depth-separated Helmholtz equation for the horizontal wavenumbers and mode shape functions when given the characteristics of the water column and ocean bottom. This is accomplished numerically by calculating the eigenvalues (horizontal wavenumbers) and eigenfunctions (mode shape functions) of the matrix Helmholtz and boundary condition equation. Additional information describing normal mode approaches [17] and a complete users guide describing the computational details of Kraken are available elsewhere [11]. While Kraken is a very robust and stable model, and it computes all of the eigenvalues and

eigenfunctions for a given location, where typical global-scale problems may require only mode 1 or the first several modes instead of the whole spectrum.

Since the modal structure is required at each geographic location in a world-wide grid, a modest time savings at a single location translates into a large time savings when calculating a global grid. A second mode model provided in HydroCAM attempts to provide a faster but more approximate calculation of the mode structure by employing the Wenzel-Kramers-Brillouin (WKB) approximation. It has the additional benefit of calculating only the desired modes. It is a hybrid WKB Finite Difference (FD-WKB) approach which estimates the modal eigenvalues using the WKB approximation, and then calculates the mode shapes and refines the eigenvalue estimates using finite-differences. The details of this method are provided in Appendix A

For either Kraken or the WKB models, the mode shapes and horizontal wavenumbers are stored in a mode file. A typical deep-water mode shape function is included in Figure 18. The rest of this section describes the equations used to calculate the waveguide parameters from the modes and the sound speed statistics

Phase Speed

The local phase speed is calculated from the horizontal wavenumber using

$$v_n = \frac{\omega}{k_n}. \tag{7}$$

The phase speed grid obtained by applying equation (7) at every lat/lon location determines how energy is horizontally refracted at frequency ω.

Group Speed

The modal group speed u_n, or its reciprocal the modal slowness S_n, is the major factor in determining the travel time along a path (See the travel time calculation section below.) One approach for calculating group speed can be obtained using perturbation theory [17] The resulting equation for the modal slowness is a function of the mode shape, the density ρ, and the sound speed profile $c(z)$

$$S_{gn} = \frac{1}{u_n} = \frac{dk_n}{d\omega} = \frac{\omega}{k_n}\int_0^D \frac{\psi_n^2(z)}{\rho(z)c^2(z)}dz. \tag{8}$$

where D is the depth of the acoustic half-space This equation is evaluated in several steps First, the sound speed and density profiles are linearly interpolated to the same depths as the mode shape function (The sound speed profiles are typically sampled at

spacings of to 100 to 1000m The.mode shape function is sampled more densely). After the mode shape function is normalized such that

$$\int_0^D \frac{\psi_n^2(z)}{\rho(z)} dz = 1,$$

equation (8) is numerically evaluated using trapezoidal integration.

The group speed could also be calculated by numerically evaluating the derivative in equation (8) using finite differences. This would require calculation of the modal eigenvalues at several frequencies. In the future, if broadband calculations are desired and the mode shape functions are not needed for either the attenuation or group slowness variances, then a finite differences approach for calculating the group speed would be recommended.

Bottom Attenuation

Two options for calculating bottom attenuation have been implemented; (1) a perturbation theory derived equation which is included in the NRL model [18], and (2) directly using the imaginary wavenumbers calculated from Kraken or WKB. The first approach gives an equation for the attenuation in dB per wavelength [19]

$$atten = \frac{\beta_0}{\lambda_0} \int_D^\infty \frac{\psi_n^2(z)}{\rho(z)} dz \tag{9}$$

where β_0 is an empirically derived constant, typically 0.1 dB, and λ_0 is the acoustic wavelength The advantages of this approach are that it is identical to the NRL model, and that NRL has measured values of β_0 for some locations. However, when more complete characteristics of the bottom are known (such as when LFBL is integrated), then it is appropriate to determine the attenuation from the imaginary part of the wavenumber computed by Kraken [18] or WKB (see Appendix A)

$$\psi(x,t) = Ae^{-i(\omega t - kx) - \alpha x}$$

The resulting expression for attenuation is [17, p 135]

$$atten = -20\log\left[e^{\frac{2\pi\alpha}{k}}\right] \tag{10}$$

Equation (10) is the default in WaveGuide.cc Equation (9) is available by changing the bottom attenuation model number in WaveGuide.cc and recompiling the software

Slowness Variance

The travel time variance depends strongly on the variance of the slowness along the path. (See section on travel time variance). HydroCAM has two models for determining the slowness variance. The channel model assumes that the sound energy propagates entirely at the sound channel depth. In this case, the slowness is the inverse of the minimum sound speed in depth at each point along the ray path. The Taylor series expansion of the channel axis slowness about the mean slowness is

$$c^{-1} = \mu_c^{-1} - (\Delta c)\mu_c^{-2} + (\Delta c)^2 \mu_c^{-3} + h.o.t.$$

where μ_c is the mean sound speed at the channel axis depth. The variance of the slowness is then determined by taking the expected values of the Talyor series expansion and using

$$\sigma_{S_c}^2 = \left\langle c^{-2} \right\rangle - \left\langle c^{-1} \right\rangle^2,$$

where the subscript indicates that the variance of the slowness S is for the channel model. The resulting expression for the channel slowness variance is

$$\sigma_{S_c}^2 = \frac{\sigma_c^2}{\mu_c^4} \tag{11}$$

where σ_c^2 is the variance of the sound speed at the channel axis.

Derivation of the modal slowness variance model starts with the expression for the modal group slowness given in equation 8. If we expand the square of the local sound speed in the denominator of equation 8 and use the same method described for the channel axis model, we obtain the following equation for the modal slowness variance

$$\sigma_{S_n}^2 = 4v_n^2 \int_0^\infty dz \frac{\psi_n^2(z)\sigma_c^2(z)}{\rho(z)\mu_c^3(z)} \int_{-z}^{\infty} d\Delta z \frac{\psi_n^2(z+\Delta z)R(\Delta z)}{\rho(z+\Delta z)\mu_c^3(z+\Delta z)} \tag{12}$$

where R in this equation is describes the correlation of the sound speed statistics as a function of depth. Details of this derivation are provided in Appendix B In Version 2, the correlation function R is given by

$$R = \exp\left\{\frac{-\Delta z^2}{2L^2}\right\}$$

where L is the 1 σ correlation length scale of the fluctuations currently set at 30m. To speed up the numerical integration of (12), the correlation function is pre-computed for $|\Delta z| < 3L$, and the integral evaluated over this same range.

Grid Files

The last step in the calculation of the modal databases is to sort the modal parameters contained in the waveguide file into spatial grid files which are readily accessible by both the horizontal ray-tracing program and the display software. No interpolation or extrapolation is performed during this procedure.

Path Prediction

Recent interest in the global propagation problem has resulted in the development of several methods for predicting acoustic paths at global scales. These methods range from the relatively simple, such as using a single sound speed for the whole ocean and a spherical model for the earth, to fully developed approaches such as horizontal raytracing on an ellipsoidal earth, to approaches that are still under development such as the horizontal PE model [20]. The design approach used in HydroCAM was to start with the simplest models, and gradually add more complex models as required and available. Early comparisons with measured data showed that the simplest appropriate model consists of geodesic (ellipsoidal earth) paths and channel sound speeds. In many cases this model predicts travel times to sufficient accuracy (less than 1% error). However, in other cases, this model does not predict the right paths and/or produces a biased travel time estimate. A model that includes the effects of horizontal refraction is required for these situations.

In HydroCAM, the prediction of paths and their characteristics is usually performed in the program GlobeRay. The original version of GlobeRay was based on the horizontal raytrace program GSOAR (Global-Scale Ocean Acoustic Raytrace) developed by NRL. The differential equations describing the ray path and the method of solving these equations in GlobeRay are identical to the methods used in GSOAR. However, the C++ implementation of GlobeRay provides great flexibility. As an example, the grid database class used for environmental data, allows the user to define areas using any resolution environmental data without software changes. In addition, GlobeRay calculates travel time, transmission loss, travel time standard deviation and provides for a number of input and output options not present in GSOAR. The current version also implements an alternate boundary value approach called Bender. This approach was also provided in standalone raytrace software for AFTAC in 1997. This section of the users guide presents a summary of the method for determining horizontally refracted ray paths, followed by the equations used for determining the path characteristics. Information on the details of the class structures used for manipulating geographic data are provided in Appendix F. Additional information on horizontal refraction methods is widely available in the literature [eg see 17,19]

A functional block diagram of GlobeRay is shown in Figure 20. Path locations are calculated first, where the only conditions stopping a ray are (1) if the ray passes over regions shallower than a user specified minimum depth, or (2) the ray exceeds the maximum range specified by the user. If reflections are desired, the location of the reflection and the new launch angle are computed and the path continued. After the locations are determined, the characteristics of the ray are calculated by numerically integrating the appropriate data over the ray path. The results are stored in one of two sets of data files, as summarized in Table 6. Path files save all information along each path. Grid files contain only the path characteristics at the endpoint of paths from the

reference point to a grid of evenly spaced endpoints. An additional matrix containing the launch angles for each path is provided for use in Sonar equation calculations (such as ambient noise) at the reference point.

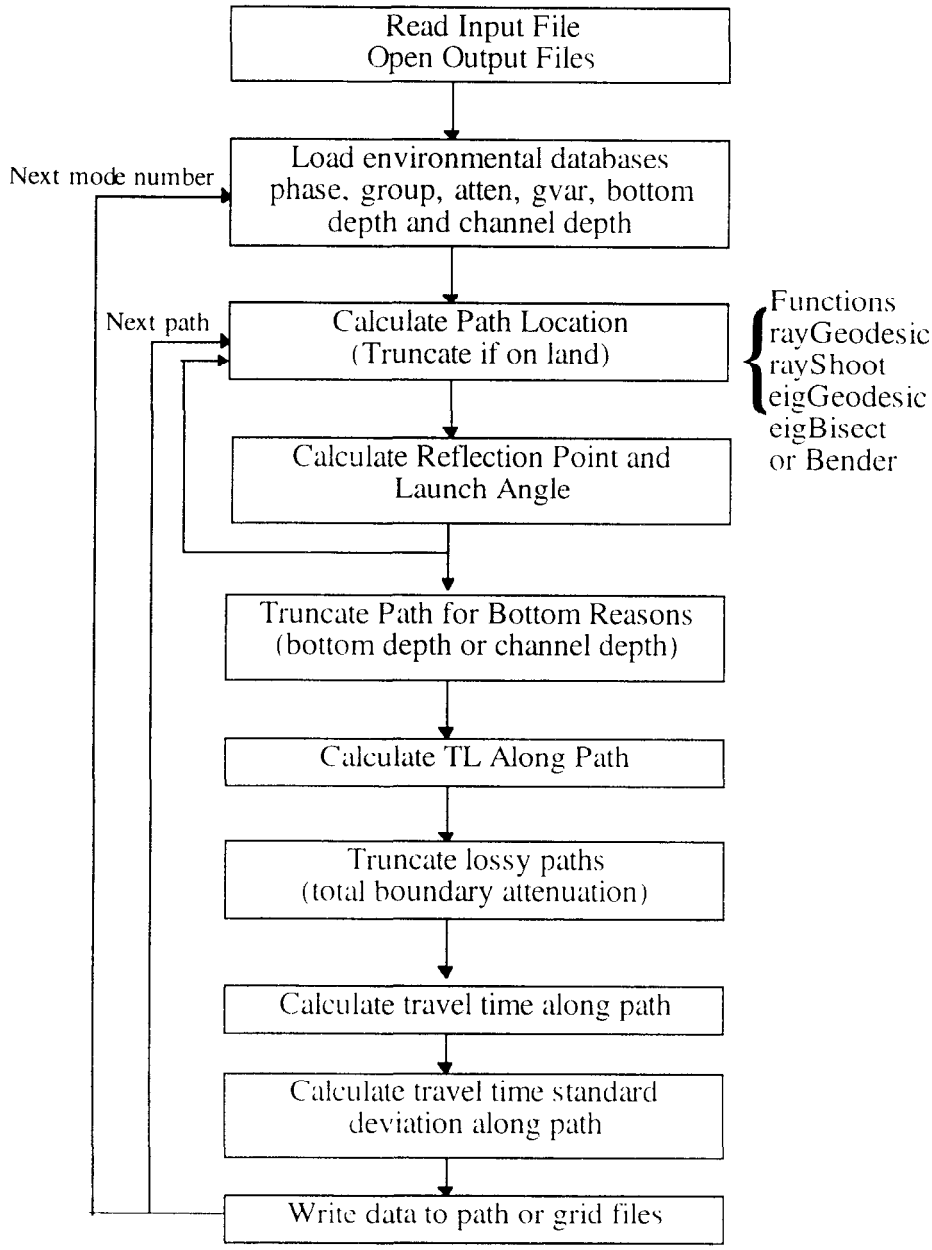

Figure 20. GlobeRay Functional Diagram

Table 6: Data files for describing ray paths and their characteristics

Path Files	
.path	lat, lon, range, angle along set of paths (deg, deg, km, deg TN)
ATTEN	attenuation due to ice coverage and bottom loss along paths (dB)
.TT	travel time along paths (seconds)
.ST	travel time standard deviation along paths (seconds)
Grid Files	
TTgrid	travel time from reference point to grid points (sec)
.STgrid	travel time standard deviation from reference point to grid points
.ANGLEgrid	launch angle of path from reference point to grid points
.Rgrid	range from reference point to grid points (km)
.ATTENgrid	attenuation due to ice coverage and bottom loss from reference point to grid points (dB)

Path Location

HydroCAM contains three path models; geodesic (ellipsoid earth) paths, horizontally refracted paths based on the NRL model [19], and horizontally refraced paths calculated using a bender method (see Appendix C). The first two approaches can be run in two ways, shooting and eigenrays. Shooting a ray is the process where the initial conditions (lat, lon and launch angle) are specified, and the ray is propagated wherever the equations for the particular model dictate (ie, an initial value problem). Solving for eigenrays is the process where both the starting point and the ending point of the desired ray path are fixed, and the locations of the intermediate points in the path are calculated (ie, a boundary value problem). In some cases, this method results in a non-linear search for the path that connects two points that may or may not converge. The bending approach is an attempt to speed up the search for eigenrays and reduce the conditions under which no connecting ray paths are found. The following sections describe the calculations performed in HydroCAM for each of these methods

Geodesic Rays

Geodesic rays are calculated in function *rayGeodesic* The function uses two routines provided by the US Geologic Survey [21] The first routine, *geod_invrse* calculates the range and bearing between two points. The second, *geod_forwd* calculates the lat/lon coordinates of a point given the range and bearing from a reference point Both routines use an ellipsoidal earth model with parameters from the Clarke66 earth model, an equatorial radius of 6370 km and an eccentricity of 0 088 When *rayGeodesic* is called, a range increment is provided as an input parameter, based on

$$\Delta r = 1.5\Delta t \cdot nsave,$$

where Δt is the base time increment specified in the user interface, 1.5 is a rough conversion factor from time to distance and *nsave* is a decimation factor that determines which ray points are returned to the calling routine. Since the horizontal refraction code uses a base time step and the geodesic code uses a base range step, we opted to simplify the control software by always requiring a time step as the input parameter, then to use simple equation above to compute the range step. However, unlike the horizontal refraction case, the range step for the geodesic computations is fixed, and does not adapt to the resolution of the environmental databases. A geodesic ray is calculated starting at the initial location and launch angle and using the range increment to calculate the latitude and longitude at the next point. After the local ray angle at the new point is calculated, the current geographic location is tested to verify that the ray is not on land, is not outside the coverage of all depth databases, and that the distance traveled does not exceed the user-specified maximum range. Latitude, longitude, local angle and distance along the path are returned for each point in the path.

Geodesic Eigenrays

These calculations are performed in function *eigGeodesic* First, the ray end-point is checked to make sure it is not on land. Then, the range and bearing between the end-points is calculated. Using this range as the maximum range and the bearing as the initial azimuth, *rayGeodesic* is called to calculate the coordinates along the path between these points. All points along the path are returned to the calling routine.

Refracted Geodesics

These calculations are performed in function *rayShoot*. A set of ordinary differential equations (ODEs) describing the ray-path are solved by starting at a defined initial condition and numerically integrating. A diagram of the method is provided in Figure 21.

The differential equations are derived starting with the equations for a refracted ray path given in [19],

$$\frac{\partial \phi}{\partial s} = \frac{\cos\alpha}{\mu(\phi)} \tag{13a}$$

$$\frac{\partial \lambda}{\partial s} = \frac{\sin\alpha}{\eta(\phi)\cos\phi} \tag{13b}$$

$$\frac{\partial \alpha}{\partial s} = \frac{\sin\alpha}{\eta(\phi)}\tan\phi - \left(\frac{\sin\alpha}{\mu(\phi)}\frac{\partial}{\partial\phi} - \frac{\cos\alpha}{\eta(\phi)\cos\phi}\frac{\partial}{\partial\lambda}\right)\ln k_n \tag{13c}$$

where

$$\mu(\phi) = \frac{r_{eq}\left(1-\varepsilon^2\right)}{\left(1-\varepsilon^2 \sin^2 \phi\right)^{3/2}} \tag{14a}$$

$$\eta(\phi) = \frac{r_{eq}}{\left(1-\varepsilon^2 \sin^2 \phi\right)^{1/2}}, \tag{14b}$$

r_{eq} is the equatorial radius of the earth, and ε is the eccentricity. Examination of (13) shows that the derivatives are taken with respect to the path length s , and that horizontal refraction is contained in the spatial derivatives of the horizontal wavenumber in (13c). A more convenient formulation be obtained by converting (13) into equations that depend on the local phase speed v_n and time by using equation (7), which relates the horizontal wavenumber k_n to the phase speed, and the relationship

$$ds = v_n dt .$$

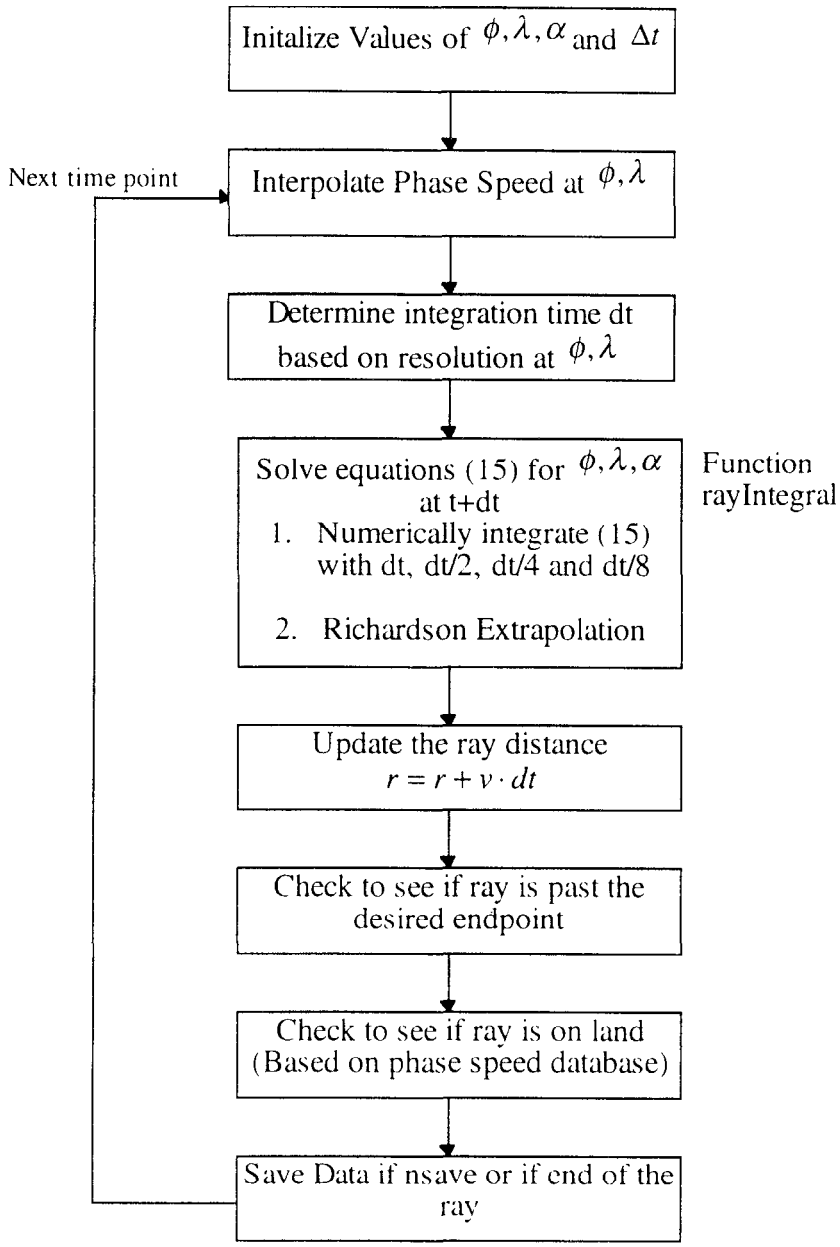

Figure 21: Block diagram of function rayShoot

The resulting equations, which are implemented in both GlobeRay and GSOAR, are

$$\frac{\partial \phi}{\partial t} = v_0 \frac{\cos \alpha}{\mu(\phi)} \tag{15a}$$

$$\frac{\partial \lambda}{\partial t} = v_0 \frac{\sin \alpha}{\eta(\phi) \cos \phi} \tag{15b}$$

$$\frac{\partial \alpha}{\partial t} = v_n \frac{\sin \alpha}{\eta(\phi)} \tan \phi + \frac{\sin \alpha}{\mu(\phi)} \frac{\partial v_n}{\partial \phi} - \frac{\cos \alpha}{\eta(\phi) \cos \phi} \frac{\partial v_n}{\partial \lambda} \qquad (15c)$$

These equations are solved independently using trapezoidal integration. The user specifies a base integration time Δt (seconds per degree) At each increment, the resolution of the phase speed databases is checked, and the actual integration time dt is calculated according to

$$dt = \Delta t \cdot res.$$

where *res* is the best resolution available at the current location. This adaptive time step procedure is used to "slow down" the integration in geographic regions where the phase velocity is rapidly changing, such as continental margins and areas near islands. (See the illustration in Figure 22). After the integration time dt is computed, the ray location at the $t+dt$ is computed by integrating the ODEs as follows: First, the phase speed is calculated at the current point using bilinear interpolation. The gradient of the phase speed is calculated at each of the four grid locations surrounding the current point using finite differences, with the latitude and longitude differences computed in units of radians. Then, the phase speed gradient at the current location is calculated by bilinear interpolation on these four gradient values. Equations (15) are now integrated from time t to $t+dt$ four separate times, using an integration step sizes of dt, $dt/2$, $dt/4$ and $dt/8$ respectively. The values of phase speed and phase speed gradient are not interpolated at intermediate times $t+dt/8$, $t+dt/4$ etc. Richardson extrapolation is used to estimate what the integrated value would be with step size dt/∞ [22].

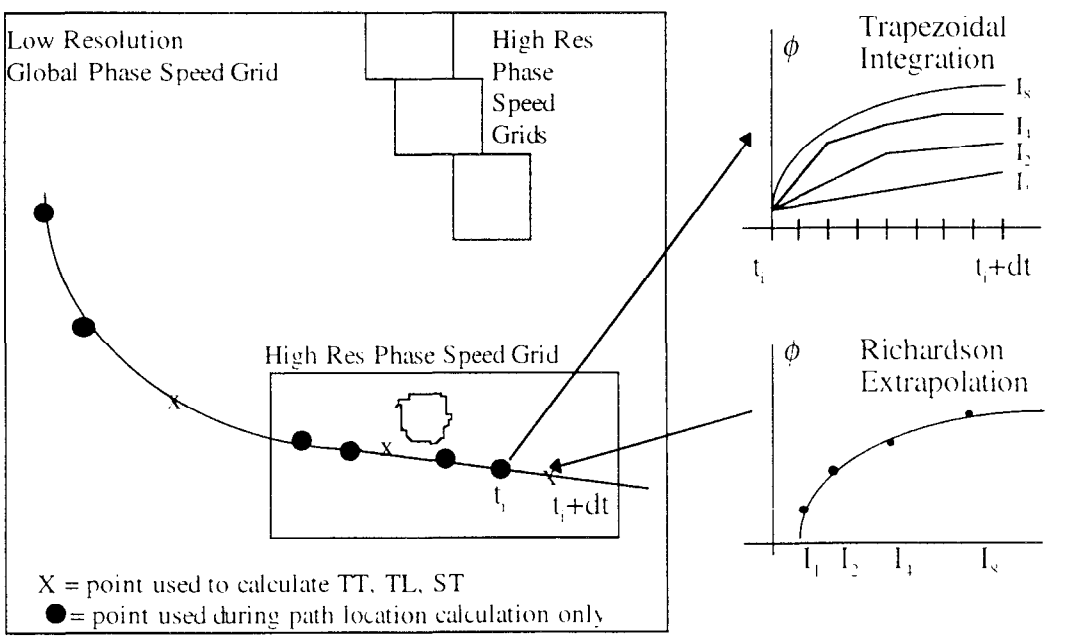

Figure 22: Ray tracing procedure

As with the geodesic ray paths, the location after each integration step is checked to verify that the point is not on land. When a desired end point has been specified, the raypath is also checked to make sure that it has not passed this end point. The procedure is verify that the current location is within 15 degrees latitude and 15 degrees longitude of the endpoint, and then stop the ray if the following condition is met

$$(\phi_i - \phi_e)\cos\alpha_i + (\lambda_i - \lambda_e)\sin\alpha_i > 0.$$

The subscript i indicates the *ith* point of the ray path, and the subscript e indicates the desired endpoint. This equation is derived by using the plane geometry of the ray path with respect to the desired endpoint. The decimation factor *nsave* is applied as the ray is being traced, with one point every *nsave* points being placed in the data arrays that are passed back to the calling routine.

Reflections

A first order model based on the law of reflection (ie angle of incidence equals the angle of reflection) is used to compute ray paths reflected from continental shelves, islands, seamounts and other types of bathymetric features. For modeling purposes, reflections are only produced when the ray path encounters sufficiently shallow water. Thus, an accurate characterization of the coastline is needed to model the reflection geometry. Once a ray path enters a geographic region where the depth is less than the user specified value (typically 50-100 meters), a reflected path is computed as described in the following paragraphs. If the user has not selected the reflections option then the path is terminated (see Path Stop Conditions below).

Figure 23 depicts the geometry of an incoming ray path approaching a coastal region. In this diagram, θ_{INC} and θ_{REF} denote the angle of the incident and reflected rays measured relative to true North, θ_I and θ_R are the angles of incidence and reflection $(\theta_I = \theta_R)$, and ϕ represents the angle that the tangent to the coastline makes with the horizontal axis. The vertical and horizontal axes represent latitude and longitude respectively Given θ_{INC} and ϕ, θ_{REF} is readily calculated as

$$\theta_{REF} = \pi - \theta_{INC} - 2\phi$$

In order to determine the angle of the tangent to the coastline at a specific point, a local characterization of the coastline behavior is needed. This can be accomplished by examining the local bathymetry surrounding the area where the incident ray approaches the coastal region Coastlines can be defined as a level curves, or contour lines, of bathymetry where the depth (D) is zero By definition, the gradient of the bathymetry (∇D) will point in the direction of steepest slope and will be orthogonal to the coastline [30] A vector which is tangent to the coastline will thus be orthogonal to the gradient of

the bathymetry. Once the gradient of the bathymetry is calculated, the angle that the tangent vector (T) to the coastline makes with respect to the horizontal axis is easily computed from

$$\nabla D \bullet T = 0$$

This determines the new launch angle for the reflected path. The gradient is computed using the same finite differences with bilinear interpolation algorithm that is used for determining the phase velocity gradient for horizontally refracted paths (see the section on *Refracted Geodesics* above).

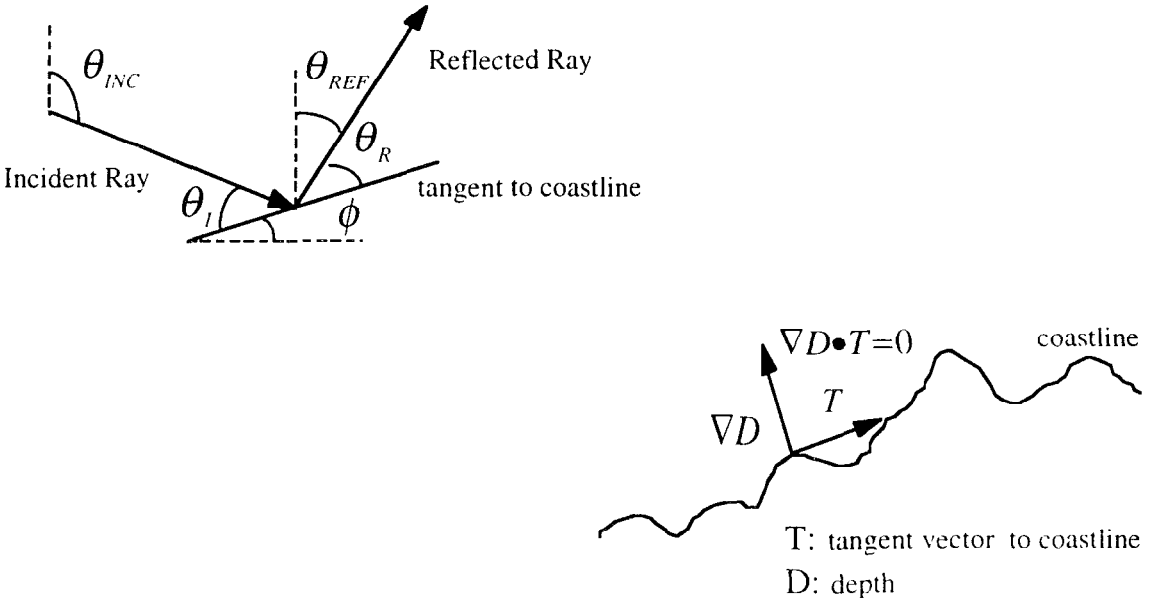

Figure 23: Reflection Geometry

Reflected rays can currently be generated only for 'shooting' rays (geodesics or refracted) and not for eigenrays. Also, a ray is reflected only when the path encounters the pre-selected minimum depth. Whether the path is actually reflected or terminated depends on a pre-selected parameter indicating the maximum number of reflections for each ray. Both of these are chosen by the user prior to generating any ray paths.

Refracted Eigenrays

Refracted eigenrays are calculated in function *eigBisect* , where the function name indicates that the bisection method is employed. Basically, the procedure is to shoot a number of refracted rays (using *rayShoot)* and search for the ray path that is closest to the desired end point. The user specifies a start angle, end angle and angle increment (relative to either true north, or to the geodesic connecting the starting point and the desired end point). After each ray is traced, a distance measure from the ray end point to the desired end point is calculated using

$$\Delta_i = \mathrm{sgn}(\lambda_i - \lambda_e)\sqrt{\left((\phi_i - \phi_e)^2 + (\lambda_i - \lambda_e)^2\right)}$$

Here the subscript i indicates the last point in the raypath using the *ith* launch angle, and the subscript e indicates the desired endpoint of the eigenray If the distance measure is smaller than the user specified *eigenray tolerance*, then the search is stopped and the current ray path is selected as the eigenray. If the current ray path is on the other side of the endpoint than the ray path at the previous launch, then these two launch angles are used to start another search and the angle increment is decreased by a factor of 10.

Figure 24 shows a block diagram of the function including all logic for terminating the eigenray search. Other methods for performing this search, such as Newton's method, may be employed in the future It should be noted that the current implementation of *eigBisect* does not perform a search in range (ie decrease the time step size during the search) or search for multiple eigenrays connecting two points

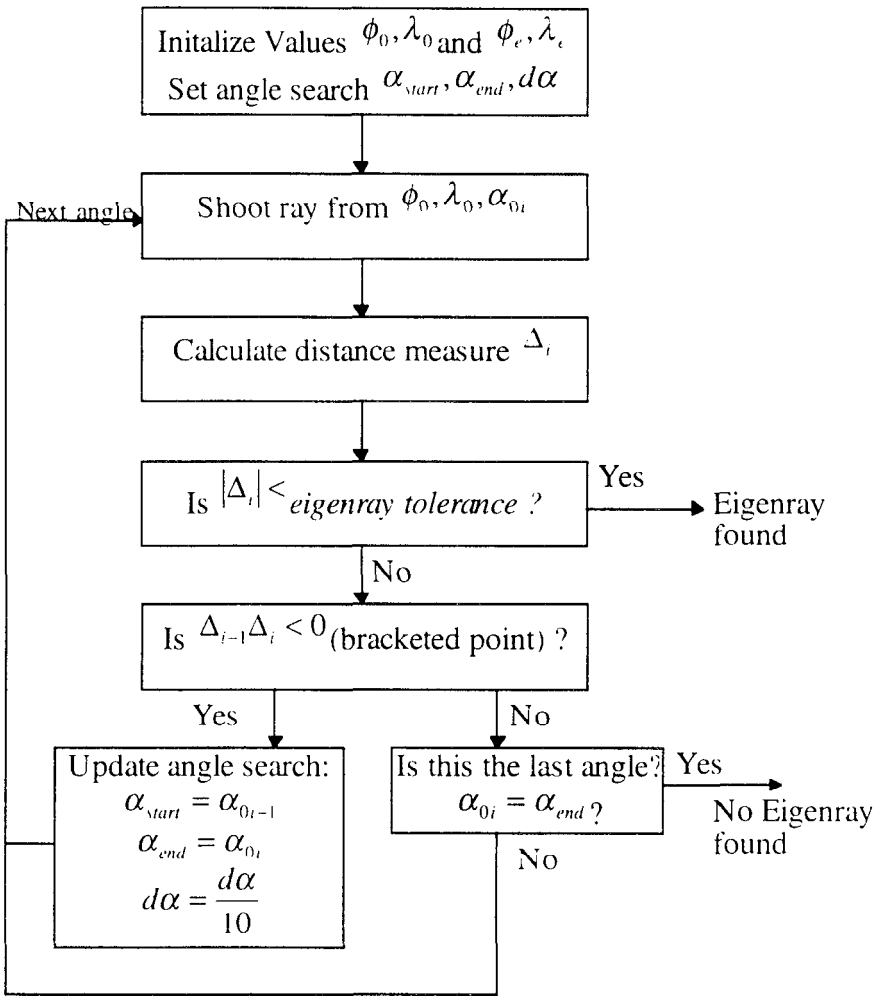

Figure 24: Block Diagram of Function *eigBisect*

Bender

As described in the *Refracted Eigenray* section above, a usual approach to determining ray paths between two fixed points is to use an iterative scheme to perturb the initial launch angle from the starting point until the refracted path passes through the known receiver position. This approach can be computationally intensive in that a large number of rays may need to be traced until an acceptable solution is found. In some cases, particularly when the source and receiver are nearly antipodal, these approaches may fail to converge.

As an alternative, HydroCAM also includes a perturbational approach where the two desired endpoints are fixed and an initial raypath is perturbed until the travel time along the path is minimized. Figure 25 graphically illustrates the difference between the two approaches. A complete derivation of the equations used in this approach is contained in Appendix C.

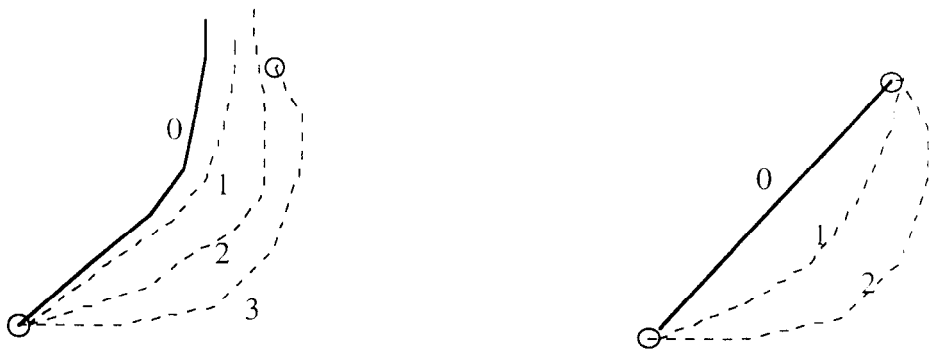

Figure 25: (a) Shooting/Searching Approach, (b) Bender Approach.

The numbers indicate the iteration on each approach. The shooting/searching method in Figure 25 stops when the ray path passes close enough to the desired endpoint. The bender approach stops when the difference between successive iterations of the locations along the entire path are smaller than a user specified tolerance.

Path Characteristics

Once the locus of geographic points along a path is computed using the methods described in the previous section, the travel time, travel time standard deviation and attenuation are calculated along each path.

Travel Time

Travel time is computed using trapezoidal integration to approximate

$$t = \int \frac{1}{u_g(s)} ds,$$

where $u_g(s)$ is the group speed obtained by bilinear interpolation of the best resolution group speed database available at location s. The integral is performed along the entire path and may use variable increments depending on the method of computing the path location and the availability of high resolution phase speed databases along the path. Other than proper selection of *nsave* to provide adequate spatial sampling of the group speed along the path, there are no other user controllable parameters for calculating travel time.

Travel Time Standard Deviation

The travel time standard deviation is an important factor in determining the performance of localization algorithms. There are three methods available in HydroCAM; the percentage model, the path integral model, and the square root model. The path integral model is a trapezoidal integration of

$$\sigma_t^2(r) = \int_0^r dl_1 \int_0^r dl_2 \sigma_s^2(l_1)\rho(l_1 - l_2) \tag{16}$$

where σ_s is the slowness variance calculated using either the channel model of equation (11) or the modal model using equation (12). In either case, the travel time variance depends on the correlation structure of the slowness, which is currently modeled using an isotropic Gaussian correlation function, given by

$$\rho(\Delta l) = e^{-\left(\frac{\Delta l}{L}\right)^2},$$

where L is the correlation scale length in km. Researchers at the Alfred-Wegener-Institute for Polar and Marine Research have analyzed their Southern Ocean Atlas, which contains temperature and salinity measurements south of 30° S, and determined that an appropriate correlation function describing those measurements is a two-dimensional Gaussian function with latitude scale length of 350 km and longitude scale length of 450 km [23]. Since a variety of ocean conditions will produce different anisotropy (such as areas near the Gulf Stream or the Antarctic Convergence), we have assumed the isotropic model, with a default scale length of 300 km. Uncorrelated conditions are selected by setting L = 0, and totally correlated conditions are selected by setting L to a large value (much greater than the length of the longest path).

Simplified models can be obtained by appropriate choice of the correlation function. If the slowness fluctuations are assumed to be completely correlated, then equation (16) becomes

$$\sigma_t^2(r) = r \int_0^r \sigma_s^2(l) dl$$

This equation shows the travel time standard deviation is a linear function of range. Interestingly enough, early efforts in quantifying the location performance of hydroacoustic networks assumed that the travel time standard deviation was a percentage of the range [6]. This option is included in HydroCAM to allow consistency checking with those previous results. The percentage model is

$$\sigma_t(r) = Cr \tag{17}$$

where r is in units of kilometers and typical values for the constant C are from 1 to 5 percent. If the slowness correlation is zero, then the expression for travel time variance in (16) becomes

$$\sigma_t^2(r) = \int_0^r \sigma_s^2(l)dl$$

and the variance is seen to be a linear function of range. In addition, if one represents the correlation structure with a triangle window, the expression in (16) can be reduced to a constant times the square root of range. This "square root" model is used in the IVSEM model under development at Sandia National Laboratories [6],and is included in HydroCAM to facilitate comparisons with IVSEM. If the range r is in units of km, then this model is

$$\sigma_t(r) = C\sqrt{r} \tag{18}$$

where a typical value of C is 0.03

Transmission Loss

Three simple models for transmission loss are provided in GlobeRay. The purpose of these models is to account for the first-order loss mechanisms and provide path attenuation predictions, which are necessary for predicting signal-to-noise ratios and detection performance, without the computational load of more sophisticated models such as RAM The first model is of the form

$$TL(r) = A + B\log(r) + Cr + I(r) \tag{19}$$

where A, B and C are constants and I*(r)* is the integrated modal attenuation along the path. The range r is in units of km and all other terms are in decibels. The first constant, A is sometimes called the *injection* constant. It specifies the energy level measured at 1 km relative to the equivalent source level at 1m For omnidirectional sources in deep water, this loss is the result of spherical spreading, so a nominal value of A is 60 dB At long ranges, B is set to 10 to account for the loss due to cylindrical spreading A and B can be chosen such that a variety of spherical-to-cylindrical spreading transitions situations can be modeled. The constant C (dB/km) accounts for attenuation due to absorption and scattering While very small at the low frequencies of interest, this attenuation can become significant at extremely long ranges For situations where energy is propagating in the SOFAR channel with little bottom interaction, these three terms can provide a reasonable model of the transmission loss Bottom interation is included in the transmission loss by computing the total modal attenuation along the path

$$I(r) = \frac{f}{V_g}\int_0^r atten(l)dl \tag{20}$$

The modal attenuation, *atten(l)* in (dB per wavelength), is found by bilinear interpolation of the modal attenuation grid calculated using equation (9) or (10). The integral in (20) is evaluated using trapezoidal integration, with a variable integration length calculated along the path using

$$\Delta l = \Delta t \cdot nsave \cdot u_n$$

Both the group speed u_n and the phase speed v_n are calculated using bilinear interpolation of the environmental grids. The second transmission loss model in HydroCAM is

$$TL(r) = A + B\log\left[r\sin\left(\frac{r}{R_e}\right)\right] + Cr + I(r), \qquad (21)$$

where R_e is the radius of the earth in km This model replaces the cylindrical spreading term in (19) with another term that accounts for the spherical nature of the earth. On a spherical earth (with no intervening land masses), all energy emitted from a source would *converge* with no loss at the opposite point on the sphere (the antipode). As land masses will remove some of the energy that would converge at the antipode, this second model is generally not used.

The AFTAC version of the transmission loss equation is defined as

$$TL(R) = 22R + 10\log_{10}(7 + 30R) + 10\log_{10}(\sin R) - 35.5$$

where R denotes range measured in geographic degrees The first term represents an absorption factor, the second is essentially cylindrical spreading and the third is a refocussing term.

Since it is unclear as to which model is generally acceptable to the hydroacoustic community, HydroCAM 2.0 provides both a range grid and a boundary attenuation (correction) grid, which includes only the $I(r)$ term These two grids can be used in conjunction with any of the above transmission loss models to provide an estimate of transmission loss They replace the TL grids which were available under version 1.0 An additional advantage of this approach is that various TL models can be tested without recomputing the path locations

In general, the $I(r)$ term in equations (19) and (21) can be thought to include

$$I(r) = L_s(r) + L_f(r) + L_v(r) + L_b(r) \qquad (21a)$$

where L_B includes losses due to the interaction with the ocean bottom (which are obtained by integrating the modal attenuation coefficient calculated by WKB or Kraken along the ray path), L_I is due to ice cover in polar regions, L_S is due to rough-surface attenuation and L_V is due to volume attenuation (absorption). Since L_V is normally accounted for using the C term in equations (19) or (21), and databases of the chemical factors affecting the term are not readily available, this term is set to zero in equation (21a) The L_I and L_S terms are new components included in HydroCAM version 2 0 The following two sections discuss these terms.

Ice Cover Attenuation

In polar regions where the ocean is covered with ice, the attenuation due to repeated surface interactions can dominate all other losses and result in the termination of acoustic paths. The magnitude of the loss is a complicated function of the ice cover characteristics (such as roughness, mean depth and ice composition), the frequency, and the grazing angle. Since detailed databases of the relevant ice characteristics are not available (and the nature of the ice cover can change from year to year), a first-order model based on results from ONR experiments performed in the central Arctic is used [29] These experiments directly measured the mode 1 ice cover attenuation as a function of frequency, as shown in Figure 26 The ice cover model employed in HydroCAM is a linear interpolation of the data shown in this figure between 10 Hz and 200 Hz.

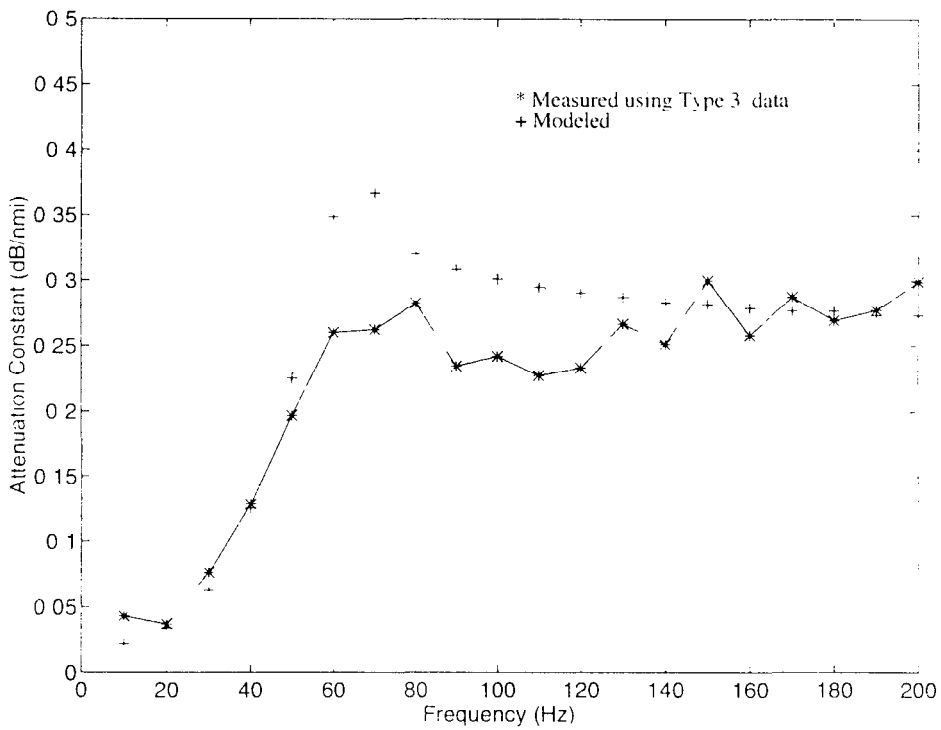

Figure 26: Measured and Modeled Attenuation Constant Vs Frequency from [29]

Now that the ice cover attenuation model has been selected, a choice for when and where to apply these losses must be made. The best available ice cover extent data seems to be the databases provided by the National Ice Center which are derived from the Defense Meteorological Satellite Program (DMSP). This database, which is updated monthly via the internet, contains ice cover extent for the northern and southern hemisphere on a polar stereographic grid (See Figure 27 and Figure 28). This database has been translated to a single lat/lon grid and integrated into HydroCAM, such that when raypaths traverse an area where ice is present, the loss derived from Figure 26 is applied.

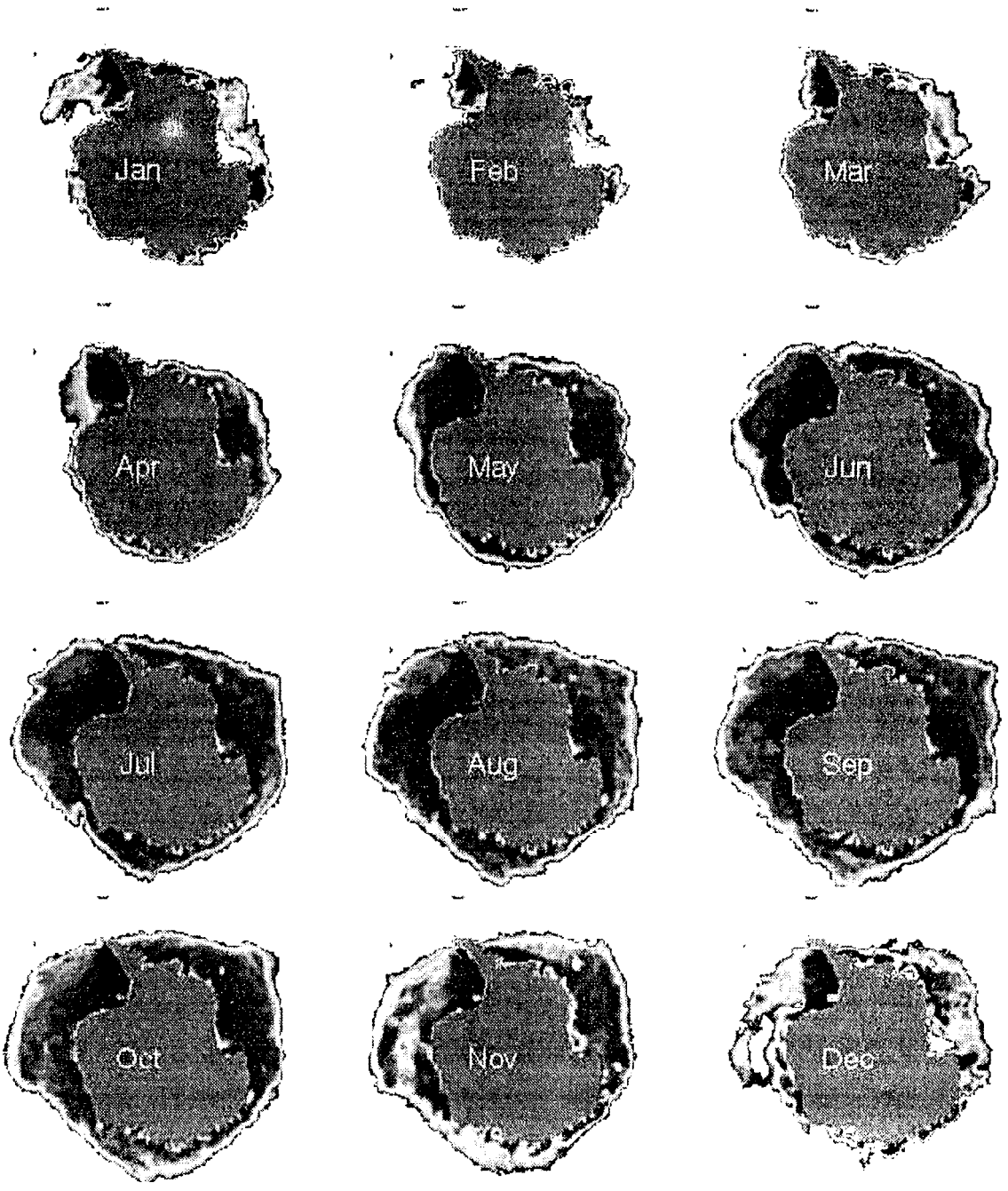

Figure 27. 1996 Southern Hemisphere Ice Cover Extent Measured by DMSP Satellite

Figure 28: 1996 Northern Hemisphere Ice Cover Extent Measured by DMSP Satellite

Rough-Surface Attenuation

Several models for the rough-surface propagation loss were investigated [28]. These models were used to calculate the magnitude of the loss for several wind speeds and several seasons. The results indicated that in mid-latitude and equatorial regions (which typically have a deep SOFAR channel), the surface loss is at least five orders of magnitude less than the ice cover and bottom losses already contained in HydroCAM. The loss is also at least an order of magnitude smaller at high latitudes, except under worst-case situations (such as local winter where the sound speed profile in high-latitude regions is strongly upward refracting *and* high 40 knot wind speeds are present). However, large areas where these conditions are present will be ice-covered, so that the rough-surface loss term would not need to be included. Due to the results of this study, we have decided not to incorporate the rough-surface model into the raytrace software at this time.

Path Stop Conditions

In addition to the conditions which terminate the path location calculations (see the *Path Location* section), there are other conditions that are used in GlobeRay to terminate paths. (See the GlobeRay functional diagram in Figure 20). These rules are used as a simple method for determining when significant (ie detectable) energy will pass bathymetric features that may be partially or completely blocking the SOFAR channel. Figure 20 shows that these conditions are applied as soon as possible to save calculations. The options are listed in Table 7

Table 7: Summary of Path Stop Conditions in GlobeRay

Condition	Description	Typical Value
Maximum Range	Used in Path Location function	30,000 km
Past End Point	Used in Path Location function	N/A
Max Atten	Maximum integrated boundary attenuation (bottom + ice cover losses) as calculated by equation (20)	40
Min Depth	Path terminated if depth is less than this value Usually used to approximate modal cutoff conditions	50
Bottom Blocks Channel	Path terminated if the bathymetry is shallower than the channel depth provided in the channel database	N/A

Detailed Vertical Environment, Mode Structure and TL along paths

There are several situations where the simplified transmission loss models contained in GlobeRay are insufficient. Examples include situations when the detailed effects of source characteristics on network performance or the nature of the arrival structure are required; when the effects of bathymetry on loss mechanisms are needed, and when the modal conversion due to bathymetric interaction is required. In these situations, the paths predicted by the path models are used to investigate the detailed structure of the vertical plane along the path. Figure 29 shows a block diagram of the procedures available

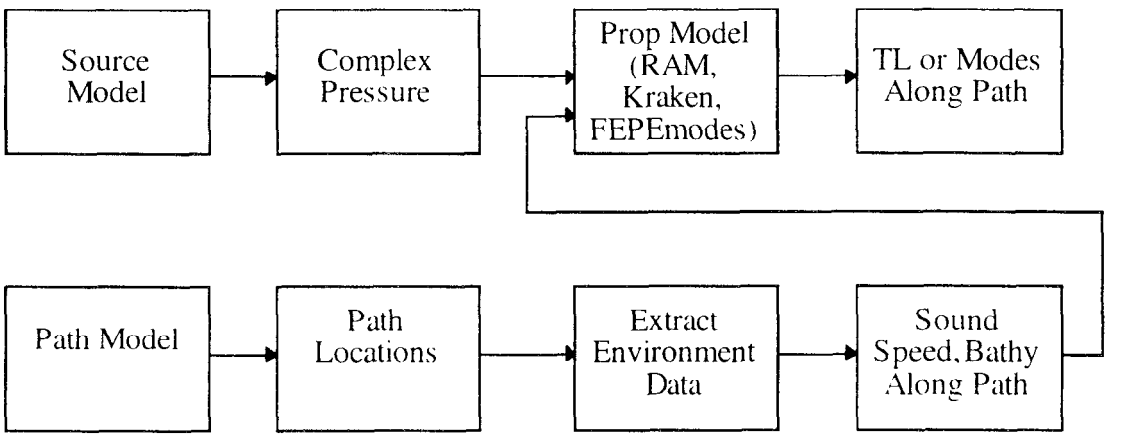

Figure 29. Detailed Analysis of Vertical Plane Along Paths

DOE funded research at LLNL and NRL has produced a combined hydrodynamic and non-linear acoustic model of the pressure signature from underwater and low-atmosphere nuclear bursts called CALE/NPE [3]. The source function is provided as pressure time series vs depth at a range where the acoustic propagation becomes linear (typically about 10 km from the burst). HydroCAM reads these files and calculates the complex pressure over a cylindrical surface in the water column as a function of depth and frequency This data is used as a "starter field" for the linear propagation model, i.e. the complex pressure is the input to a range dependent propagation model which estimates the complex propagation transfer function, and hence transmission loss (TL) at multiple frequencies along selected bearings from the event position The result is the estimated received spectral level, for each frequency, to any selected range and depth along these radials The principal development effort for the source portion of HydroCAM was to couple the source functions produced by this model to the linear acoustic propagation models contained in HydroCAM This interface required modification of the RAM source code to read in the starter field from a file which is created by HydroCAM

Example output products from this analysis are shown in Figure 30 After the path model is run to determine the horizontal trajectories, environmental data can be extracted

along the path(s) using any of the available sound speed and bathymetry databases. The sound speed profiles along a path from Ascension Island are displayed in Figure 30(a). The sound channel depth is overlayed on this data using a thick solid line. Section (b) of this figure shows the transmission loss at 20 Hz along the same path as calculated by RAM. Section (c) shows the received level from a 1kT explosion at 50m depth. This option must be used with care as there are many technical details which affect the results as discussed in the HydroCAM Final Report [9].

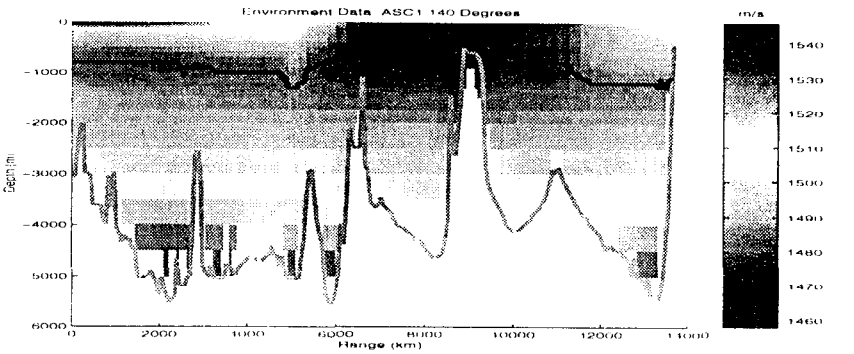

(a)

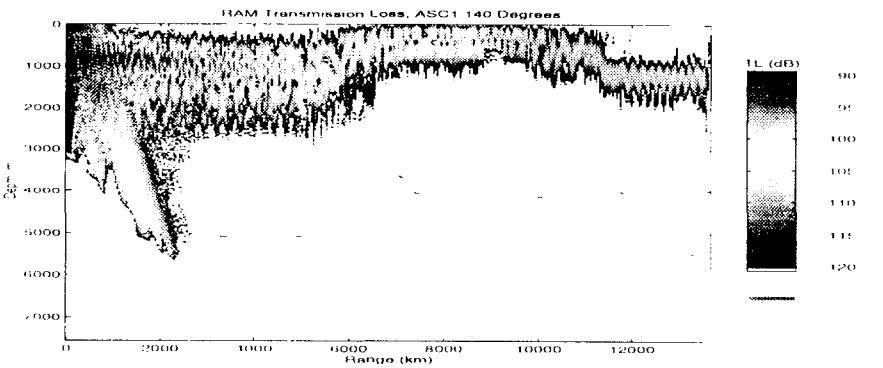

(b)

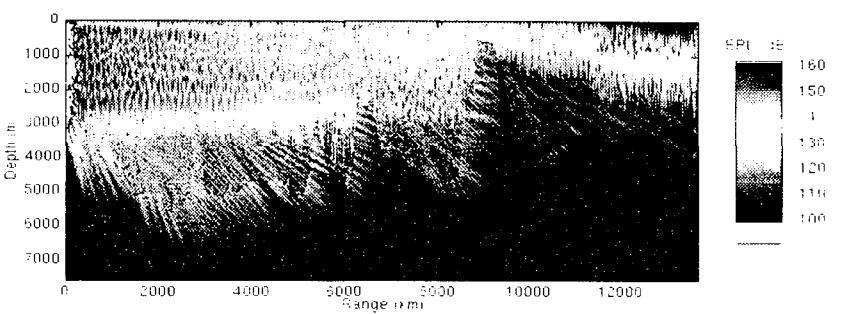

(c)

Figure 30: Detailed Vertical Plane Analyses (a) Sound Speed and Bathymetry Along Geodesic Path from Ascension Island at 140 Degrees Azimuth, (b) Transmission Loss at 20 Hz Predicted with RAM, (c) received level from 1kt explosion at 50m level.

Network Performance Prediction

The network performance prediction software uses the outputs of the path model, source model and receiver models to determine the detection and localization performance of the network as a whole. These calculations are performed in the C++ program HydroNET. This section of the *HydroCAM Users Guide* describes issues concerning path interpolation needed before network performance can be determined, the calculation of detection performance using the signal-to-noise ratio, and calculations of the location Area of Uncertainty (AOU). Figure 31 shows a block diagram of the network performance model.

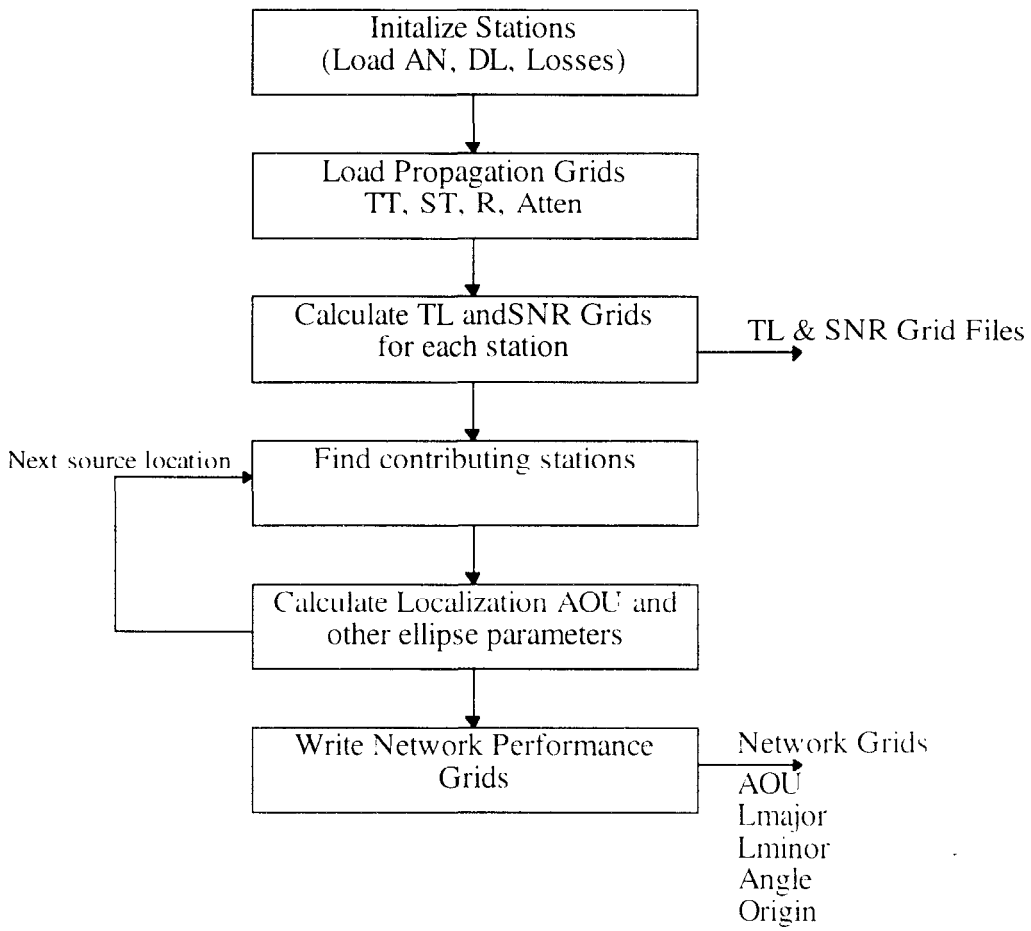

Figure 31: Network performance model

Measurement Grids and Path Interpolation

A common method of predicting acoustic coverage is to run a propagation model along a set of radials emanating from a source or receiver. An illustration of the radials used for two receivers is provided in Figure 32

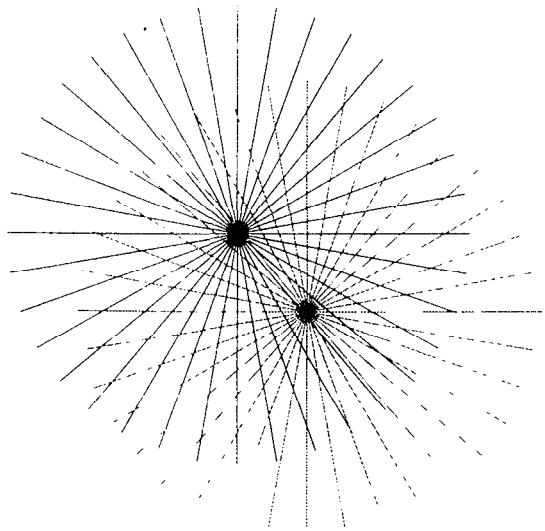

Figure 32: Star Scenario for Two Receivers

The figure shows that when path characteristics are needed from a common point to many receivers, two-dimensional interpolation will be required. If a robust interpolation procedure can be identified, it is likely that a significant amount of computation could be saved by using Star scenarios for each receiver and interpolating onto a common grid versus directly calculating a large number of eigenrays required for a grid scenario. HydroCAM provides a capability for analyzing the effectiveness of number of path-to-grid interpolation procedures

The available interpolation methods are: quantize, nearest, average and weighted. When *quantize* is selected, HydroCAM loops through each point on each path and places each data value into the grid cell that contains the point The last data value placed into the grid cell is used.

When *nearest* is selected, HydroCAM calculates the distance (in latitude and longitude space) between each point on each patch and all of the grid cell locations The data value closest to each grid cell center is used for that cell.

The *average* method collects all path data points that fall inside a grid cell. The average of these points is used

Weighted uses the "inverse distance" method of interpolation [24]. All path data points are collected that fall inside a grid cell The returned value is an average weighted by the inverse of the distance between the cell center and the path location If p is the collection of indices of the path points contained in the grid cell, then the returned value is given by

$$value = \frac{\sum_{i \in p} \frac{z_i}{(d_i)^w}}{\sum_{i \in p} \frac{1}{(d_i)^w}}$$

where zi is the data value of the ith path point, w is a user selected weighting factor. The term di is the "distance" measure defined as

$$d_i = abs(\phi_i - \phi_b) + abs(\lambda_i - \lambda_g)$$

where the subscript g indicates grid cell as opposed to path location.

Several tests were made using each of these methods comparing interpolated geodesic paths to geodesics on a uniformly spaced grid. The results using each of these four methods exhibited substantial errors and the methods were determined to be inadequate to accurately produce the propagation characteristic grids delivered to AFTAC [28] Thus, an alternate approach to the interpolation procedure was considered This approach is contained in a C++ software program called PathToGrid which is distributed with HydroCAM 2 0. A block diagram of the program is shown in Figure 33.

The basic interpolation problem is to compute the values of travel time, travel time standard deviation, range and attenuation at the center of each grid cell from a set of points non-uniformly spaced throughout the cell The non-uniform spacing of the points is primarily a result of the radial sampling of the ray paths shot from a station location. This sampling is then complicated by the ellipsoidal nature of the earth, the effects of horizontal refraction, multipath and blockage from land masses Of the quantities to be computed, travel time is the most difficult, since we usually require accuracies on the order of 1 second (out of 10000 seconds) Under the first order assumption that the travel time varies linearly with distance along a ray path, a reasonable approach is to perform a least mean squares estimate to a plane containing the points in the geographic cell Here, the x- and y-coordinates of the plane correspond to the longitude and latitude of the cell points, and the z-coordinate corresponds to travel time (or travel time standard deviation, range, attenuation, etc). Once the equation of the plane has been determined, the z-coordinate of the cell center is readily computed given its latitude and longitude

Special processing is necessary for three cases, locations where there is an over-abundance of points (such as in the near field close to the receiver or in high resolution areas), places where the points are sparse (such as in the far field near the end of rays), and multipath In the former case, only the points which are closest to the center of the cell are used to obtain the least squares estimate; in the second case, several points are artificially added to the cell prior to the interpolation process.

Finally, the path-to-grid interpolation procedure accounts for multipath. Rays within a cell which arrive from different directions may exhibit markedly different travel times and transmission loss. The degree to which these quantities vary within a particular cell is a function of the specific path geometry and depends on the path length and whether or not the paths interacted with islands or other land masses. If a cell contains multipath rays, certain assumptions need to be made concerning which path(s) are chosen as input to the lms algorithm in order to obtain a reasonable estimate of the propagation parameters. A primary concern is to choose the paths which are the strongest (least attenuation) and/or arrive first (least travel time). The following approach is used to detect the presence of multipath within a cell, and to determine which paths should be used as input to the interpolation procedure:

1) Sort rays in a given cell by launch angle from the receiver station.

2) Separate rays into groups (successive rays having launch angles that differ by more than 1° belong to different groups).

3) Sort groups of rays by (average) TL.

4) Retain only those groups of rays for the strongest arrivals (groups having 1 dB more of transmission loss than the previous group are eliminated from the interpolation process).

Several studies have been performed to verify the accuracy of this interpolation procedure [28] The results indicate that with a large number of paths (about 1 path launched every 1/4 degree) that path characteristics can be interpolated onto a 1 degree lat/lon grid with accuracies better than 0 1 sec for travel time and 02 dB for attenuation. [28]

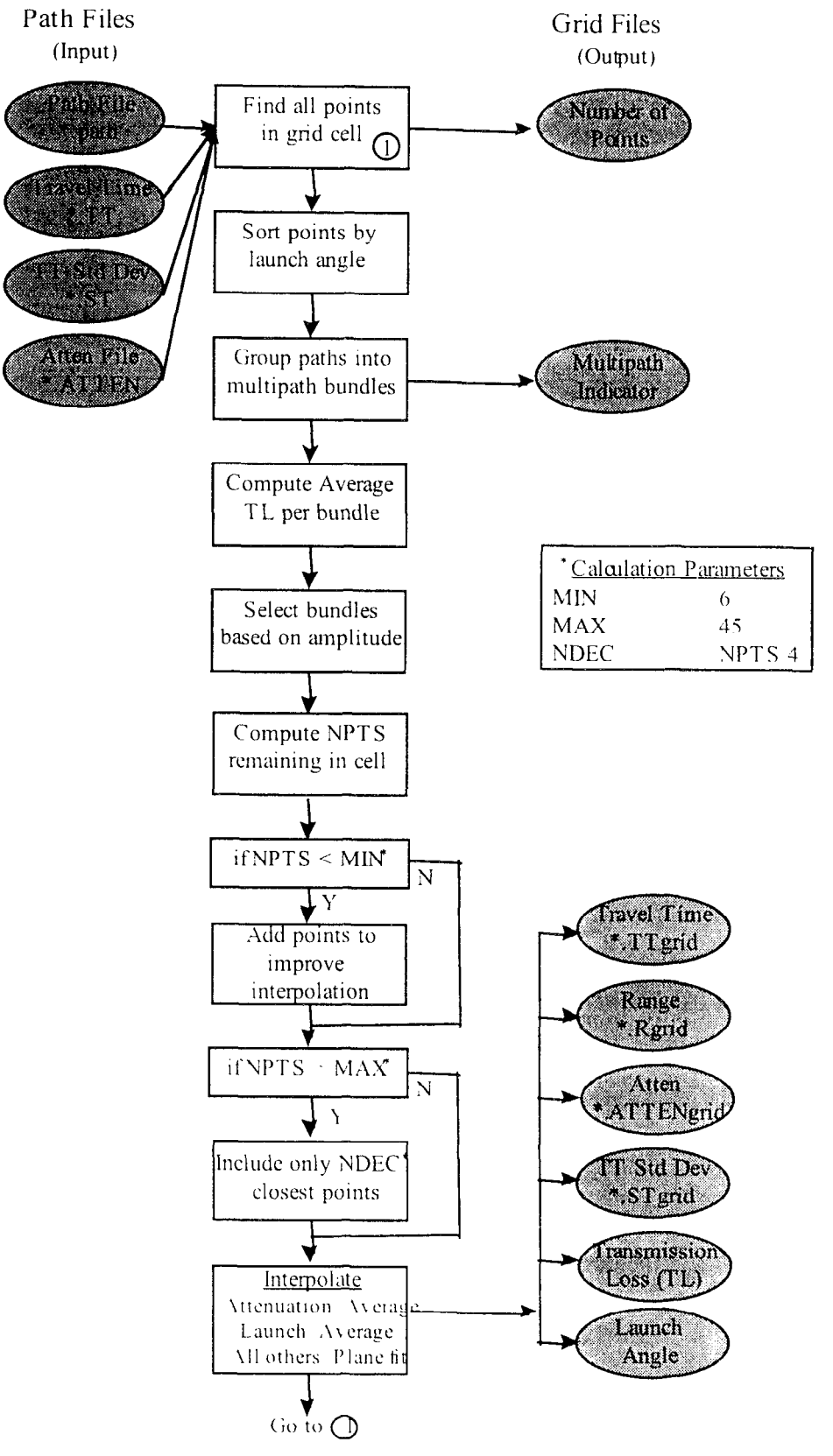

Figure 33: Path To-Grid Interpolation Process

Detection Performance

The performance of a monitoring network is described in terms of the ability to detect and locate sources. One measure of detection performance is the signal to noise ratio (SNR). SNR is usually defined as the peak value of the receiver output relative to the background level, and may be calculated for a complete event or for a single component phase. It can be related to a number of other performance metrics, such as detection probability and arrival time accuracy. However, since the transformation into detection probability requires a model for the receiver output statistics and specification of a detection threshold which are not currently available, HydroCAM does not compute probability of detection.

SNR Model

HydroCAM uses a spectral model in which the SNR is evaluated in a 1 Hz band centered at a given frequency *f*. Even though broadband detection processing may be used in operational monitoring systems, a narrowband model was chosen since the calculations required to predict the path attenuation (mode calculations for the phase speed and group speed grids, path calculations and transmission loss calculations along the paths) are all computationally intensive and are a strong function of frequency. Reasonable, if conservative, detection coverage maps can be obtained by running narrowband SNR predictions near the frequency where the source energy is a maximum. Additional suggestions for approximating the broadband detection performance are provided at the end of this section. The SNR model is derived using an energy form of the SONAR equation

$$SNR(f) = ESL(f) - TL(f) - (NL(f) + 10 \log T) + AG(f) - L(f) \qquad (22)$$

ESL is the energy spectral level of the source (*dB re uPa^2 sec*) at a reference distance of 1 meter in a 1 Hz band. This value is either calculated from the pressure time series files (see the *Source Models section)* or is provided as a user specified input to the model. Since the pressure time series is often produced at ranges greater than 1 meter (typically 10 km for the CALE NPE source model), a correction factor can be applied to scale the ESL to an "equivalent" range of 1m.

TL is the transmission loss (path attenuation) expressed in dB relative to the energy level at 1 meter. It is computed using the path attenuation model contained in GlobeRay or a more detailed propagation model such as RAM.

The remaining terms are included in the data files describing the capabilities of each receiving station. A complete description of the use and format of these data files is provided in the *Receiver Models* and the *Receiver Form* sections. The noise power spectral level, *NL* (dB re μPa^2 in a 1 Hz Band) is stored as a function of frequency and

azimuth in the receiver ambient noise file AG is receiver spatial processing (array) gain, which is included in the "directionality file" L is the "system loss factor" which contains all processing gains and losses not accounted for elsewhere. L is typically used to include the SNR loss of island seismic stations compared to hydroacoustic stations T, the receiver integration time in seconds, must be set to a value that is at least as large as the time duration of the expected received signal. Equation (22) shows that T effectively converts the noise *power* from the ambient noise model into the noise *energy* which is included in the data during the integration time. T and L are both included as a function of frequency in the receiver "system loss file". The decision to include the integration time in the "system loss file" was made to allow receiver specific integration times which can change as a function of frequency.

As shown in the block diagram of the network performance model (Figure 31), equation (22) is evaluated separately for each receiver. A "hypothesized" source is placed at each desired location in the coverage map (usually a regular grid obtained through a grid scenario), and the SNR is calculated using equation 22. The transmission loss grids calculated by GlobeRay are used without interpolation to calculate the TL for each source location. Noise level and array gain are determined by using the input frequency and the launch angle grid to interpolate the respective tables. Linear interpolation is used in azimuth, while logarithmic interpolation is used for frequency.

The SNR grids may be used individually to display the detection coverage of each receiver or combined to compute the performance of the hydroacoustic network as a whole. Many related data products are available, including geographic plots of the following:

- SNR for a specific receiver, corresponding to different event locations (for evaluation of existing assets)
- SNR for a specific event location, yield and depth/height for various receiver locations (for evaluation of alternative locations for new sensors).
- The minimum SNR seen by all receivers in the network
- The Mth largest SNR value seen by the network
- The number of receivers receiving the event above a specified SNR threshold The interpretation of this option is discussed in the *Contributing Receivers* section below.

Since the path model can be run for each mode (if phase and group speed grids have been computed for each mode), the SNR can be computed for each mode Note that the propagation grids produced by the model contain the path characteristics for a *single* path for each mode (ie horizontal multipath is not included)

A broadband model could be obtained by calculating each term in equation (22) over a range of frequencies, and numerically integrating the source terms over frequency and receiver terms over frequency In cases where the terms in equation (22) are not expected

to vary over the band, the narrowband SNR numbers obtained are identical to the broadband SNR since the effect of increasing the bandwidth on the received signal energy and noise energy cancel.

Contributing Receivers

For reasons mentioned previously, HydroCAM does not predict the probability of detection. However, there is a need to make a detection decision based on the predicted SNR; both for the production of detection coverage maps and for determining when arrival time measurements can be made for use in localization algorithms. HydroCAM uses a user specified SNR threshold to make this detection decision. If the signal plus noise statistics are known, then this threshold can be set to obtain a specified probability of false alarm and probability of detection using standard formulas from detection and estimation theory [25] When the SNR threshold is used to determine which receivers detect the source and can make accurate arrival time estimates which contribute to a localization solution, the receivers exceeding the threshold are called *contributing receivers* HydroCAM produces a grid on the number of contributing receivers for each source location. Depending on the choice of threshold, this grid can be used as a network detection coverage map, or as a tool to understand the contributions of each receiver in the network to the localization performance.

Localization Performance

Localization performance is measured using the area of uncertainty (AOU), which summarizes the effect of all the uncertainties in the localization calculation, including propagation model uncertainties The AOU model in HydroCAM assumes that the localization algorithms use arrival time measurements of one specific phase at multiple receivers, and that these measurements are statistically independent Additional measurements, such as bearing, can be readily added to the AOU model The size of the AOU is a function of the accuracy of the travel time model, the ability to correctly measure the arrival time of the modeled phase, and the sensor-event geometry. The effects of sensor geometry can be investigated by simply changing the source and receiver locations The accuracy of the travel time model is included through the travel time variance calculations described in the *Path Characteristics* section above Measured sound speed statistics are included in the travel time variance calculations by using a perturbation model for the slowness variance of propagating modes (See Appendix B). Measurement uncertainties, which depend on signal-to-noise ratio and the specific signal shape, are currently modeled parametrically, as an independent "picking" error added to the travel time error More sophisticated models of measurement uncertainties will be included in the future if necessary

The primary output products of the localization model are geographic plots of the AOU and a specialized display format showing contributing receivers and path characteristics

for a particular source location. This section summarizes the calculations performed in HydroCAM for predicting the AOU. A complete derivation of these equations is provided in Appendix D for reference.

AOU Calculations

The AOU calculations are performed in three stages. In the first stage, the propagation conditions (transmission loss, travel time and travel time standard deviation) are calculated from a set of source locations (typically on a grid) to each receiver in the network using GlobeRay. In the second stage, which is shown in the block diagram in Figure 31, "Normalized" network performance parameters are calculated using the software program HydroNET. The last set of calculations occurs when the user requests a display of an AOU map or concentration ellipses. These items are calculated from the "normalized" performance parameters in the MATLAB display software.

Normalized Network Parameters

At each source location, the normalized network performance parameters are calculated using the following information:

- Source geographic coordinates in radians, $[\phi \quad \lambda]$
- List of contributing receivers
- Locations of the contributing receivers $\{\phi_i \lambda_i \; i = 1,2,\ldots N\}$
- Predicted travel time and travel time variance grids for each of these receivers

A block diagram of the calculations is shown in Figure 34

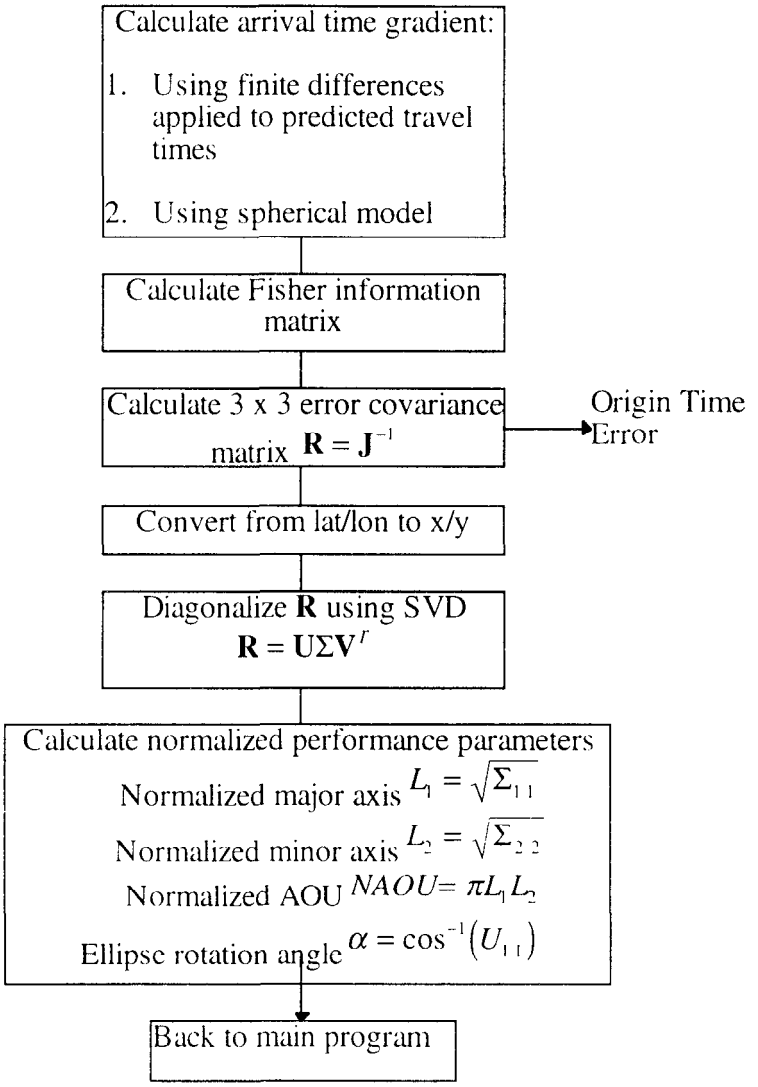

Figure 34. Calculation of Normalized Network Performance Parameters

For each source location, a source state vector **s** can be assembled

$$\mathbf{s}^T = [\phi \quad \lambda \quad t_o]$$

which contains the source latitude ϕ, longitude λ and origin time t. The first step is to calculate the gradient of the arrival time $h_i(s)$ with respect to the source state vector

$$\nabla_s\left(h_i(\mathbf{s})\right) = \begin{bmatrix} \dfrac{\partial h_i(\mathbf{s})}{\partial \phi} \\ \dfrac{\partial h_i(\mathbf{s})}{\partial \lambda} \\ \dfrac{\partial h_i(\mathbf{s})}{\partial t_o} \end{bmatrix} = \begin{bmatrix} \dfrac{\partial f_i(\mathbf{s})}{\partial \phi} \\ \dfrac{\partial f_i(\mathbf{s})}{\partial \lambda} \\ 1 \end{bmatrix}, \tag{23}$$

where the subscript i indicates the *ith* receiver and the function $f_i(\mathbf{s})$ is the travel time from a source at $\mathbf{s}$ to the *ith* receiver. Two methods for evaluating equation (23) are available: (1) using finite differences, calculate the latitude and longitude derivatives using the predicted travel time grids from the propagation model, or (2) use an analytic expression derived from a simple spherical earth model of the travel time (See Appendix D for the derivation)

$$\nabla_s\left(h_i(\mathbf{s})\right) = \begin{bmatrix} \dfrac{\mathrm{Re}}{c\sin(\theta_i)}\left(\cos\phi_i \sin\phi \cos(\lambda - \lambda_i) - \cos\phi \sin\phi_i\right) \\ \dfrac{\mathrm{Re}}{c\sin(\theta_i)}\left(\cos\phi_i \cos\phi \sin(\lambda - \lambda_i)\right) \\ 1 \end{bmatrix}. \tag{24}$$

The Fisher information matrix is then computed using the gradient from each contributing receiver

$$\mathbf{J} = \sum_{i=1}^{N} \frac{1}{\sigma_i^2}\left(\nabla_s h_i\right)\left(\nabla_s^t h_i\right). \tag{25}$$

The variance in equation (25) is the total arrival time measurement error, which is obtained by assuming that the travel time variance σ_m^2 and the picking error σ_{pi}^2 are independent

$$\sigma_i^2 = \sigma_m^2 + \sigma_{pi}^2$$

The ability of the localization algorithm to estimate the source state vector is given by the 3 x 3 source state error covariance matrix **R**, which contains the variances of the source latitude, longitude and origin time estimate. The covariance matrix is computed by inverting the Fisher information matrix

$$\mathbf{R} = \mathbf{J}^{-1} = \begin{bmatrix} \sigma_\phi^2 & \sigma_{\phi\lambda} & \sigma_{\phi t_0} \\ \sigma_{\phi\lambda} & \sigma_\lambda^2 & \sigma_{\lambda t_0} \\ \sigma_{\phi t_0} & \sigma_{\lambda t_0} & \sigma_{t_0}^2 \end{bmatrix}. \tag{26}$$

The origin time error $\sigma_{t_0}^2$ is saved into the Origin grid file. Although the spatial estimation error is given by the top 2 by 2 submatrix of **R**, the AOU cannot be calculated directly from (26) because these variances are in units of radians, and the AOU is required in square kilometers. The mapping between lat/lon and x/y in km depends on latitude. The arc length in the east-west (x) direction and north-south (y) direction between two points separated in angle by $\Delta\phi, \Delta\lambda$ on a sphere is approximately

$$x = \mathrm{Re}\ \cos(\phi)\Delta\lambda$$
$$y = \mathrm{Re}\cdot\Delta\phi.$$

This relationship shows that the covariance matrix can be transformed into the appropriate units using

$$\mathbf{R}_{xy} = \begin{bmatrix} \sigma_x^2 & \sigma_{xy} \\ \sigma_{xy} & \sigma_y^2 \end{bmatrix}, \tag{27}$$

where

$$\sigma_x^2 = R_e^2(\cos^2\phi)\sigma_\lambda^2 \tag{28a}$$
$$\sigma_{xy} = R_e^2(\cos\phi)\sigma_{\phi\lambda} \tag{28b}$$
$$\sigma_y^2 = R_e^2\sigma_\phi^2 \tag{28c}$$

If the arrival time errors are Gaussian, then contours of constant probability are ellipses given by

$$\begin{bmatrix}\Delta x & \Delta y\end{bmatrix}\mathbf{R}_{xy}^{-1}\begin{bmatrix}\Delta x \\ \Delta y\end{bmatrix} = C^2 \tag{29}$$

where the constant C depends on the desired probability contained inside the ellipse. Diagonalizing the matrix using Singular Value Decomposition (SVD) into

$$\mathbf{R}_{xy} = \mathbf{U}\Sigma\mathbf{V}^t \tag{30}$$

rotates the error ellipse until the major axis is aligned on a new x-axis and the minor axis is aligned on a new y-axis. (See Figure 35). The parameters describing the error ellipse can now be derived using equations (29) and (30). The major and minor axis lengths (a and b respectively) are related to the (1,1) and (2,2) elements of the diagonal matrix Σ by

$$a = C\sqrt{\Sigma_{11}} \tag{31a}$$

and

$$b = C\sqrt{\Sigma_{22}}. \tag{31b}$$

The area of the ellipse is simply

$$AOU = \pi ab \tag{32}$$

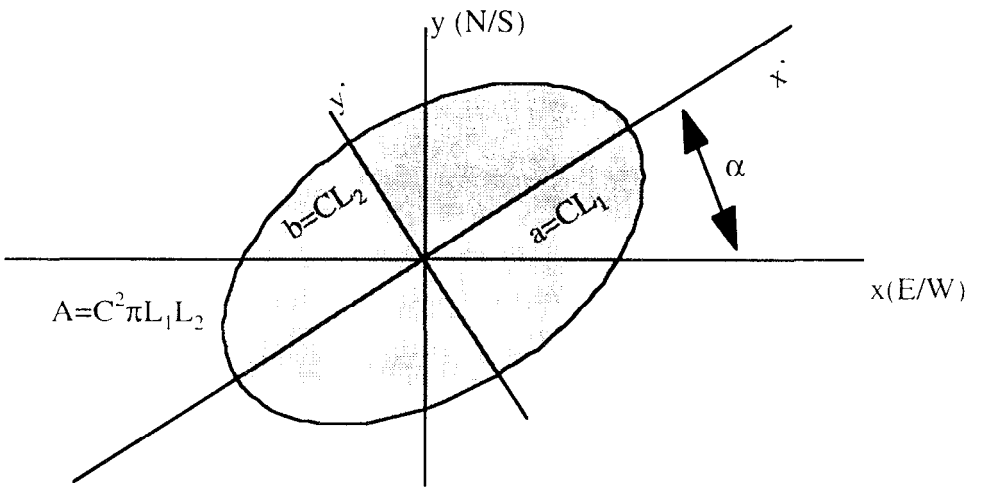

Figure 35. Location Error Ellipse

The *normalized* major axis length, L_1, minor axis length, L_2, and area of uncertainty, AOU', are computed using equations (31) and (32) with the constant $C = 1$. This normalization allows the AOU and ellipse to be calculated and displayed for different values of C (and therefore different confidences) without recalculating many of the previous equations. The normalized parameters are saved to grid files after all source locations have been completed. The only remaining parameter, which is also saved in an output file, is the ellipse rotation angle, α. Since the matrices **U** and **V** in equation (29) are rotation matrices, α can be determined from any of the elements in these matrices. In HydroCAM, the angle is calculated using

$$\alpha = \cos^{-1}(\mathbf{U}_{11}) \tag{33}$$

Although the coordinates of the ellipse could be calculated directly from (29), the parametric representation of the ellipse in polar coordinates is a more convenient method. The required parameters could be calculated using standard formulas applied to the covariance matrix. However, use of the SVD will allow the extension to higher dimensional cases without major software changes.

Calculation and Display of the AOU and error ellipse

The display software in HydroCAM can produce a number of localization performance output products such as geographic displays of the origin time uncertainty and geographic displays of each of the error ellipse parameters. In addition, the error ellipse for any selected source location can be analyzed using the display format shown in Figure 36. The data required for these displays is generated from the normalized performance parameter grids produced by the network performance model.

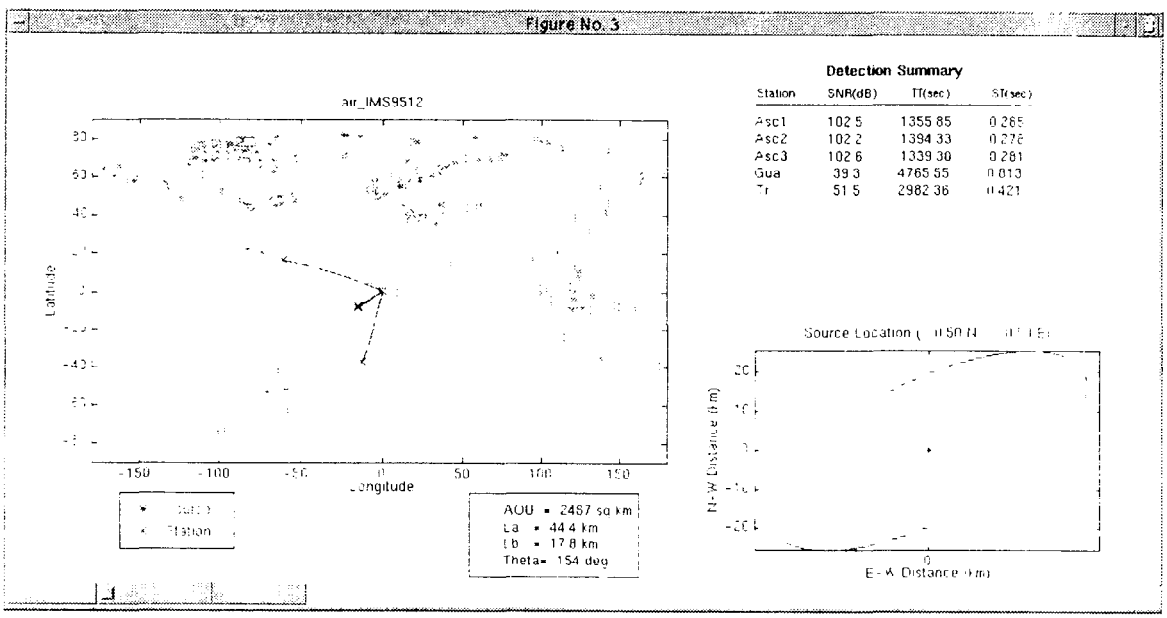

Figure 36: Example Error Ellipse Analysis Display

First, the user selects a desired AOU probability, P. The concentration parameter C is then calculated such that probability that the true localization solution lies within the error ellipse is P. The defining relationship is (See Appendix D)

$$1 - P = \exp\left(-\frac{C^2}{2}\right), \tag{34}$$

After the normalized performance parameter grids are read, the actual ellipse parameters are calculated using C from equation (34) and equations (31) and (32).

If a display of the error ellipse has been requested, then the locus of points on the ellipse in the rotated coordinate space x', y' is calculated using

$$x' = CL_1 \cos\theta$$

and

$$y' = CL_2 \sin\theta$$

where 360 values of θ are used, evenly spaced between 0 and 2π. The ellipse is rotated into x/y (east/west) space according to

$$x = x'\cos\alpha - y'\sin\alpha$$

and

$$y = x'\sin\alpha + y'\cos\alpha$$

and displayed on the bottom right of Figure 36. The ellipse shown on the geographic display is generated by calculating the range and bearing of each point from the source location and using the geographic routine *geod_forwd* to compute latitude and longitude.

Using HydroCAM

HydroCAM consists of a collection of environmental databases, acoustic propagation models, network detection and localization performance models, and graphical user interface software for running the models and displaying the results. The software programs included in HydroCAM are listed in Table 8 below This section of the Users Guide describes how to setup and run each portion of the model A separate set of instructions for installation is available in *Installation Notes for HydroCAM version 2.0.*

Table 8: Software programs contained in HydroCAM

Program Name	Language	Description
HydroCAM	Various	The entire collection of programs and interface software
DBTool	MATLAB	Environmental database access software now incorporated in HydroCAM
WaveGuide	C++	Calculates derived databases
Kraken	Fortran	Calculates modal eigenvalues and mode functions
WKB	C/C++	Calculates modal eigenvalues and mode functions
MakeGridDB	C++	Collects waveguide outputs and produces geographic grids of phase, group, atten and slowness variance
GlobeRay	C++	Calculates refracted and geodesic paths, travel time, travel time variance and attenuation.
HydroNET	C++	Network performance model, calculates SNR and AOU
RAM	Fortran	Calculates transmission loss versus range and depth along a path
Path to Grid	C++	Interpolates from raypaths into lat/lon grid

Version 2.0 of the software distribution is provided with executables that run under *Solaris 2.5* or higher The following configuration is recommended:

Workstation running UNIX, with X-Windows software
MATLAB Version 5.1 or higher
2.2 GB Disk space for all environmental databases and software
At least 500 MB disk space for analysis results
At least 64 MB RAM

HydroCAM has been developed and tested with the following compilers

Sun SPARCompiler FORTRAN 3.01
GNU C compiler version 2.7.2.3
GNU C++ compiler version 2.7.2.3

Data Products

Figure 37 shows a block diagram of the functional components of HydroCAM. The variables listed in the rightmost column are each available as output products for display or as data files for additional manipulation. The text below each box indicates the toolbar option that is used to calculate and/or display the data contained in the box. A description of each of these "forms" is provided in *Description of the Tools*

Getting Started

Before getting started, make sure that your system administrator has installed the HydroCAM software using the instructions outlined in *Installation Notes for HydroCAM Version 2.0.* Log into a users account, and make sure that you have an X-window capability running. Verify that the following environment variables are set:

Variable	*Description*	*Example*
HYDROHOME	top level HydroCAM directory	/export/home/hydro
HYDRO	top level HydroCAM matlab source directory	/export/home/hydro/matlab
HYDRODB	top level HydroCAM databases directory	/hydro1/databases
SGRIDPATH	colon delimited path list for grid database files	/hydro1/databases/hydroCAM
MATLABPATH	colon delimited path list used by MATLAB to look for source files	see table below

These variables must be defined in your *~/.cshrc* file so that they are set every time a new process is started. These variables specify the directories where HydroCAM looks for source code, configuration files, MATLAB source files and environmental databases. The *MATLABPATH* variable should include all of the directories in the table below in the same order as they appear in the table.

Directory	Contents
$HYDRO/html	on-line help files
$HYDRO/dbtool	environmental database access software
$HYDRO/hydroCAM	hydroCAM gui software
$HYDRO propagation	interface software for propagation models
$HYDRO utils	general MATLAB utilities
$HYDRO/oceans	oceans toolbox from WHOI
$HYDRO/mathworks_names	name collision software
$HYDRO/mex	compiled software callable from Matlab

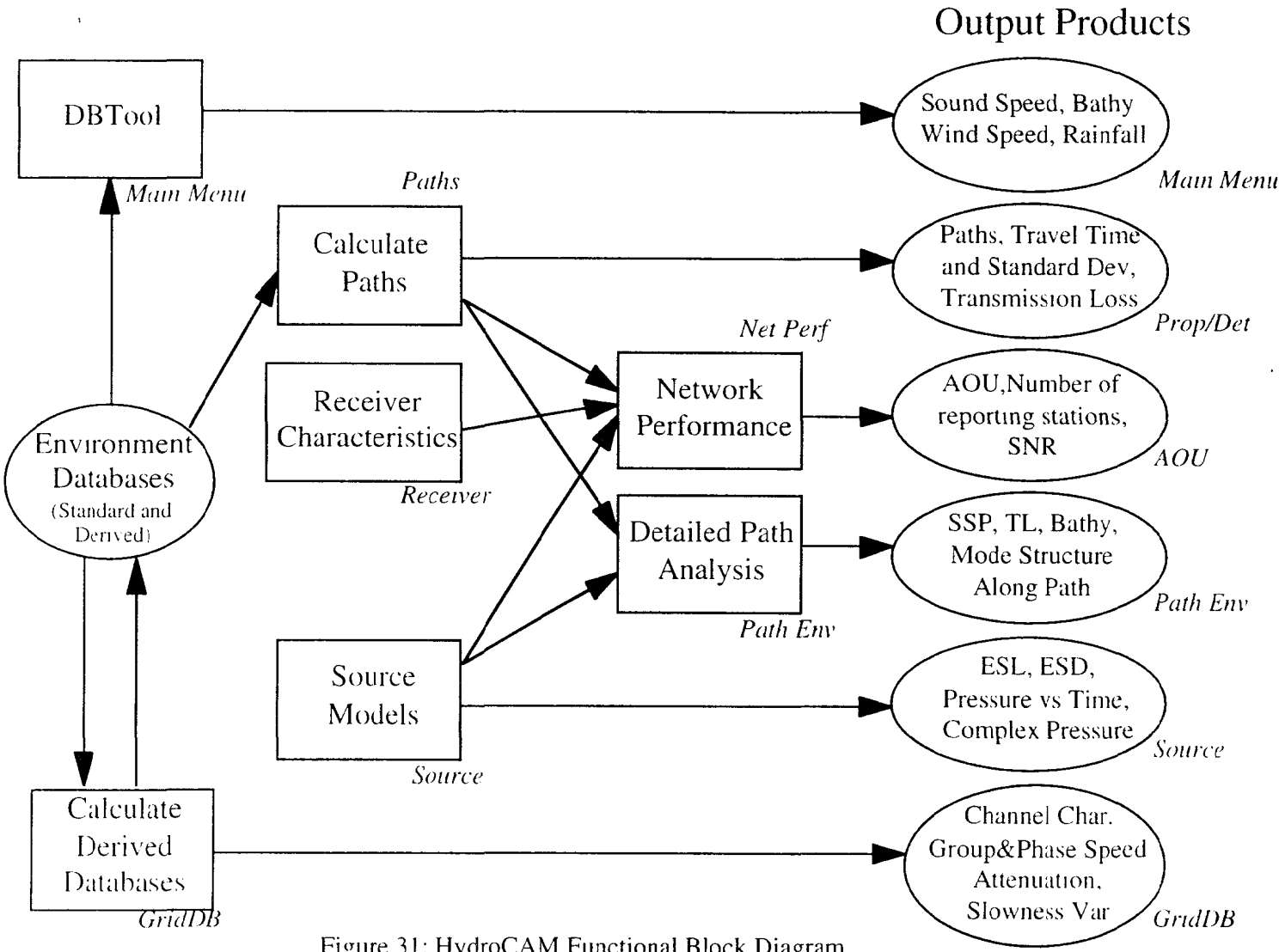

Figure 31: HydroCAM Functional Block Diagram

Each of the environment variables is used to specify the location of a different set of databases or software. The table below summarizes the directories that are needed by the HydroCAM software and their relationship to the environment variables

Directory	Contents
$HYDROHOME/config	configuration (setup) files
$HYDROHOME/config/source	source time-series files
$HYDROHOME/config/scenario	source location files
$HYDROHOME/config/receiver	receiver files
$HYDROHOME/config/network	network files
$HYDROHOME/config/prop	propagation model parameter files
$HYDRO	matlab m-files
$HYDRO/dbtool	environmental database access software
$HYDRO/hydroCAM	hydroCAM gui software
$HYDRO/propagation	interface software for propagation models
$HYDRO/utils	general MATLAB utilities
$HYDROHOME/models	all non-matlab hydroCAM software
$HYDROHOME/models/RAM	the Range-dependent Acoustic Model
$HYDROHOME/models/WKB	the WKB approximation software
$HYDRODB/gdem	GDEM sound speed database
$HYDRODB/etopo5	ETOPO5 bathymetry database
$HYDRODB/hydroCAM	hydroCAM derived grid databases (eg phase speed, group speed, etc)

To begin, start MATLAB and type "hydroCAM" at the MATLAB prompt. Although no specific knowledge of MATLAB is necessary to use HydroCAM, those who are unfamiliar with it will benefit from reviewing the demonstration programs and documentation Type "help" or "help demos" at the MATLAB prompt for more information. Since many HydroCAM data products are available in MATLAB variables, new analyses can easily be performed by using standard MATLAB commands to manipulate and display these variables To see a list of the available variables at any time, type "whos" at the MATLAB prompt

After an introductory window is displayed, two windows will pop up as shown in the figure below. The MATLAB command window on the bottom right of the figure, is used to analyze any variables available in the MATLAB workspace The main geographic display, shown in the top left of the figure, includes a set of pull-down menus for reading and manipulating oceanographic databases. The button menu called Tools is used to control HydroCAM Each button brings a new figure onto the display. These figures, or forms, are used to setup and run the models contained in HydroCAM The form for computing paths is shown in the example display figure

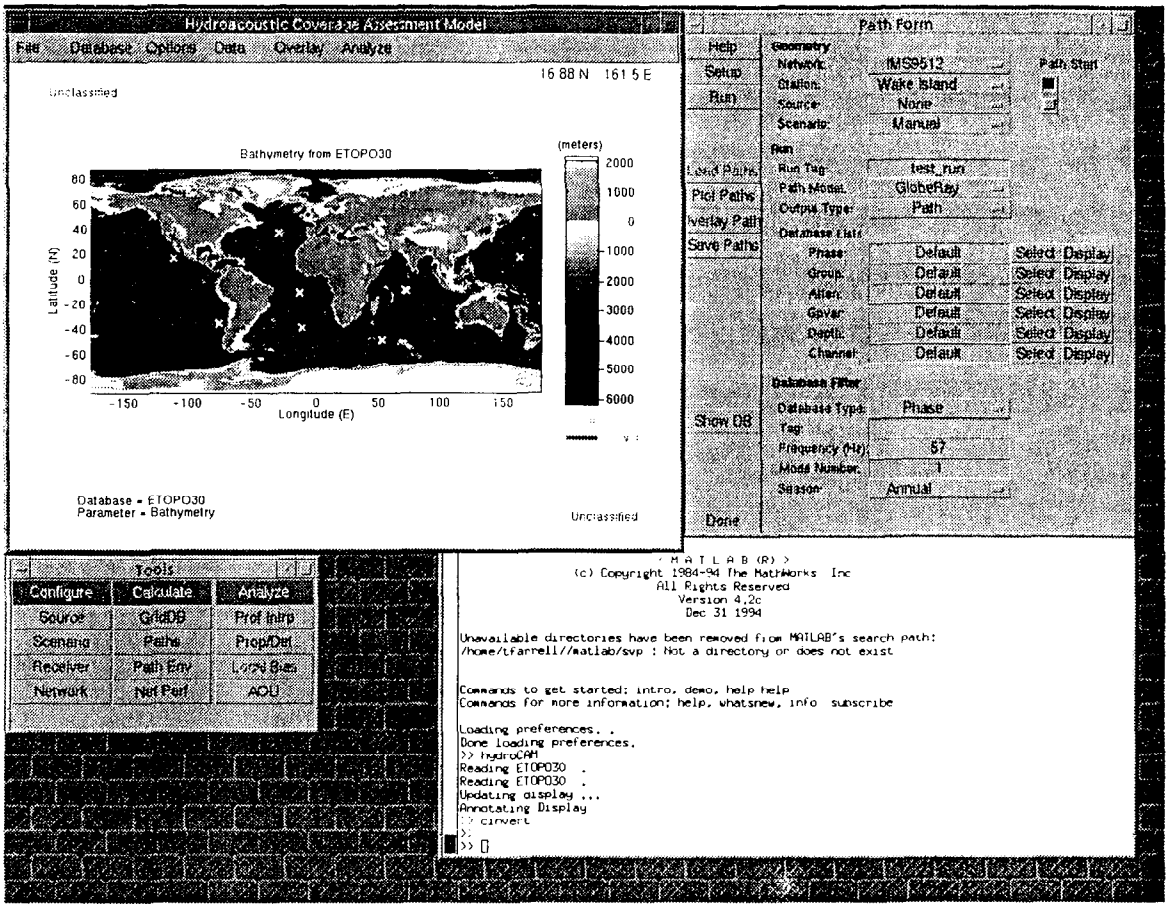

Example Screen Showing HydroCAM Windows

The remainder of the Users Guide is divided into two parts. The first section describes the functions and data that are available on the Geo Display. Then a reference section describing the use of each form on the Toolbar is provided.

Referring to the path form above, buttons are indicated using bold typeface (**Setup**), sections on the form are indicated using bold italic typeface (***Geometry***) and variables on the form, or within the MATLAB workspace are italicized (*frequency*)

Geo Display

The purpose of the main geographic display is to interactively manipulate environmental data, and to display source and station locations in geographic context. The features of the display are controlled through a set of pull down menus at the top of the figure. At all times, a cursor readout showing the current location of the mouse is provided at the top right of the display.

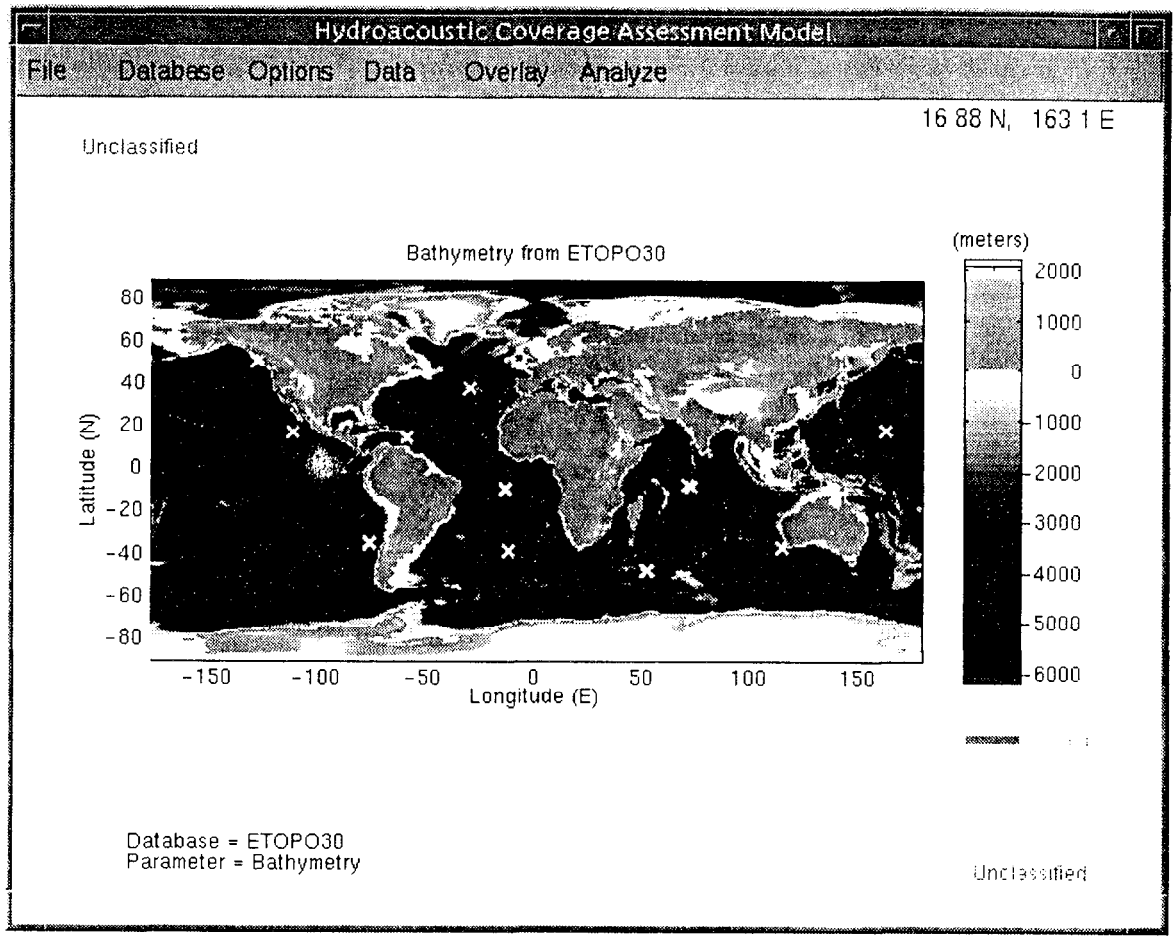

File Menu -- This menu performs some general purpose functions

About	Displays HydroCAM version information
Help	Access help display
Print	Print the geo to a printer or save to a postscript file
Exit	Exit the system

Database Menu – This menu is used to select environmental databases for analysis and display. The databases are organized by the physical properties into the following categories.

Bathy/Topo	Various bathymetric and topographic databases
Sound Speed	Various sound speed databases
Ocean Volume	Ocean volume database
Ocean Bottom	Ocean bottom information
Meteo	Meterological data
Shipping	Shipping density

When a user selects a database, a new figure for reading the database is created. The figure below shows the form for loading data from the World Ocean Atlas Analyzed database (WOA_ANALYZED1). A description of each of the databases is provided in the *Environmental Databases* section of this report. Additional information is also available on-line using the **About** button on the database form.

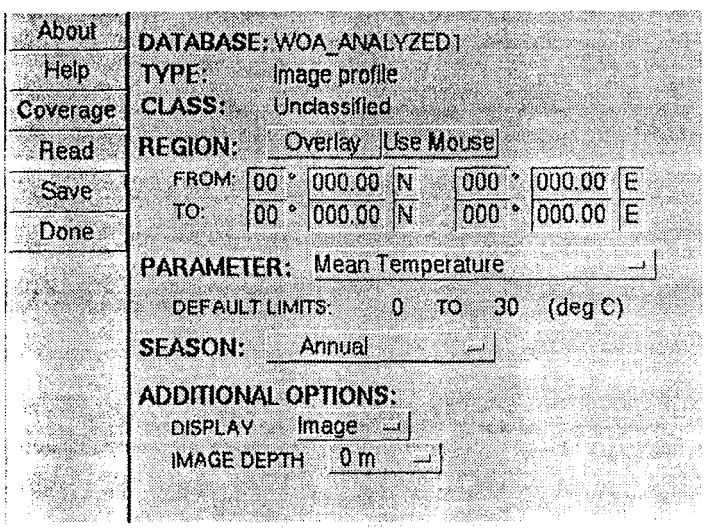

The **Coverage** button overlays the coverage of the database onto the geographic display. This option is most useful for block-image type databases (like DBDB1) which have many small grids and do not cover the entire region of interest. Each entry on the right side of the form (the "data entry side") must be chosen before the database can be read. Three options are available for defining the geographic region. The first is to manually enter the coordinates of two corners of the region into the form, and press **Overlay** to display the region on the geo. The second option is to press **Use Mouse** and then move the mouse to one corner of the geo, press and hold the left mouse button while you drag the mouse to the second corner of the desired area. The last option is to manually define the MATLAB variable *region* to describe the area of interest.

Two general types of environmental data may be accessed, image (raster) data and profile data. Any time image data is read in using the HydroCAM interface, it is stored in the two MATLAB variables *image_data* and *image_loc*. Image data is a matrix which contains the raster data (such as bathymetry) with latitude in rows and longitude in columns. The data starts at the southwest corner of the image, and works to the east and then north. The four element vector *image_loc* contains the minimum latitude, maximum latitude, minimum longitude and maximum longitude respectively of the raster data. All lat/lon values are referenced to the center of the cells Figure 2 below summarizes the image data structure in MATLAB. The user can modify or load any raster data into these variables and show a plot of the data in the geographic display by typing "update_display" at the MATLAB prompt.

$$image\_loc = [\phi_{min} \quad \phi_{max} \quad \lambda_{min} \quad \lambda_{max}],\ image\_data = 3 \text{ x } 4 \text{ matrix}$$

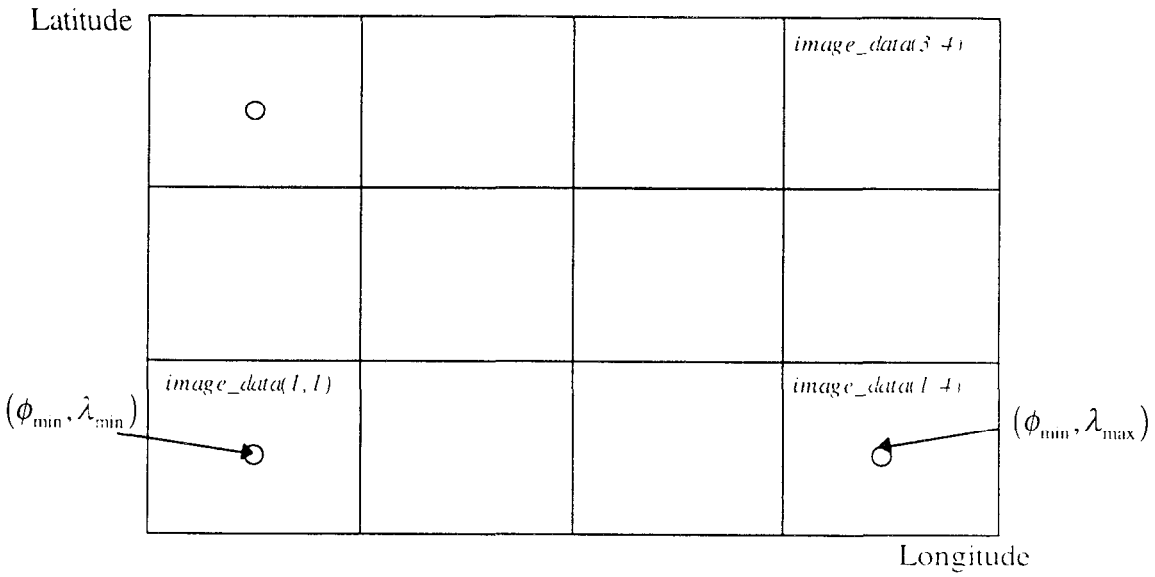

Figure 2: HydroCAM Image Data Structure

Likewise, profile data is stored in these MATLAB variables:

prof_data -- matrix of profiles data, one per column
prof_depth -- matrix of depths for each profile (one profile per column)
prof_lat -- vector of latitudes, one per profile
prof_lon -- vector of longitudes, one per profile

After profile data is read into these variables, the routine *update_display* plots a symbol at each latitude and longitude where profile data is available A second figure containing a line plot of all of the profile data is also created

Options Menu -- General plotting options are provided under this menu.

Plot Type	Controls the type of plot produced in the main window. The current options are *image* -- A color image (default) *surface* -- A three dimensional surface plot *globe* -- A three dimensional sphere plot *map* -- Map projection
Map Projection	Not normally used
Colormap	Several colormaps are available for the display: *Topo* -- Normal map for topographic data *Jet* -- Spectrum like scale used for most other data *Grayscale* -- 64 element grayscale *Zebra* -- NOAA developed colormap for identifying features in satellite images

Data Menu -- This menu is used to manipulate the data on the geographic display.

Reset	Reset the display to its original state
Select Region	Use the mouse to select a region the variables describing this region are place into MATLAB variable *region*. This option is used for the analyses available under the *Analyze* pull-down menu
Zoom On	Use the mouse to select a region to zoom into
Zoom Out	Zoom out to original view
Zoom Off	Turn off mouse mapping to zoom
Save Data (Matlab)	Save image data in matlab format
Save Data (GMT)	Save image data in GMT format
Remove Overlays	Remove all overlays on geo display

In addition, other windows may have a zoom feature controlled by a button. To operate, press the **Zoom On** button and drag a box with the mouse. Press the **Zoom Out** button to revert to the window's original size. To stop the zoom feature, press the **Zoom off** button.

Overlay Menu -- This menu controls some general purpose overlays on the main geographic display. The color and symbol used for each overlay is specified using two matlab global variables. As an example, the color and symbol for network locations is controlled through *ColorNetwork* and *SymbolNetwork*. Use the MATLAB command "help plot" for details on the color and symbol options available.

Overlay	Description
Contours	Plots contours of *image_data*. Contour levels are specified by the MATLAB vector *contours* Contour color is set by *ColorContour*
Map	Overlay of map features from the CIA world databases (see the Map option under ***Options Menu***).
Grid	Plot grid lines
Gazateer	Display information on oceanic features
DCW	Display island names from the Digital Chart of the World

Analyze Menu -- This menu is used to analyze environmental data that has been loaded.

Extract Point	Select this option and move the mouse to the desired area on the geographic display. The coordinates and data value at that point will be printed in the MATLAB text window when you press the left mouse button. To exit this mode, press the right mouse button This option uses only image databases (not profile databases).
Extract Line	Select this option and move the mouse to the desired start point. Hold the left mouse button down and drag the mouse to the desired end point. After releasing the mouse button, a new figure will be displayed containing the environmental data along the geodesic path connecting the two selected points. This option uses the available image databases (not profile data).
Extract Profile	After profile data has been read, move the mouse to the geographic window over the circle indicating the location of the desired profile. Press any mouse button to create a new figure containing the profile data at the selected location.
Profile EOF	Once profile data has been loaded using the appropriate database form (see ***Data Menu*** above), an analysis of the Empirical Orthogonal Functions which describe this set of profiles can be performed First, use the *Select Region* option under the ***Data*** menu to select a region for analysis. Then, set the energy threshold variable *eof_thresh* to a number between 0 and 1 using the MATLAB command window Select *Profile EOF*, and follow the instructions to display the EOFs and profiles reconstructed using only those EOFs above the energy threshold.
Bathymetry Analysis	Perform an analysis on the bathymetric slope of a selected region First, use the *Select Region* option under the ***Data*** menu to select a region for analysis Selecting *Bathymetry Analysis* will cause the statistics of the bathymetry and the local slope at each resolution cell in the selected region to be computed and displayed This option was used primarily for oceanographic studies of shallow water areas.

Description of the Tools

The tools panel consists of three sections: Configuration, Calculation and Analysis. The configuration forms allow parameters to be set for the runs The calculation forms execute prediction programs such as KRAKEN and GlobeRay and create output files. The analysis forms provide utilities for displaying and investigating the results of the prediction models. Each of these forms can also be started from the *Tools* menu on the main geographic display.

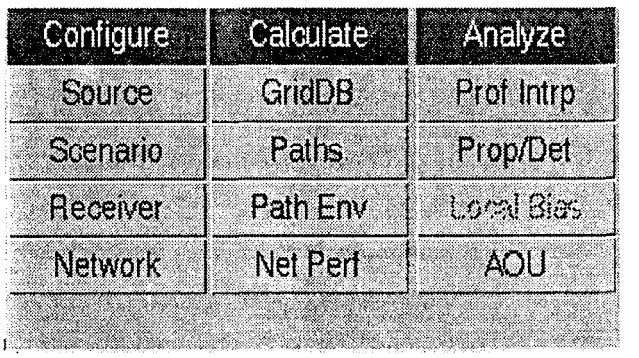

Configuration Forms		
Source	Load and display source characteristics	p. 84
Scenario	Define/Modify source locations	p. 85
Receiver	Define/Modify Receiver Parameters	p 87
Network	Display/Modify stations in a network	p. 91

Calculation Forms		
GridDB	Create grids containing ocean waveguide parameters using Kraken, WKB and WaveGuide	p 92
Paths	Create files containing paths, TL, TT, ST and angle using GlobeRay and Bender	p 94
Path Env	Extract environment along paths, Run detailed TL models along paths including RAM, Kraken and FEPEModes	p 101
Net Perf	Calculate network detection and localization performance using GenAOU	p 106

Analysis Forms		
Prof Intrp	Display profile data using different interpolation methods	p 109
Prop/Det	Display path characteristics and SNR	p 111
AOU	Display and analyze AOU	p 114

Source Form

Network performance and arrival structure details are dependent on source characteristics. One model available is a combined hydrodynamic and non-linear model of the hydroacoustic signature from underwater and low-atmosphere nuclear bursts. All models calculate pressure time series vs depth, which are saved into files in the config/source subdirectory. This form allows users to read and display the data from existing source files, as well as compute spectral characteristics, complex pressure and the energy level as a function of depth and frequency.

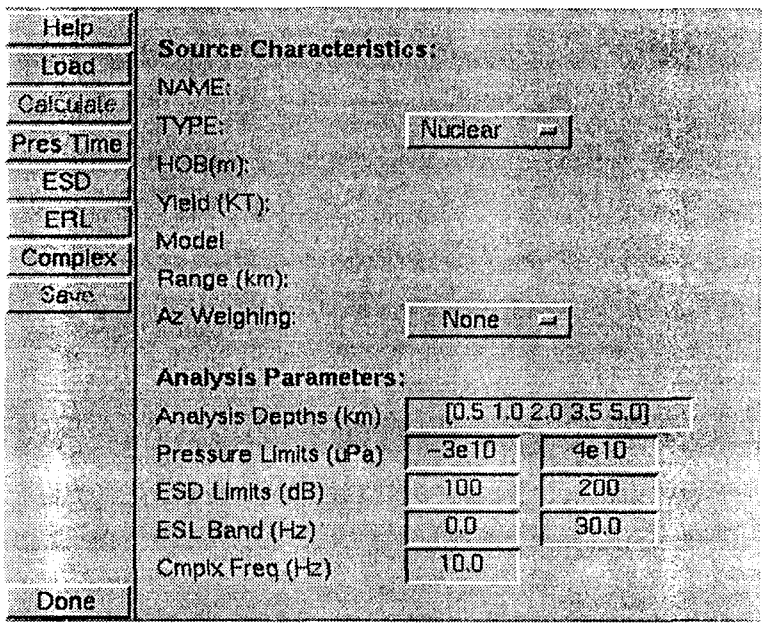

Button	Description
Load	Load a source file into the MATLAB Workspace
Pres Time	Plot Time series data vs depth and time; and vs. time at several depths
ESD	Plot Energy Spectral Density vs depth and frequency
ERL	Plot Energy level in a band vs depth
Complex	Plot complex pressure vs depth

Analysis Parameter	Description
Analysis Depths	Depths used for the Pres Time and ESD plots
Pressure Limits	Limits on the plots generated by the Pres Time button
ESD Limits	Limit on plots generated by ESD button
ERL Band	Limit on plots generated by ERL button
Complex Frequency	Frequency used for the plot generated by Complex button

Scenario Form

A scenario is a description of a set of path end-points This form is used to choose the type of scenario and specific scenario parameters, and save this information into a file in the config/scenario subdirectory Scenario files can also be created manually They must have a *scen* extension

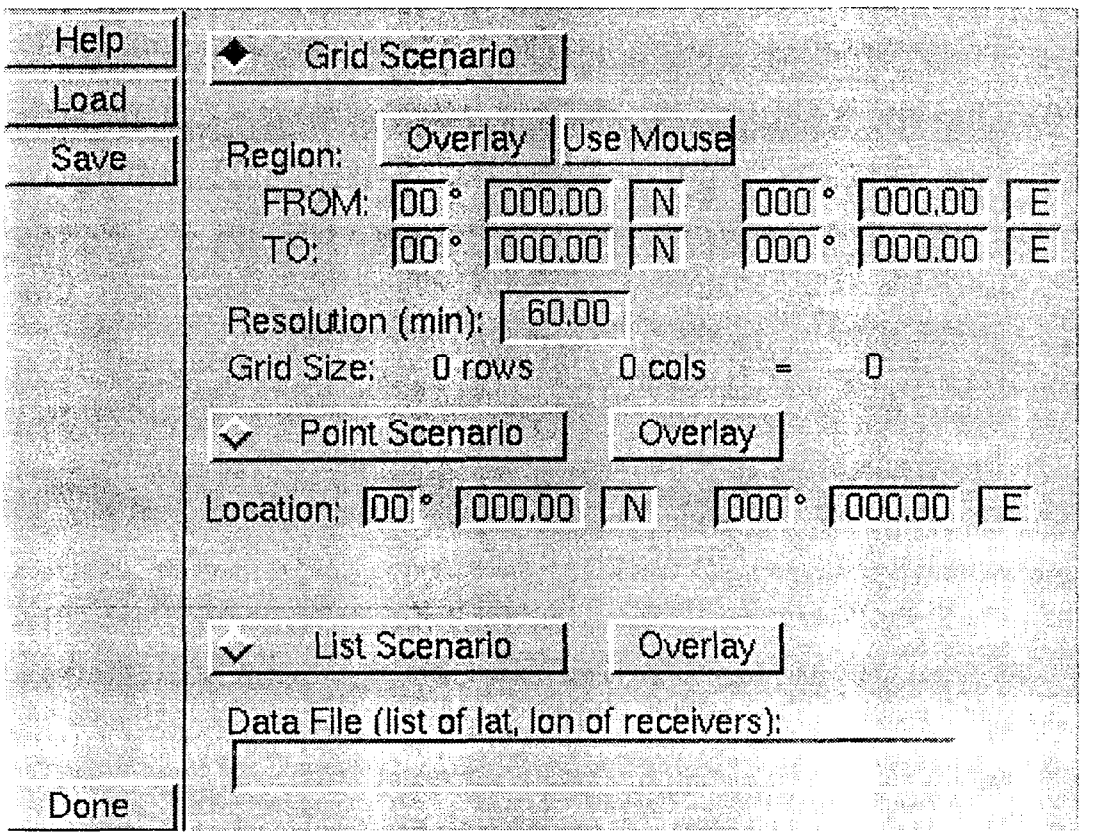

Grid Scenario A grid scenario is an evenly sampled rectangular region in latitude and longitude Enter the boundary of the grid by typing the coordinates of the lower left and upper right corners into the edit fields on the form; or select the **Use Mouse** button and drag a rectangle in the geographic display window Select a resolution (in minutes) for the granularity of points The grid size is calculated and displayed in number of rows and columns for reference purposes only Source positions are calculated from each point on the grid A sketch of a grid scenario is shown below

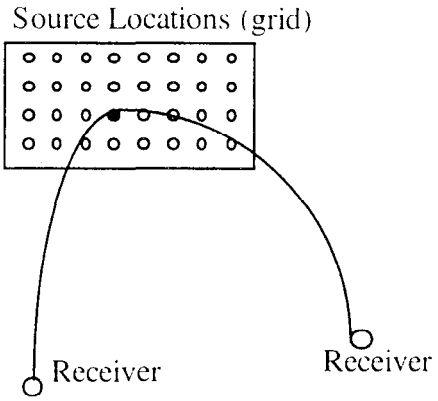

Point Scenario: A point scenario is a single source location. This option is usually used for analyzing data from specific events or experiments Example point scenarios included with HydroCAM are the Heard Island Feasibility Test (HIFT scen), and the September 1995 French Nuclear Tests (Mururoa.scen).

List Scenario: A list scenario is a file containing a list of source locations in degrees latitude and longitude This type of scenario is used for data analysis of a set of earthquake positions or other explosions heard by the same sensor An example file is provided in *config/scenario ExampleList scen*

In general, the scenario form is used with the **Paths** form. However, it is not necessary to create a scenario file each time you wish to predict propagation paths To avoid saving data on the form to a file, keep the form on the screen and select the "Manual" option on forms that require scenario input HydroCAM will then read the data from the open **Scenario** form instead of a file

Receiver Configuration

Receiver characteristics are contained in four data files which are stored in the config/receiver directory. The primary file, called simply a receiver file, contains the receiver location, type, name, and the names of three other files; the ambient noise file (extension .an), the directionality file (extension dir) and the system loss file (extension sloss). The receiver form loads, displays and creates receiver files.

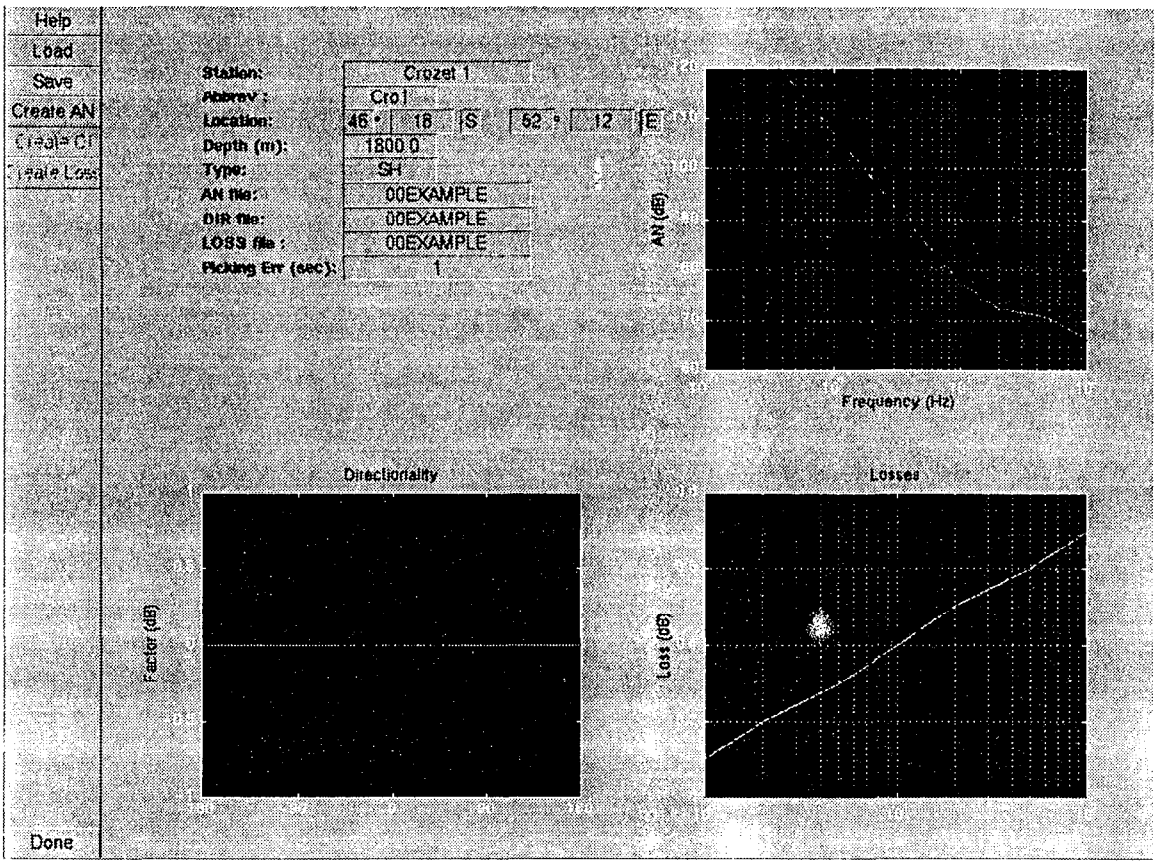

Button	Description
Load	Load a receiver file and display its contents on a new form
Save	Save a receiver in the config/receiver directory The filename name is created using the *Abbreviation* in the Input Parameters section. For the form shown above, the filename is *Cro1 rec* in the SHYDROHOME/config/receiver subdirectory
Create AN	This option brings up a new form which creates a new ambient noise file for a receiver (See **Create AN** below). Add a file name to the Ambient Noise form and adjust any of the parameters Pressing enter after changing the values of Frequency, wind speed or shipping level will modify the level vs frequency graph.

Input Parameter	Description
Station	Complete station name (Can include spaces and other symbols Does not have to be unique)
Abbreviation	Common abbreviation, this also is the filename used when the *Save* button is pressed, this must be unique
Location	Receiver location (lat, lon)
Depth	Depth of receiver in positive meters
Type	Simple seismic (SS), Simple hydroacoustic (SH), Seismic array (SA), Hydroacoustic Array (HA), Infrasonic Array (IA)
AN File	Set to default file, create new files as described below
DIR file	Set to default file, create new files as described below
LOSS File	Set to default file, create new files as described below

Ambient Noise File (.an) -- New files can be manually created in the config/receiver directory These files can be also be created using the **Create AN** button The file contains a table of the ambient noise as a function of direction and frequency The example file provided with HydroCAM illustrates the format Do NOT include comments in these files The numbers in the table need to be delimited by spaces *not* commas.

Listing of config/receiver/00EXAMPLE.an

```
7                       ! Number of Frequencies
1 2 5 10 20 50 100      ! Frequencies in Hz
-180 180 180            ! Azimuth Start, Stop, Increment (deg TN)
100 110 70              ! AN at first frequency vs direction
85 90 70                ! AN at second frequency vs direction
80 85 70                ! AN next frequency vs direction
75 80 70                ! AN next frequency vs direction
70 75 70                ! AN next frequency vs direction
70 75 70                ! AN next frequency vs direction
70 75 70                ! AN last frequency vs direction
```

Directionality File (.direct) -- This file contains a weighting factor applied to the sonar equation as a function of azimuth and frequency See the *Receiver Characterization* section of this report for a more detailed description of the uses of this file An example is provided with HydroCAM Do NOT include comments in these files The numbers in the table need to be delimited by spaces *not* commas

Listing of config/receiver/00EXAMPLE.dir

```
7                    ! Number of Frequencies
1 2 5 10 20 50 100   ! Frequencies in Hz
-180 180 180         ! Azimuth Start, Stop, Increment (deg TN)
0 0 0                ! Az weighting at first frequency vs direction
0 0 0                ! Az weighting at second frequency vs direction
0 0 0                ! Az weighting at next frequency vs direction
0 0 0                ! Az weighting at next frequency vs direction
0 0 0                ! Az weighting at next frequency vs direction
0 0 0                ! Az weighting at next frequency vs direction
0 0 0                ! Az weighting at last frequency vs direction
```

System Loss File (.sloss) -- This file is used to account for all losses occurring in the sensor, receiver, and processing systems that are not accounted for elsewhere A typical use is to include the island seismic station loss in this file. Four columns are provided to contain four different types of losses. The total of these four columns is used for the loss factor at each frequency. Do NOT include comments in these files. The numbers in the table need to be delimited by spaces *not* commas.

Listing of config/receiver/00EXAMPLE.sloss

```
7                                    ! Number of frequencies
1.00   0 1   0.0   0.0   0.0        ! Frequency and 4 loss data pts
2.00   0.2   0.0   0.0   0.0
5 00   0.3   0.0   0.0   0.0
10.00  0 4   0.0   0 0   0 0
20.00  0 5   0 0   0.0   0.0
50 00  0.6   0.0   0 0   0 0
100.00 0.7   0.0   0 0   0.0
```

Create AN

This form is used to generate ambient noise files for hydroacoustic stations. The Wenz ambient noise model is used. Files can be saved in the config/receiver subdirectory for use by any hydroacoustic station.

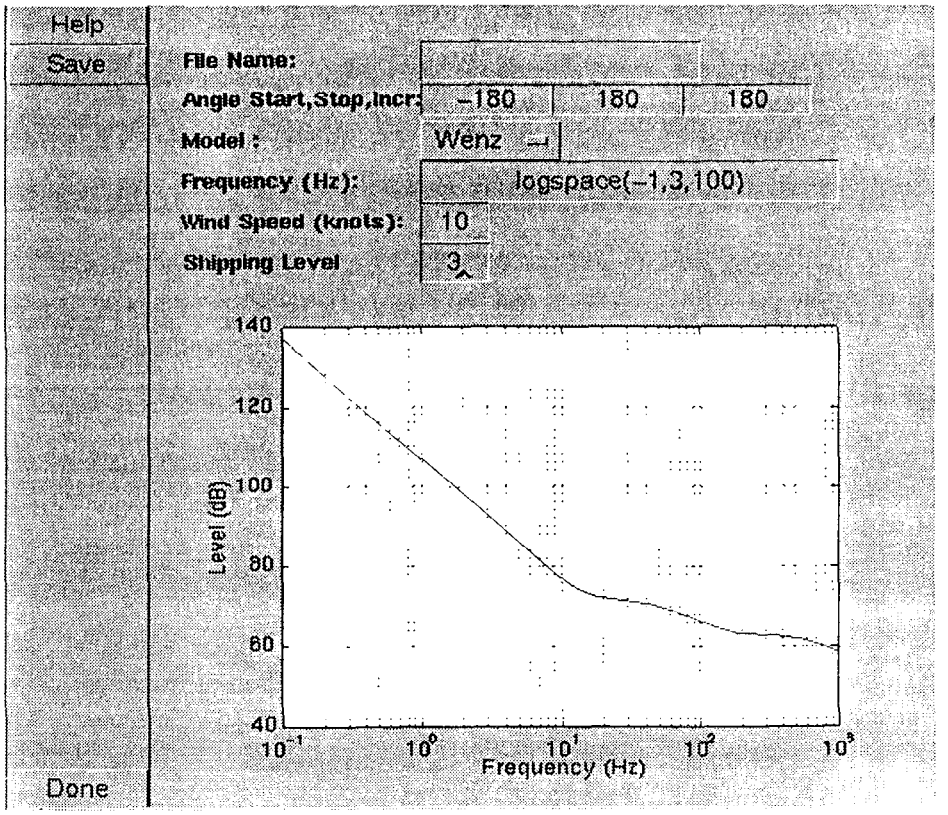

Variable	Description
File Name	Name of the ambient noise file. This name is used in the receiver file
Angles	Start, stop and increment. The Wenz model is omnidirectional, so these values have no effect. Three values are required for the interpolation routines to work correctly
Model	The Wenz model is the only available option
Frequency	Any valid MATLAB statement can be used to specify the vector of desired frequencies in Hz
Wind Speed	Wind speed in m/s This parameter effects the ambient noise level between 100 and 1000 Hz
Shipping Level	Level between 1 and 7. Primarily effects the ambient noise level below 200 Hz

Network

Networks are groups of receivers. Network configuration files are stored in the config/network subdirectory and consist of a list of receiver filenames (without the extension). This form is used to display networks on the main geographic display, add or remove receivers from a network, or to print a summary of the network characteristics to a text file.

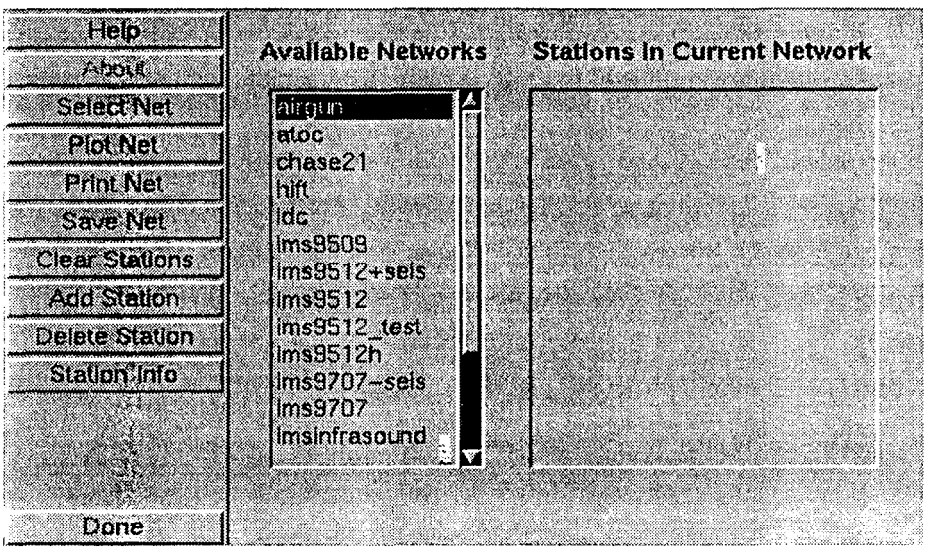

Button	Description
Select Net	Load station information from network selected under "Available Networks"
Plot Net	Plot stations listed under "Current Network"
Print Net	Print stations information listed under "Current Network" to a text file
Save Net	Save the stations under the "Current Network" into a new network file
Clear Stations	Clears stations under the "Current Network"
Add Station	Add a new station to the "Current Network"
Delete Station	Deletes the selected station from the "Current Network"
Station Info	Displays the characteristics of the selected station

The *Available Networks* listbox displays all the currently available networks in the configuration directory. New networks are created by modifying an existing network and saving it to a new filename. When a network is selected, its stations will appear in the *Stations in Current Location* listbox. Specific information on the station may be obtained by selecting a station and then clicking **Station Info**.

GridDB

This form is used to setup calculations of the ocean waveguide on a geographic grid. At each lat/lon point on the grid, the wavenumbers and modes for a range-independent waveguide are calculated. The phase speed, group speed, attenuation and slowness variance of propagation are then calculated and placed into 4 grid files for use in predicting propagation paths and their characteristics.

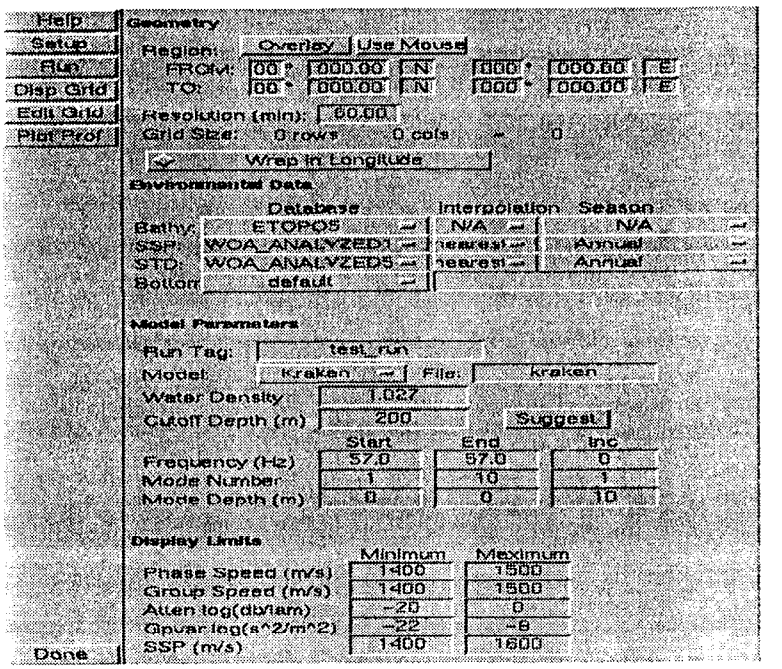

Button	Description
Setup	Produces a form containing all of the model-specific parameters needed to calculate the modal eigenvalues and eigenfunctions. The model is selected under ***Model Parameters***
Run	Runs a shell-script that (1) extracts environmental data at each point on the grid, (2) Runs the mode model to predict the modes at each point on the grid, (3) Runs the waveguide program to calculate the waveguide parameters at each point on the grid.(4) collects the results and places them in 4 grid files in the current directory, phase grid, group.grid, gpvar grid and atten.grid
Disp Grid	Displays color images of the four grid files
Edit Grid	Not functional Will eventually allow users to modify points on the grids
Plot Prof	Produces a display of the phase speed grid When the mouse is clicked on a point in this grid, details of the mode/waveguide calculations are displayed in a separate figure The sound speed, sound speed variance, density and mode shape profiles, and the numeric values of the phase speed, group speed, attenuation and slowness variance are shown for the selected point

Geometry -- The geometry section of this form is used to select the parameters of the grid to be calculated Any grid is specified by the latitude and longitude coordinates of the corners of the grid, the spatial resolution, and a flag indicating whether points to the east of the grid should be "wrapped around" to the western edge of the grid.

Environmental Data -- The environmental databases used for the mode and waveguide calculations are selected here. These databases are read, then interpolated onto the desired grid selected in the ***Geometry*** section. Interpolation options are listed in order of decreasing speed (ie *Table* is the fastest). The results are saved into an input file used by the mode and waveguide prediction programs.

Model Parameters -- The model-independent parameters are chosen here. Model-specific parameters are defined using the **Setup** button on the left of the form. The independent parameters include:

Run Tag:	This character string is prepended to the grid file names
Model:	The options are Kraken, and the WKB approximation model.
File:	Name of the file containing the model-specific parameters
Water Density:	Like it says, in gm/cm3
Cutoff Depth:	Locations where the water depth is less than this value will not be used in the predictions. This option saves disk space and cpu time for shallow water areas where modes do not propagate (cutoff). The "Suggest" button suggests a cutoff based on the Pekeris waveguide model for the frequency and mode numbers selected on the form.
Frequency	Frequency used for the mode calculations
Mode Number:	Limits on the mode numbers to save. Increasing the number of modes increases both the run time and the size of the mode and grid files.
Mode Depth.	Depths where the modes should be calculated. If the ending depth is set to "0", then the model is run from the surface to the bottom at each grid point with increment as selected here

Display Limits -- Limits for the displays produced by **Disp Grid** and **Plot Prof**

Paths

This form is used to predict the characteristics of acoustic ray paths including amplitude, travel time, travel time standard deviation along the paths. The models all require ocean database grids produced by **GridDB**. The paths can be examined using **Prop/Det** or **Path Env.** A setup form for the selected path model (either GlobeRay or Bender) is displayed with the path form.

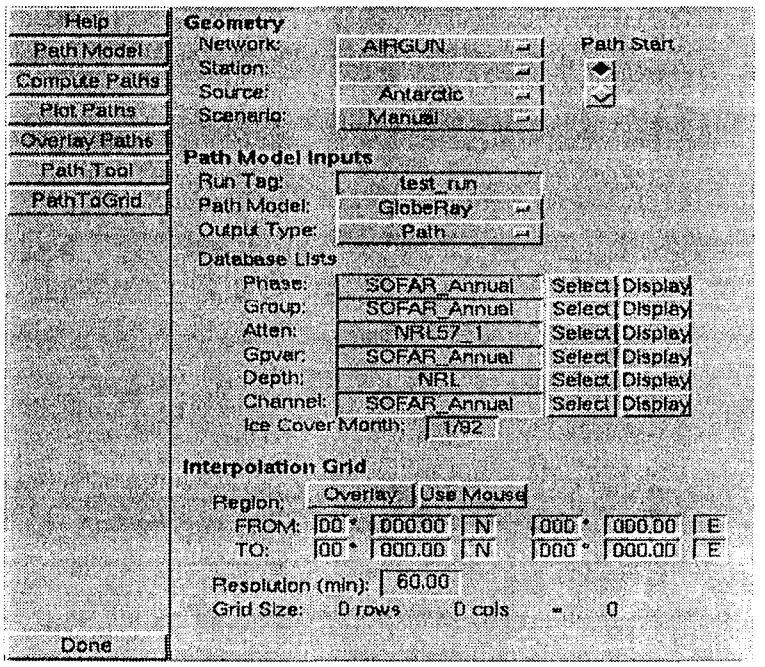

Button	Description
Path Model	Allows the user to load, modify and save parameters specific to the path model chosen on the *Path Model* pop-up menu.
Compute Paths	Runs the path model for each receiver in the selected network. The results are saved in grid or path files containing the path location, transmission loss, travel time and travel time variance. The environment variable SGRIDPATH must contain the directory where the desired ocean grid files are located
Plot Paths	Produces a geographic display of the paths
Overlay Paths	Overlays the paths on an existing display, which is selected by moving the mouse to the desired figure (and axis) and using the left mouse button
Path Tool	Opens another form that displays all of the paths It plots the travel time, nominal transmission loss, attenuation, travel time standard deviation, and the local path angle for a selected path (See **Path Tool** below)
PathToGrid	Interpolate path data into a rectangular region in latitude and longitude The grid's location, size and resolution are specified in the ***Interpolation Grid*** section of the form

Geometry -- The geometry of the path predictions are defined here Paths can start from either source locations or receiver locations by choosing the appropriate checkbox. If a "point" scenario is chosen, the predicted paths end at either source locations or receiver locations. If a "manual" scenario is chosen, then the scenario information is obtained from the currently open **Scenario** form All other scenario options describe the names of scenario files (such as a grid of hypothesized sources), which can be created or modified by the **Scenario** form on the tool-bar.

First choose the network. Each network file in the *config/networks* subdirectory is provided as an option. When a network is selected, all the available receivers in the network are placed in the *Station* menu. Choose a station and source from the pull down menu; select whether the path will start at the station or the source using the radio button under *Path Start*

Path Model Inputs -- This section contains all of the parameters necessary to run the path model.

Run Tag	A prefix used on all of the output files
Path Model	GlobeRay - Geodesic or "Shooting" refracted path model
	Bender - Bending refracted path model
Output Type	Path - the characteristics along each path are saved. Warning shooting paths over grid scenarios can be compute intensive
	Grid - the values at the end of a path are saved. These paths must end on a grid of points.
Database Lists	The environmental databases required for computing paths are selected in this section. As described in the *Detailed Model Descriptions* section of this report, the data for each environment variable can be composed of a number of grids at different resolutions A data file that contains the name of each grid file in the collection is called a *Database List* Database list files must be located in the *config/dblists* subdirectory The edit field next to each variable is used to enter the desired database list filename **Select** allows you to choose from the currently available lists **Display** overlays the locations of the grids in the list onto the main geographic figure. Clicking on the outline of any of these grids produces a new figure displaying a color image of the data in the grid Make sure that you set the *SGRIDPATH* environment variable to include all directories where the data files contained in each database list are located.
Ice Cover Month	Month and year (MM/YY) of DMSP ice coverage to use

Interpolation Grid - Grid specifications for interpolation using PathToGrid.cc Enter the boundary of the grid by typing the coordinates of the lower left and upper right corners into the edit fields on the form; or select the **Use Mouse** button and drag a rectangle into te geographic display window. Select a resolution (in minutes) for the granularity of points. The grid size is calculated and displayed in number of rows and columns for reference purposes only

Path Tool

This form allows the user to see additional information on each path. The user can click on a path to get the path number. Enter that number in the *Path Number* field on the bottom and hit **Select** to display the travel time, nominal transmission loss, attenuation, travel time standard deviation, and the local path angle for that path.

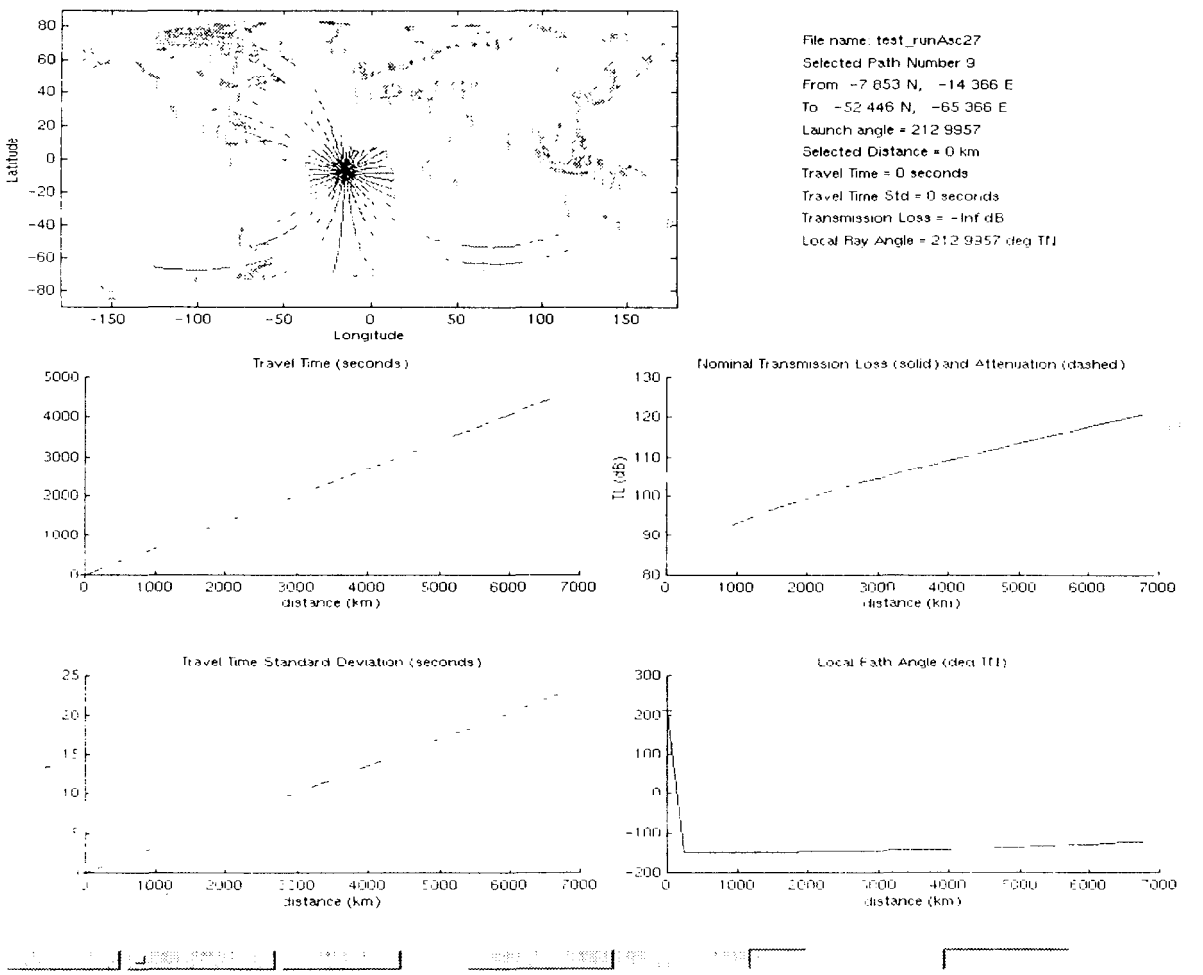

Setup Globeray

This form contains the model input parameters that are specific to the GlobeRay propagation model. It is called from the **Path** form whenever GlobeRay is selected. The parameters can be saved and/or loaded into files in the config/prop subdirectory. The default values are stored in *config/prop/Defaults.globeray*

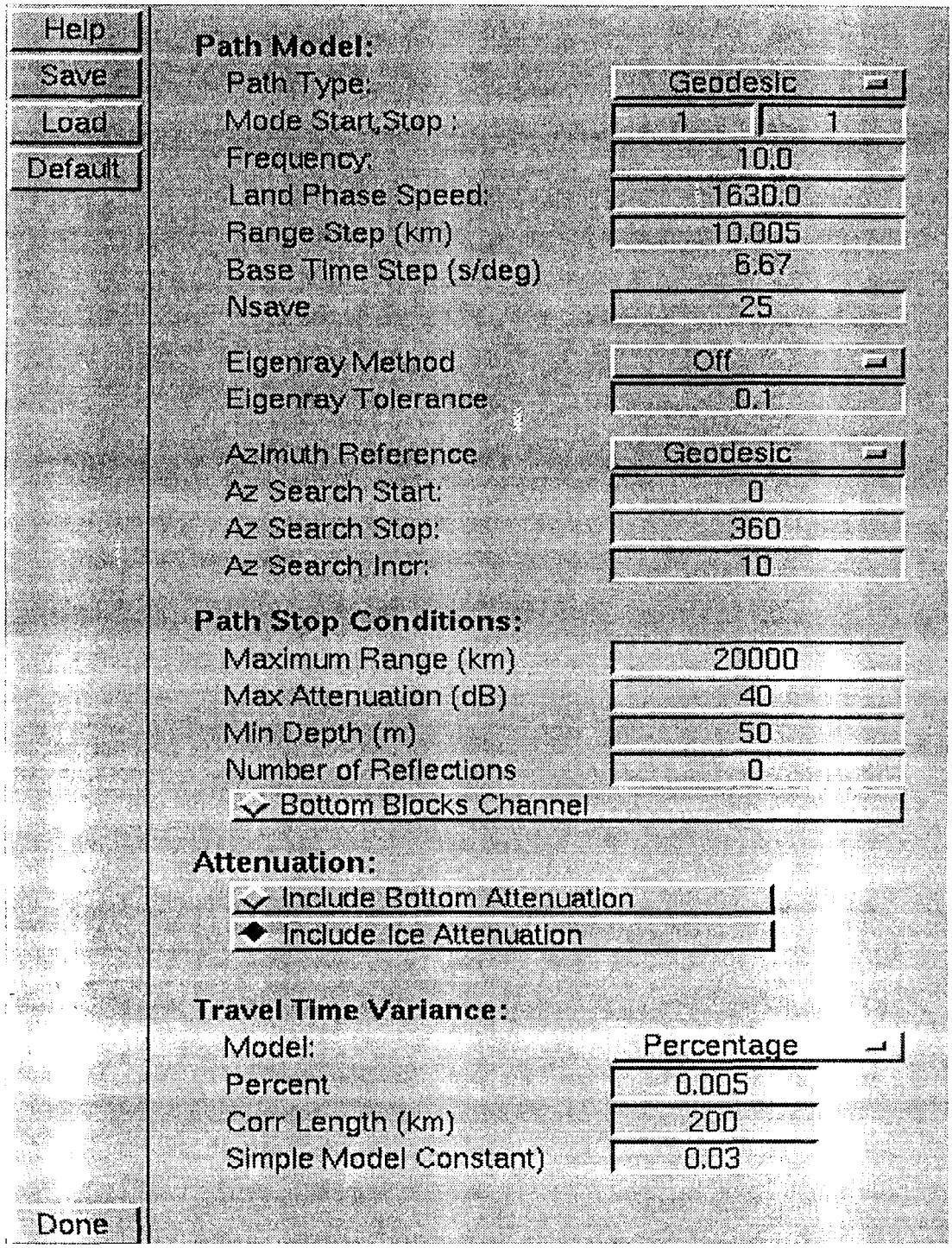

Path Model -- The parameters in this section affect how the ray path is predicted.

Path Type	Paths can be calculated using geodesics, horizontal refraction or read in from a previously calculated path file.
Mode Start, Stop	Paths are calculated for each mode in this range The environmental database files must contain valid phase speeds, group speeds, attentions and slowness variances for the requested modes.
Frequency	Used to compute the wavelength from the phase speed database. Wavelength is needed to predict bottom attenuation.
Land Phase Speed	Used to allow paths to bend away from land (where phase speed data is not available) without generating a high resolution database.
Range Step	Step size used in the solution of the ray path
Base Time Step	This value is used in the horizontal refraction model It is calculated on the input form from the *Range Step* using a sound speed of 1500 m/s. The value is a *Base* time step since it is multiplied by the resolution of the phase speed database to determine the actual time step. See the *Path Location* section in the Detailed Model Description section for more details
Nsave	Decimation factor. Ray paths are calculated using the *Range Step*, but every *Nsave* points are saved and used for computing transmission loss, travel time and travel time standard deviation.
Eigenray Method†	Four options are available: *Off* -- Eigenrays are not calculated *Geodesic* -- The geometric path connecting points is computed *Bisect* -- Bisection method used to search for refracted eigenrays *Bender* - C++ version of the Bender algorithm
Eigenray Tolerance	Acceptable distance between the ray end point and the desired endpoint in degrees lat/lon
Azimuth Reference	The search for refracted eigenrays requires an initial range of launch angles. These angles can be specified with respect to *True North*, which is useful when only one path is desired, or with respect to the *Geodesic* path that connects the desired points
Az Search Start	Initial launch angle in degrees
Az Search Stop	Final launch angle in degrees
Az Search Increment	Launch Angle increment

† The selection of *Eigenray Method* must take into account the scenario chosen on the **Paths** form. The table below summarizes how these two options are inter-related

Scenario Type	Eigenrays	Result
Point	On	One path between start and end point
Point	Off	Set of paths from *Az Search Start* to *Az Search Stop* with the paths terminated when they pass the desired end-point.
Grid	On	Set of paths from the start point to the grid points.
Grid or List	Off	Not Valid
List	On	Set of paths from the start point to each of the end points in the list scenario.

Path Stop Conditions -- Paths are terminated whenever any of the following conditions hold.

- Distance from the start of the path is greater than the *Maximum Range* (km)
- Total boundary attenuation (ice loss and bottom loss) along the path exceeds *Maximum Attenuation* (dB).
- The depth at any point is shallower than *Min Depth* (m)
- The number of reflections exceeds *Number of Reflections*
- When *Bottom Blocks Channel* is selected, paths are terminated whenever the bottom depth at any point in the path is shallower than the channel depth contained in the channel database (see the **Path** form for selection of this database)

Attenuation -- Two attenuation models are available. A complete description of these models is provided in the *Detailed Model Description* section of this report

Travel Time Variance -- Three models are available as described in the *Detailed Model Description* section of this report. The *Percent* edit field contains the value used in the model where the travel time standard deviation is a constant percentage of the travel time The *Corr Length* is used for the slowness correlation length in the *Path Integral* model. The *Simple Model Constant* at the bottom of the form is used in the model where the travel time standard deviation is a constant times the square root of the path length

Setup Bender

This form contains the model input parameters that are specific to the Bender propagation model. It is called from the **Path** form whenever Bender is selected. The parameters can be saved and/or loaded into files in the *config/prop* subdirectory. The default values are stored in *config/prop/Defaults.bender*.

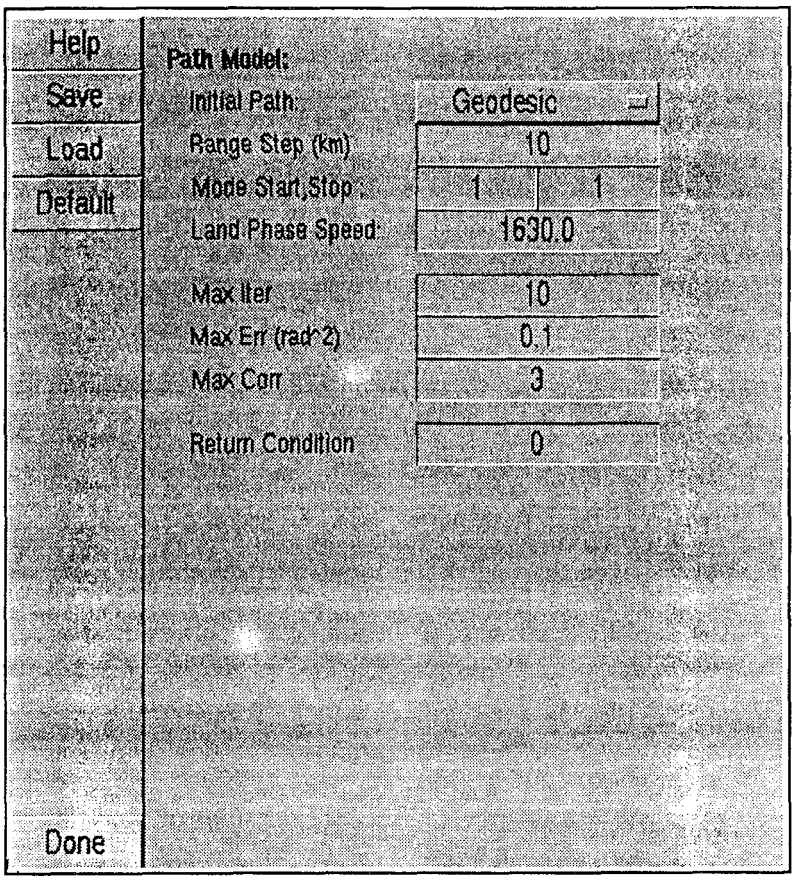

Initial Path	The Bender model iteratively perturbs an initial path until it finds the path with the smallest travel time. At this time, all initial paths are *Geodesic*
Range Step	Increment between points on the path
Mode Start, Stop	As with the GlobeRay model, Bender can be run for several modes provided that the input environmental databases include those modes
Land Phase Speed	Without high resolution databases covering all continental margins and regions around islands, a phase speed value is required to allow paths to gradually bend away from land.
Max Iter	Maximum number of iterations
Max Err	Maximum error tolerated for convergence (default = 0.01 rad^2)
Max Corr	Maximum error before corrections are scaled by $\frac{MaxCorr}{MaxCorr + error}$

Path Env

This form is used for extracting sound speed profiles and bathymetry in a vertical plane along paths. In addition, the extracted environmental data can be passed on to "standard" vertical plane propagation models such as RAM. This capability is used for determining detailed propagation characteristics along the paths, effects of bathymetric features on loss mechanisms and mode structure, and the detailed structure of the arrival from a specified source.

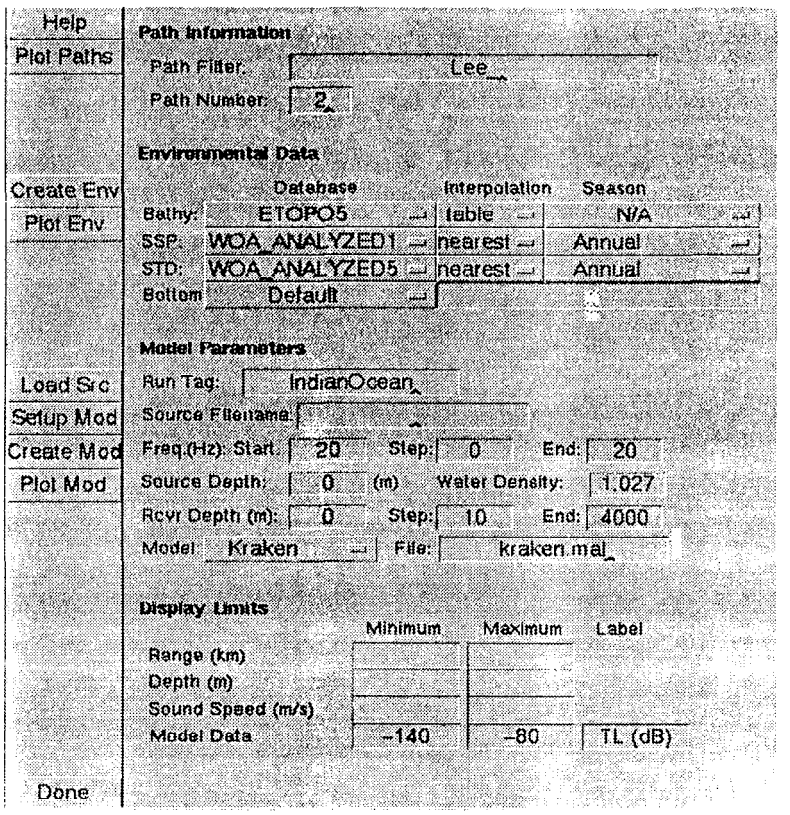

Button	Description
Plot Paths	Plots path files that match the prefix specified in the Path Filter. Clicking on a path gives a dialog box containing the path number, launch angle and mode number.
Create Env	Creates the following environment files for the specified paths: run-tag.bathy (bathymetric data along path), run-tag.ssp (sound speed profiles), run-tag.std (sound speed standard deviation). The databases and interpolation methods are selected using the pull down menus under the *Environmental Data* section of the form. This button must be used *before* propagation model input files can be created.

Plot Env	Plots sound speed profiles, sound channel depth and bottom depth versus range for the paths specified in *Path Number*.
Load Src	Initializes RAM prediction with complex pressure from the selected source file. If source file is not chosen, RAM uses a default "self-starter" to initialize the prediction, and computes transmission loss instead of received level.
Setup Mod	Displays a dialog box that creates a model specific setup file.
Create Mod	Runs selected model. Choosing path number 0 runs model on all paths.
Plot Mod	When RAM has been selected, plots transmission loss vs depth and range for the path number selected in the Path Information section. When Kraken is chosen, plots the modal exitation verus range. Make sure that Create Mod has been run on this path number.

Path Information -- The *Path Filter* is used to determine which path files are used to extract information. All path files passing the filter are included. As an example, "test*" would result in files "test1.path" and "test2.path" being included. Users must be careful when using the filter not to include all path files, especially in directories where network calculations have been performed. The *Path Number* determines which path in each path file is used. Choosing *Path Number* as 0 extracts data for all paths in the path files.

Model Parameters -- These are the generic parameters needed for all propagation models

Run Tag	Character string used as a prefix to all model output filenames. As an example, if the path file is named *testAsc1.path*, and the Run Tag is *RAM*, then the output file would be named *RAMtestAsc1 tlplane* which contains the transmission loss in a vertical plane along a selected path in *testAsc1.path*.
Source Filename	optional; see **Load Src** button description above
Freq Start, Step and End	define the frequencies to run the model over; separate input and output files are created for each frequency
Source Depth	Nominal source depth used for model run Not used if a source filename is selected. When KRAKEN is selected, this depth determines where the modal exitation is calculated when **Plot Mod** is executed
Receiver Depth	Nominal receiver depth in meters for the model run RAM generates an additional data file which contains the transmission loss from the source to this receiver depths as a function of range. When KRAKEN is selected, these depths determine where the mode shape functions will be calculated

Model	Name of the model to run along the specified paths At this time, RAM and KRAKEN are available.
File	Setup file containing the model specific parameters for the selected model. This file can be examined and changed using the **Setup Mod** button. **Load** and **Save** buttons on the **Setup** forms are used to save these parameters into the *config/prop* subdirectory. See the **Setup RAM** and **Setup Kraken** sections for descriptions of the available parameters.

Display Limits -- Controls the scaling on the displays generated with **Plot Env** and **Plot Mod**. If any of these parameters is left blank, automatic scaling is used.

Setup RAM

This form contains the model input parameters that are specific to the Range-dependent Acoustic Model (RAM). It is called from the **Path Env** form when transmission loss predictions are needed in a vertical plane along a specific path A detailed description of the RAM model, including specific information on each input parameter, is provided in the RAM Users Guide [10]. MATLAB files containing these parameters are loaded and saved into the current working directory.

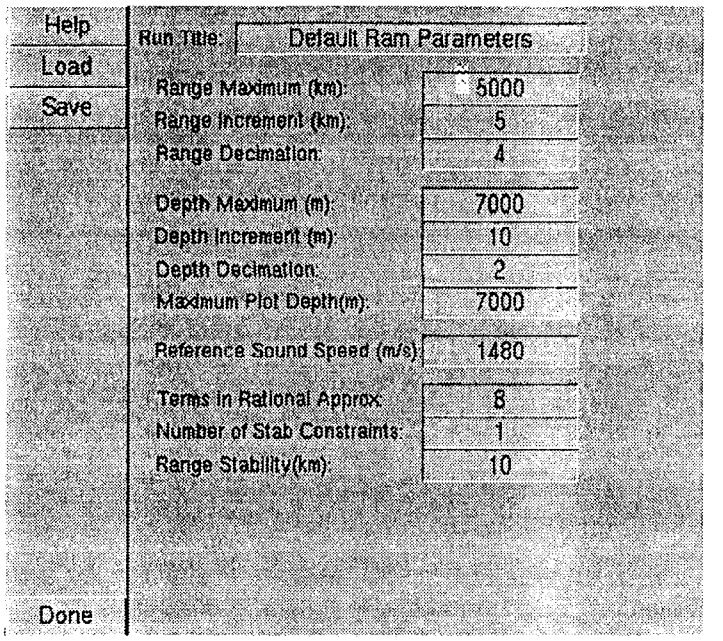

RAM Parameter	Description
Run Title	Character string describing RAM run Used only in RAM input files -- not HydroCAM or displays
Range Maximum (km)	Maximum range for the RAM run
Range Increment (km)	Range increment for calculating TL
Range Decimation	Decimation factor for saving TL grid
Depth Maximum (m)	Maximum depth used in calculating TL Experience has shown that this number should be about 1000m deeper than the deepest bathymetry point in the path
Depth Increment (m)	Depth increment for the PE mesh
Depth Decimation	Decimation factor for the TL grid that is saved
Maximum Plot Depth (m)	Only these depths are saved to the RAM output file
Reference Sound Speed	Starting point for the PE, default value is 1480 m/s
Terms in Rational Approx	Number of terms in rational approximation, typically 8
Number of Stab Constraints	Number of stability constraints (1 or 2)
Range Stability	Maximum range of stability constraints to avoid attenuation over very large ranges

Setup Kraken

This form contains the model input parameters that are specific to the KRAKEN normal model. It is called from the **Path Env** form when the modal structure is needed in a vertical plane along a specific path, and from the **GridDB** form when a new set of phase speed and group speed databases are generated. For additional information on each input parameter, see the KRAKEN Users Guide [11]. Matlab files containing these parameters are loaded and saved into the current working directory.

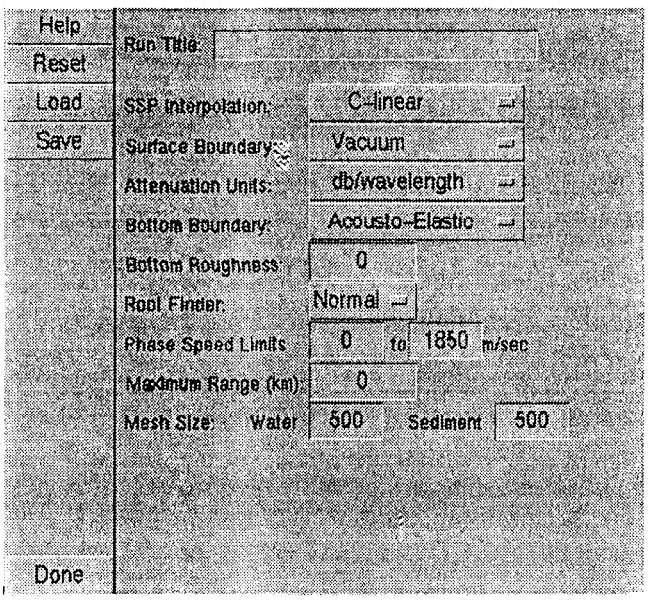

Run Title	Character string describing KRAKEN run. Used only in KRAKEN input files -- not HydroCAM or displays
SSP Interpolation	Method for interpolation versus depth
Surface Boundary	Use vacuum over open ocean, See Kraken Users Guide, p 82
Attenuation Units	db/wavelength for attenuation grids calculated using **GridDB**
Bottom Boundary	Use *Acousto-Elastic* for the default HydroCAM bottom. See *Bottom Characteristics* section of this users guide and Kraken manual p. 86
Bottom Roughness	Normally set to zero
Root Finder	The normal root finder is acceptable for most HydroCAM runs.
Phase Speed Limits	The larger high value is, more modes are calculated and saved
Maximum Range	Not used in HydroCAM since field calculations are not performed
Mesh Size	The mesh size is the number of points used as a function of depth to solve the finite difference equations in KRAKEN. In the water column, the rule of thumb is $10D/\lambda$, where D is the water depth and λ is the wavelength. For sediments, the rule is $20D/\lambda$ where D is the thickness of the sediment layer. The interface code uses the maximum of the input values on the form and these rules.

Net Perf

This form runs the network performance model to predict single sensor detection performance (SNR) and network localization performance. An SNR file (and a transmission loss TL file) are created for each receiver in the network, and a set of six files describing the network performance are also created. Grid files containing the attenuation, range, travel time and travel time standard deviation are required inputs to this model. These grid files can be generated directly using the **Paths** form. If path files were generated, they must be interpolated onto grids using the **Prop/Det** form before running the network model, or using the PathToGrid option in the **Paths** form.

After the SNR is calculated, each point on the grid is examined and compared to the SNR threshold specified under ***Network Model Parameters***. If the SNR is greater than this threshold, the receiver can "see" the source and the arrival time information for the receiver is included in the AOU calculation. The NDET grid contains the number of receivers at each point that meet this test. When the AOU is calculated, five grids are built in addition to the total number of detections (NDET): AOU, Lmajor, Lminor, ANGLE and Origin. The grids contain the AOU, the major and minor axis lengths of the error ellipse, the angle of the error ellipse and the origin time estimation error respectively. These grids can be displayed and analyzed using the **AOU** form. The SNR grids are normally displayed using the **Prop/Det** form.

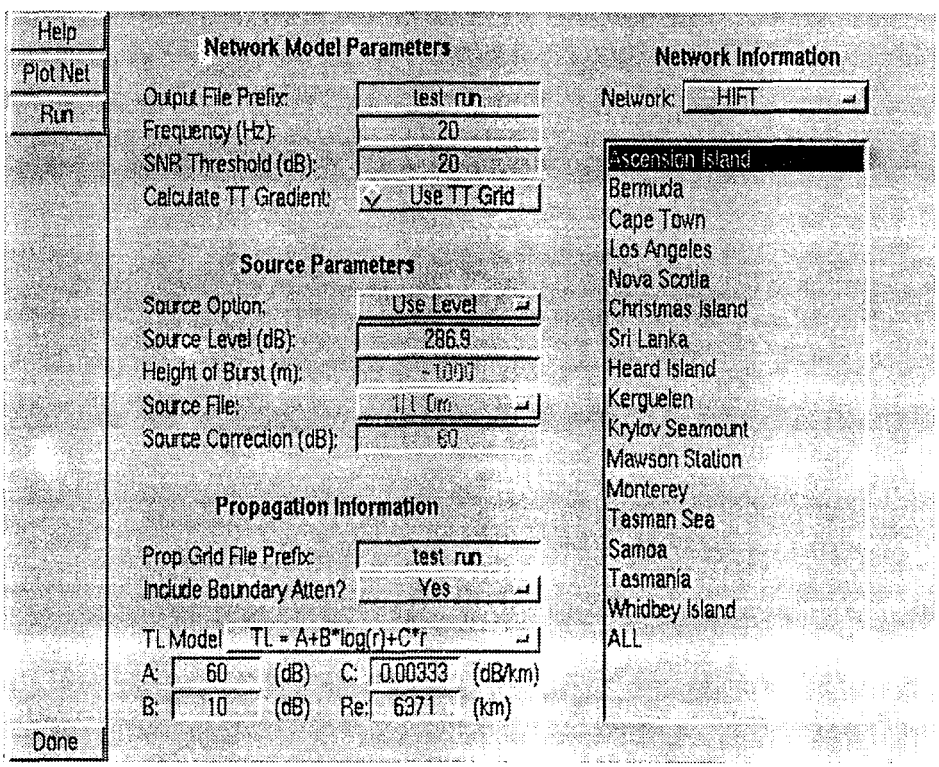

Button	Description
Plot Net	Plots station locations on the main geographic display
Run	Runs the network performance model. Requires a network list and range, attenuation, angle and standard deviation grid for each receiver in the network. Make sure SGRIDPATH is set to point to the directory where these grids are located. These grids are generated using the **Paths** form to run the propagation models. The Transmission Loss grid is generated from the range and attenuation grids using parameters specified under the ***Propagation Information*** section.
Done	Closes this form

Network Model Parameters -- These parameters are passed into the network prediction program.

Output File Prefix	Output file prefix added to the NDET, AOU, Lmajor, Lminor, ANGLE and Origin grid files. For the example form shown above, the output NDET file would be *test_runHIFT.NDETgrid*
Frequency	Used to interpolate values of ambient noise, directionality and system loss for each station Also used to interpolate the *Source Level* when the "Use File" *Source Option* is selected
SNR Threshold	Detection criteria used to determine which receivers contribute information to the localization solution
Calculate TT Gradient	If selected, the gradient of the measurements with respect to the source vector are calculated using finite differences applied to the travel time grid supplied for each receiver. Otherwise a simple analytic model for a spherical earth is used. (See the *Detailed Model Description Section)*

Source Parameters -- These parameters determine the source level that is passed into the network prediction program.

Source Option	Select "Use Level" to use the value in the *Source Level* field. Select "HOB model" and enter a source height in meters under *HOB* to use the 1kt source level table. Otherwise, select "Use File" and choose from the available files listed under *Source File*. When "Use File" is selected, the ESD is calculated from the file, the level at *Frequency* is interpolated, and the *Source Correction* is added to the level calculated from the file.
Source Level	Value used when "Use Level" is selected under *Source File*
Height of Burst	Height above the surface in meters of the source. Used to interpolate the 1kt ESL table developed at LLNL to determine the ESL.
Source File	File name of a CALE/NPE format pressure-time series file, located in the *~/config/source* directory
Source Correction	This factor corrects the source levels calculated using the *Source File* to equivalent source level at 1 m (required for the Sonar Equation).

Propagation Information -- This section of the form is used to specify the propagation paths to use for the predictions. *PropGrid File Prefix* is a character string prefix which is added to the abbreviation of each receiver in the network in order to determine the names for the propagation grid files. In the example form shown above, the transmission loss grid file would be *test_run.TLgrid* for the first receiver (Ascension Island) in the HIFT network

The transmission loss models are available from the popup menu. When *Include Boundary Atten* is selected, the boundary attenuation is added to the transmission loss calculated using the formula in the popup menu. A complete description of the transmission loss options is provided in the *Detailed Model Description* section of this report

Network Information - Used to display stations in the currently selected network

Profile Interpolation

This form is used to investigate the effects of different interpolation methods on temperature, salinity, sound speed or any other profile data.

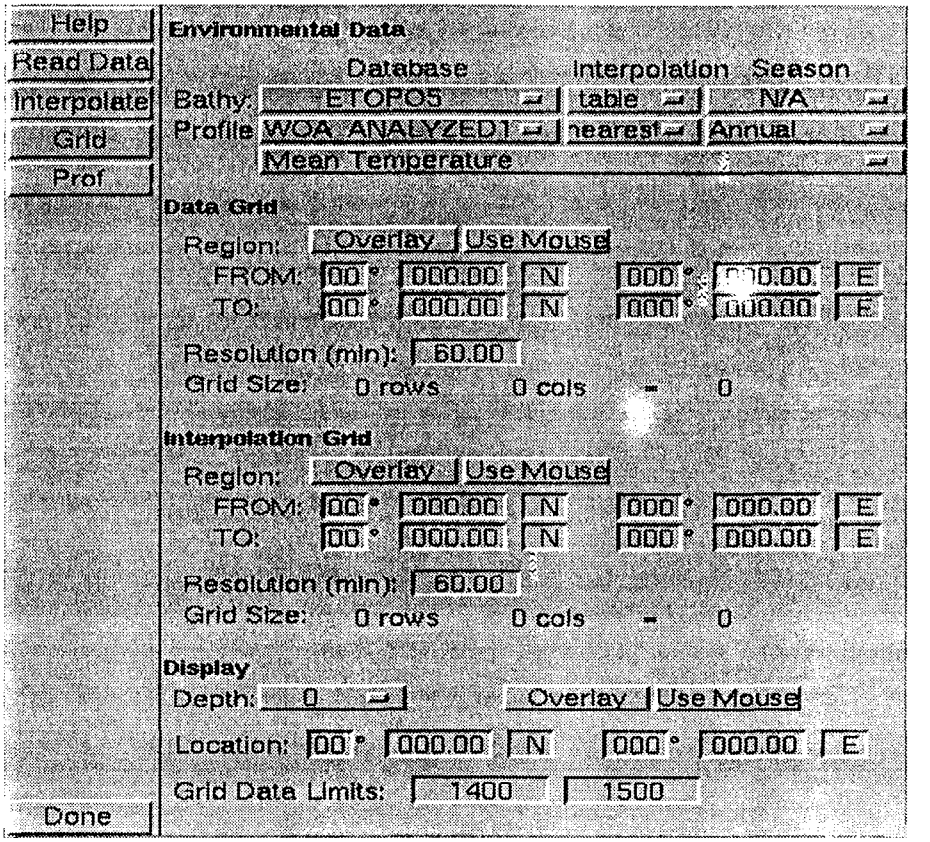

Button	Description
Read Data	Under the ***Environmental Data*** section of the form, select the database of interest and choose the parameter for the analysis. Available parameters include mean temperature, mean salinity or mean sound speed Select a region of interest in the ***Data Grid*** section Read Data extracts the region of interest from the selected databases and plots the profiles in a new window. The data is stored in the following MATLAB variables available to the user *prof_data* -- Matrix containing the profile data (one profile per column) *prof_depths* -- Matrix containing the profile depths in meters *prof_lat* -- Vector containing the profile latitudes *prof_lon* -- Vector containing the profile longitudes -- Vector describing the coordinates of the requested region *prof_res* -- Resolution of the grid in degrees

Interpolate	Select a depth in the ***Display*** section and a region/resolution to interpolate to under ***Interpolation Grid***. Interpolate uses the selected interpolation method to interpolate the profile data onto the new grid. Use Grid or Prof to display the interpolated data. The interpolated data is available to the user in the following Matlab variables: *intrp_data* -- Matrix containing the profile data (one profile per column) *intrp_depths* -- Matrix containing the profile depths in meters *intrp_lat* -- Vector containing the profilelatitudes *intrp_lon* -- Vector containing the profile longitudes *intrp_loc* -- Vector describing the coordinates of the requested region *intrp_res* -- Resolution of the grid in degrees
Grid	Displays the raw data and interpolated data grids at the depth selected under ***Display*** within the given limits. **Interpolate** must be run before **Grid** can be used.
Prof	Displays a plot graph of raw profile and interpolated profile vs depth at the location closest to the value specified under ***Display***. Interpolate must be run before Prof can be used.

Prop/Det

This form displays the results of propagation predictions and predicted SNR for single receivers. Note that some data such as SNR is by default a grid file; it will not load in if file type is set to Path.

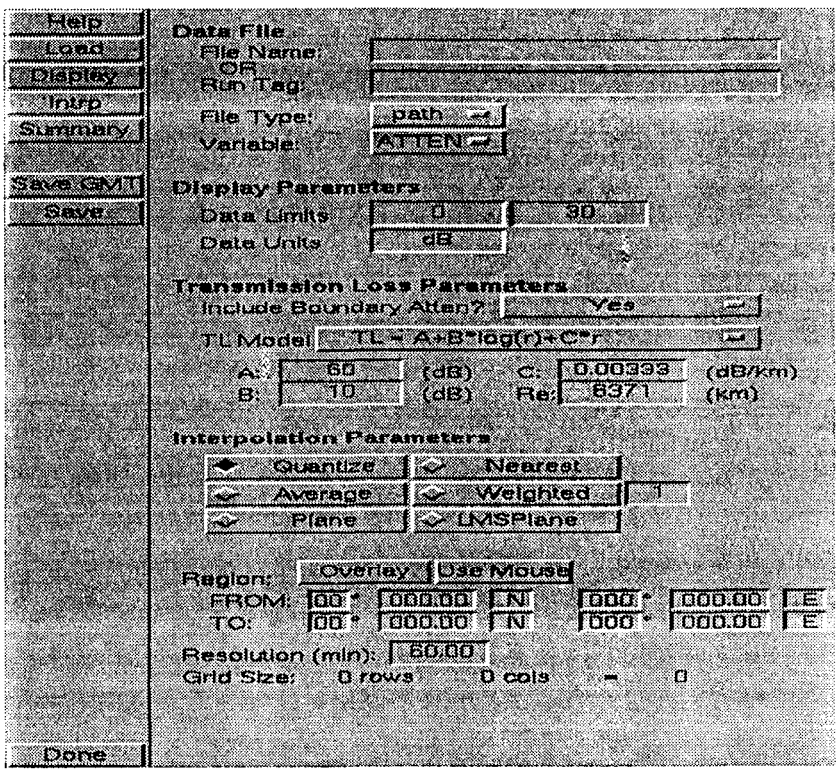

Button	Description
Load	Load file using complete *File Name* or using the *Run Tag*. *Run Tag* will search for a file name with the prefix from *Run Tag* and of type *Variable*. If the file is a path file, the data is loaded into the following MATLAB variables in the workspace: *PropVar:* Name of the variable that was loaded (eg "ATTEN") *PropType.*"Path" *PropVar1* is a matrix of data along each path (paths are in columns) *PropVar2* is a matrix containing the latitude of each path *PropVar3* is a matrix containing the longitude of each path The matrices are sized according to the number of points in the longest path. Any points after the end of the path are indicated by *NaN*. If the file is a grid file, the data is loaded into these variables in the MATLAB workspace: *PropVar* Name of the variable that was loaded (eg "ATTEN") *PropType.* "Grid"

	PropVar1: Geographic matrix containing the data and *PropVar2:* Vector of the coordinates bounding the data image.
Display	Plot the data loaded with **Load.** Uses predefined values as seen in the ***Display Parameters*** section of the form. Change these parameters to adjust the amplitude scale on the display.
Intrp	Interpolate the path data onto a grid covering the region entered under ***Interpolation Parameters*** at the chosen resolution. The interpolated grid is displayed in a new figure. The interpolation methods available are: *Quantize* -- Loops through each point on each path and places the data value into the grid cell that contains the path location. *Nearest* -- Uses the path value closest to each grid cell center. *Average* -- Uses the average of all path locations inside each grid cell. *Weighted* -- This option uses the "inverse distance" of interpolation with the weighting factor provided next to the pop-up menu. *Plane* - Constructs a plane which contains the 3 closest points in a cell. *LMS Plane* - This method uses a least mean squares estimate to a plane containing the points in a geographic cell. See the *Path Interpolation* section of this users manual for a complete description of each of these methods. The results are saved into MATLAB workspace variables *PropData,* which is a geographic matrix containing the data, and *PropLoc,* which is a four element vector containing the minimum and maximum latitudes and longitudes bounding the grid.
Summary	Displays a geographic figure summarizing a set of paths in a single path file. An example figure is shown below. This option is normally chosen when using a *List Scenario* to compare multiple paths arriving (or leaving) the same point.
Save GMT	Save the grid data contained in variables *PropVar1* and *PropVar2* in GMT format.
Save	Save the grid data contained in *PropVar1* and *PropVar2* in MATLAB format.

Data File -- This section of the form selects the propagation model or SNR data file to load. If an entry is present in *File Name* it is used, otherwise the values in *Run Tag, File Type* and *Variable* are used to select the file. The available variables are TL (transmission loss), TT (travel time), ST (travel time standard deviation), and SNR (signal to noise ratio). SNR is calculated by the network performance prediction program using the **Net Perf** button on the tool bar. The other variables are created by the propagation models and the **Path** tool.

Display Parameters – The limits and units for the data display are set here.

Transmission Loss Parameters - This is used with **Summary** to display TL grid data generated from range (and optionally attenuation) grid data. Three transmission loss models are available form the popup menu. When *Include Boundary Atten* is selected, the boundary attenuation is added to the transmission loss calculated using the formula in the popup menu. A complete description of the transmission loss options is provided in the *Detailed Model Description* section of this report.

Interpolation Parameters – Parameters used to interpolate path data onto a grid are selected here. See the *Path Interpolation* section of this users manual for a complete description of each of the available methods.

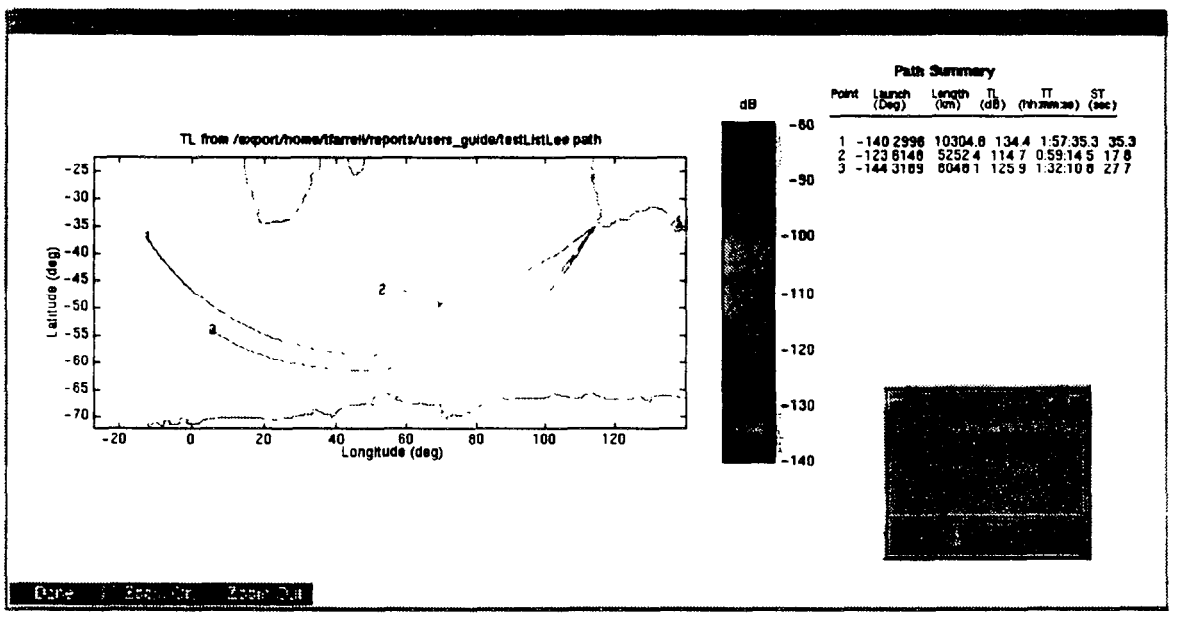

Example propagation path analysis figure generated using the **Summary** button on the *Prop/Det* form. The geographic display shows all paths included in the selected path file. The paths are color coded using the data from the *Variable* selected under ***Data File*** section, with the color limits specified by the values in *Data Lmits* under the ***Display Parameters*** section of the form. The transmission loss, travel time and travel time standard deviation from the start to the end point of each path is listed in the table on the top right of the display. This information is also available by clicking on the numbers at each path endpoint in the geographic portion of the display. The bottom right shows the figure that is created when a user has clicked on end point 1 of this geographic display.

AOU

This form displays network performance results, including SNR and localization AOU.

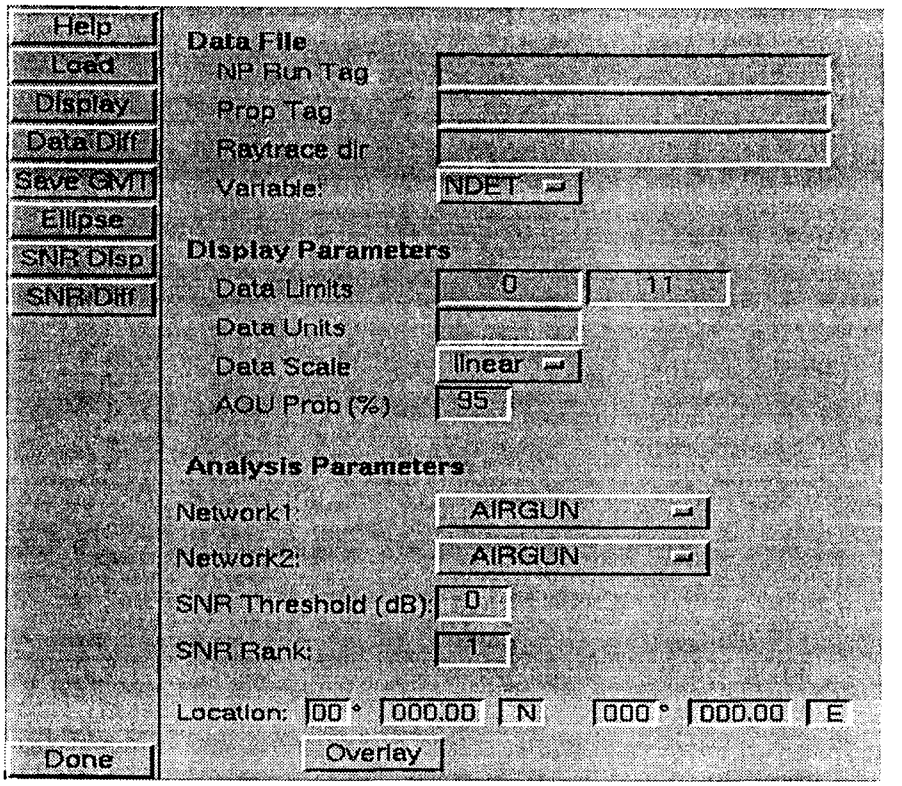

Button	Description
Load	Loads a datafile of type specified in *Variable* from the ***Data File*** section. Data is loaded into the MATLAB workspace variable *aou_data*, and the geographic coordinates describing the boundaries of the grid are provided in *aou_loc*.
Display	Plots *aou_data* from the file retrieved with the **Load** button The limits of the color scale are set using the values under ***Display Parameters***. The color scale may be linear or logarithmic as chosen using *Data Scale* (log is usually preferred for AOU coverage maps). The value in *AOU Prob* is used to scale the normalized AOU parameters calculated by the network performance model to the parameters for the error ellipse containing the selected percentage probability. Increasing this value will increase the size of the error ellipse Choosing very large values (above 95%) may result in invalid AOU displays as the linearity assumptions inherent in the network performance model may not hold.
Data Diff	Prompts the user to load two data files using the parameters from the ***Data File*** section It then plots the difference in these values in the same manner as **Display**

SNR Disp	Displays a SNR grid summarizing the detection performance for all of the networks selected under ***Analysis Parameters***. The display shows the *Nth* largest SNR value in each grid cell, where the value of *N* is specified in the *SNR Rank* edit field. Entering a *1* results in a display of the best SNR seen by all receivers in the network.
Ellipse	Displays details of the AOU for a specific source location, as shown in the figure below. Select a network and source location in the ***Analysis Parameters*** section. The SNR grids files which start with *Run Tag* are loaded for each receiver in the network. The travel time (TT) and travel time standard deviation (ST) grid files which start with *Prop Tag* are also loaded. Only receivers whose SNR is above the *SNR Threshold* are included in the display. As the threshold on the AOU form may not be the same threshold used in the network prediction, these receivers may not be the same receivers contributing to the AOU shown on the display.
SNR Diff	Displays the difference in SNR Grids of *Network1* and *Network2*.
Save GMT	Saves the data loaded into *aou_data* and *aou_loc* in a GMT format file.

Data File – These parameters control which data files are available for loading. The *Run Tag* is a prefix applied to the output files of the network prediction software. The *Path Tag* is a prefix applied to the output files of the propagation software. Note that the *Run Tag* and *Path Tag* must include the full path if those files are in another directory. *Raytrace Dir* is the directory containing the raytrace files. The variables available for loading are:

Variable	Description
NDET	Number of receivers whose SNR is above the threshold specified in the performance prediction run (NOT THE THRESHOLD ON THIS FORM).
Lmajor	Length of the major axis of the error ellipse in km.
Lminor	Length of the minor axis of the error ellipse in km
Angle	Angle in degrees true north of the error ellipse
AOU	Area of Uncertainty in square km.
Origin	Standard deviation of the origin time error (seconds)

Display Parameters -- Limits and units and scale for the plot generated using the **Display** and **Display SNR** buttons. AOU values are usually plotted using a log scale. *AOU Prob* is the probability included in the error ellipse, and is used for all displays and calculations of the ellipse parameters (AOU, Lmajor, Lminor). This option is required since the error ellipse values generated by the network performance software are normalized. The default is 95%.

Analysis Parameters -- These variables are used when the **SNR Display** and **Ellipse** displays are generated. When an **SNR Display** is requested, the *SNR Rank* is used to form a single plot containing the *Nth* largest SNR seen by the network at each source location in the grid. The grid cell locations nearest to the *Location* provided in this section is used for the error ellipse display generated using the **Ellipse** button. In addition, the contributing receivers listed on the right hand side of the display (see the figure below) are selected if the SNR is predicted to be above the threshold specified in *SNR Threshold.*

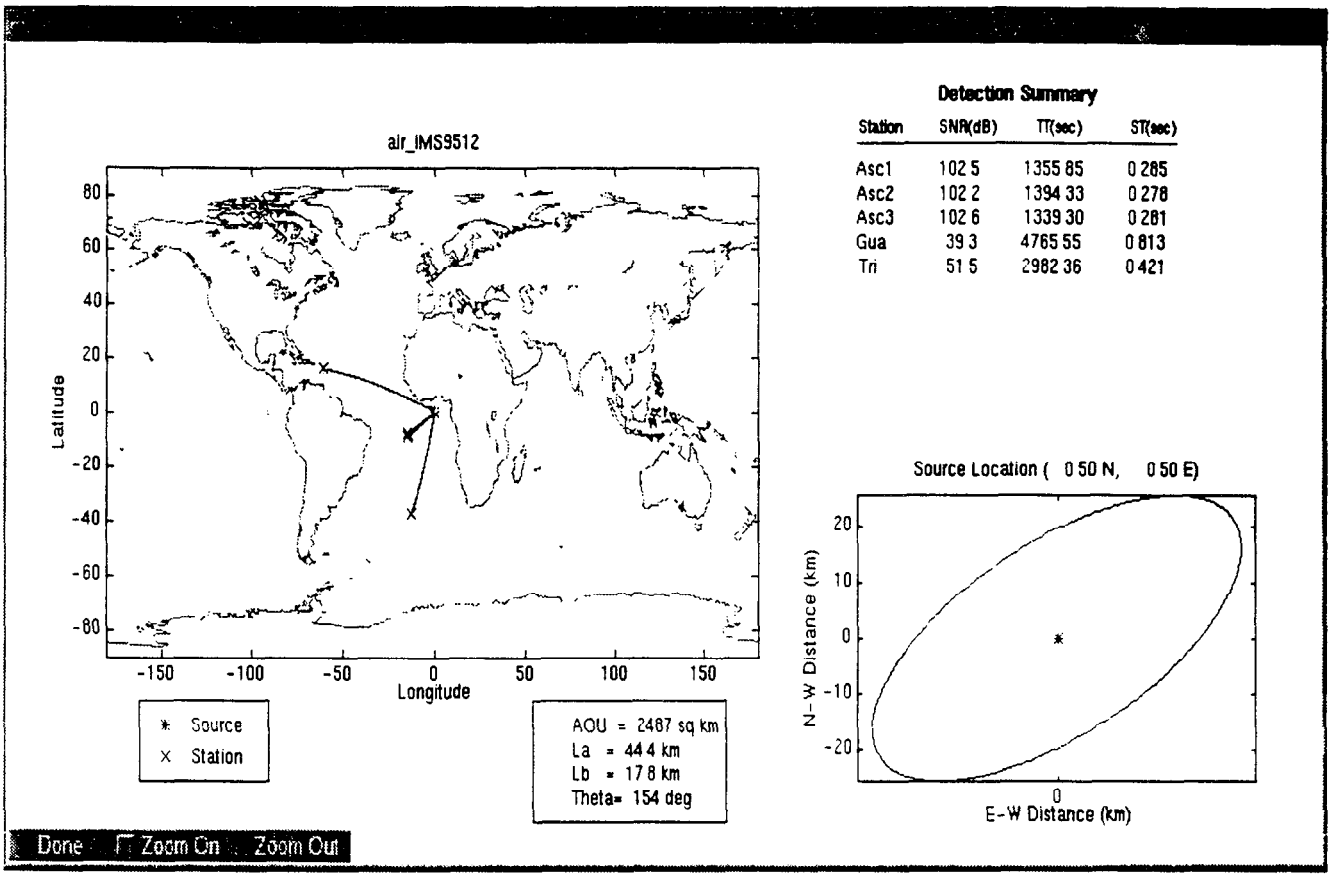

Example error ellipse analysis figure generated using the **ellipse** button on the *AOU* form. The geographic display shows the source location specified on the form and all receivers with SNR greater than the SNR threshold. The paths connecting the source and receivers are calculated in the display software using geodesic paths and do not necessarily represent the paths used in the propagation and AOU prediction software. The SNR, travel time and travel time standard deviation along each path is listed in the table on the top right of the display. This information is also available by clicking on the receivers in the geographic portion of the display. The bottom right of the display shows a blowup of the error ellipse in kilometers near the source location.

References

[1] T.R. Farrell and K.D. LePage. *Travel time variability and localization accuracy for global scale monitoring of underwater acoustic events.* JASA 99(4), April 1996.

[2] R.M. Jones, J.P. Riley, and T.M. Georges, *HARPO: A Versatile Three-Dimensional Hamiltonian Ray-Tracing Program for Acoustic Waves in an Ocean with Irregular Bottom.* NOAA Wave Propagation Laboratory, October 1986.

[3] D.B. Clarke, *Pressure Time Histories Derived from Hydroacoustic Coupling Calculations: The Transition to Long Range Linear Acoustics.* LLNL Report UCRL-ID-122595, December 1995.

[4] J. Wakeley, *Pressure Signature Model for an Underwater Explosive Charge*, US Navy Journal of Underwater Acoustics Vol 27, No2. April 1977.

[5] G.M. Wenz, *Acoustic Ambient Noise in the Ocean, Spectra and Sources.* JASA 34(12), December 1962.

[6] D.B. Harris, Personal Communication.

[7] JASA **96** (4), October 1994. This issue contains a collection of papers describing the Heard Island Feasibility Test (HIFT).

[8] R.C. Shockley, J. Northrop and P.G. Hansen. *SOFAR Propagation Paths from Australia to Bermuda: Comparison of Signal Speed Algorithms and Experiments*, JASA **71**(1) p. 51, January 1982.

[9] T.R. Farrell, K.D. LePage. *Development of a Comprehensive Hydroacoustic Coverage Assessment Model Final Report*, BBN Technical Report W1278, September 1996.

[10] M. Collins, *User's Guide for RAM Versions 1.0 and 1.0p*, NRL, 1995.

[11] M. B. Porter, *The KRAKEN Normal Mode Program*, SACLANT Undersea Research Centre, October 30, 1995.

[12] H. Weinberg, *Generic Sonar Model*, NUSC Technical Document 5971D, 6 June 1985.

[13] *Database Description for the Master Generalized Digital Environmental Model (GDEM) Version 5.0*, OAML DBD-20F, Naval Oceanographic Office, Stennis Space Center MS. September 1995.

[14] Levitus and Boyer "World Ocean Atlas 1994 Volume 4: Temperature", NOAA Atlas NESDIS 4, Washington, DC. June 1994.

[15] Mackenzie, "Nine-term Equation for Sound Speed in the Oceans", JASA **70**, p. 807, 1981.

[16] Larsen and Marx, An Introduction to Mathematical Statistics and Its Applications, Prentice-Hall, 1981, p. 124.

[17] F.B. Jensen, W.A. Kuperman, M.B. Porter, H. Schmidt, *Computational Ocean Acoustics,* AIP Press, 1994.

[18] G. Orris, Personal Communication

[19] K.D. Heaney, W.A. Kuperman and B.E McDonald. "Perth-Bermuda sound propagation (1960): Adiabatic mode interpretation", JASA **90**(5), November 1991, p. 2589.

[20] M.D. Collins, B.E McDonald, K.D. Heaney and W.A. Kuperman. *Three-dimensional effects in global acoustics,* JASA **97**(3), March 1995, p 1567.

[21] G.I. Evenden. *USGS Cartographic Projection Software (PROJ.4)* . Available over the internet at *kai.er.usgs.gov.* Email to gie@kai.er.usgs.gov.

[22] Ralston, A First Course in Numerical Analysis, McGraw-Hill, 1965, p120-121.

[23] Hydrographic Atlas of the Southern Oceans. Http://www.awi-bremerhaven.de/

[24] Lynch, et al. "Three dimensional Ray Acoustics in a Realistic Ocean" in Oceanography and Acoustics: Prediction and Propagation Models, AIP 1994.

[25] Van Trees, Harry L. Detection and Estimation Theory, Part I. John Wiley and Sons, 1968.

[26] W.H.F. Smith, D.T Sandwell. "Global Seafloor Topography from Satellite Altimetry and Depth Soundings", Science 277 (5334): 1956, September 26, 1997. Available at topex.ucsd.edu/marine_topo/mar_topo.html

[27] Available from the National Snow and Ice Data Center at: www -- nsidc.colorado.edu

[28] J.S. Angell, T.R. Farrell and K.D. LePage. "Hydroacoustic Propagation Grids for the CTBT Knowledge Database",. BBN Technical Memorandum W1303, October 1997.

[29] Duckworth, Farrell, LePage and Atkinson. "Article LFA Final Report", BBN Technical Report W12226, ONR/AEAS Technical Report 94-5102, September 30, 1994 (SECRET).

[30] D.F. Watson, Contouring: A Guide to the Analysis and Display of Spatial Data, Pergamon, 1994.

Appendix A
Faster mode computations using the WKB approximation

This appendix describes a technique by which the computation of modal eigenvalues and the corresponding mode shapes can be accelerated through the use of approximate techniques. This approach is motivated by the fact that HydroCAM requires evaluations of a large number of modal properties over a global grid. These properties are required by the model for the purposes of estimating travel time, travel time variance and refracted geodesics for global propagation studies. Currently modal properties are calculated using the KRAKEN model, which is a general purpose research grade propagation code. However, the precision of KRAKEN comes at some computational cost. What is desired is a technique which can acheive results close to what KRAKEN obtains with less precision but greater speed.

The approach is a hybrid Wenzel-Kramers-Brillouin-Finite-Difference (WKB-FD) scheme which estimates the modal eigenvalues using the WKB approximation, and then refines this estimate and simultaneously estimates the mode shapes through the use of a finite difference scheme. This technique is faster than KRAKEN, which is also a FD formulation, because the eigenvalue estimate obtained with the WKB approximation is much more quickly obtained than determining the eigenvalue directly from the FD matrix. KRAKEN is also slowed by the fact that it returns all the mode shape functions and eigenvalues which fall between user supplied phase velocity limits. In interactive global propagation studies, often only one mode at a time is required.

WKB approximation

The WKB approximation is useful for estimating the modal eigenvalue because it can be used to define a simple cost function for the total phase accumulated by a ray as it travels one cycle distance. This cost function is a non-linear function of the modal eigenvalue. Since a ray which constructively reinforces itself is a resonance to the Helmoltz equation and therefore a mode, non-linear optimization of the cost function may be used to directly estimate the eigenvalue. As seen below, the estimated eigenvalue is not the true eigenvalue because of the approximations taken in the WKB approximation.

The WKB approximation is quickly derived by seeking an approximate solution to the depth separated Helmholtz equation [1]

$$\left\{\frac{\partial}{\partial z^2} + k_z^2\right\}\hat{\psi}(z) \equiv 0 \qquad \text{(A1)}$$

where

$$\hat{\psi}(z) \equiv \chi(z) e^{\imath \eta(z)}$$

and the vertical wavenumber is

$$k_z = \sqrt{k_0^2(z) - k_m^2}$$

where k_m is the desired modal eigenvalue, also known as the horizontal wavenumber. Evaluation of the second order partial derivative in equation (A1) leads to the following requirements for the real and the imaginary parts of equation (A1) to hold separately:

$$\Re\left\{\left\{\frac{\partial}{\partial z^2} + k_z^2\right\}\hat{\psi}(z) = 0\right\} \rightarrow -(\eta')^2 \chi + \chi'' + k_z^2 \chi = 0 \qquad \text{(A2)}$$

and

$$\Im\left\{\left\{\frac{\partial}{\partial z^2} + k_z^2\right\}\hat{\psi}(z) = 0\right\} \rightarrow \eta'' \chi + 2\eta' \chi' = 0 \qquad \text{(A3)}$$

Equation 2 may be approximately satisfied by the identification

$$\eta' \approx k_z \qquad \text{(A4)}$$

if the second derivative of the envelope function χ is small compared to the vertical wavenumber, a requirement which is generally met except in the vicinity of the locale $k_m \approx k_0$ which is the turning point of the ray. Inserting equation A4 into equation A3 in turn yields the differential equation

$$k_z' \chi + 2 k_z \chi' = 0. \qquad \text{(A5)}$$

Solution to equation A5 is found by substituting the rational parameterization

$$\chi = k_z^{\alpha}$$

and solving for α. Doing this and integrating equation A4 once yields the WKB approximation for the modal eigenfunction

$$\hat{\psi}(z) = \frac{e^{\imath \int k_z(z) dz}}{\sqrt{k_0^2(z) - k_m^2}} \qquad \text{(A6)}$$

A mode exists when the phase accumulated between the turning points of the ray (depths at which $k_z=0$) equals an integer multiple of 2π. It is important to include the $\pi/2$ phase advance accompanying each ray turning event in the accumulated phase [2]. The requirement that the accumulated phase for a trial modal eigenfunction must meet is given by the relation

$$2\int_{z_l}^{z_u}\sqrt{\omega^2 c^{-2}(z)-k_m^2}\,dz = 2m\pi - \pi \qquad \text{(A7)}$$

The lower and upper turning points z_l and z_u of the integral in equation A7 satisfy the requirements

$$c(z_l) = \omega / k_m$$

and

$$c(z_u) = \omega / k_m$$

The reasons that satisfaction of equation A7 does not give the exact eigenvalue k_m are 1) the $\pi/2$ phase accumulation at the turning points is a high frequency approximation, and 2) the argument to the exponential in the numerator of equation A6 as an approximation for the vertical phase accumulated by a mode. Despite these inaccuracies, iterative solution of equation A7 yields estimates for the modal eigenfunctions which are in very close agreement to those determined by KRAKEN, even at low frequencies or when modes interact with boundaries. When mode shapes interact at the upper free surface, the accumulated phase requirement must be modified to account for the π phase change at the surface

$$2\int_{z_l}^{z_u}\sqrt{\omega^2 c^{-2}(z)-k_m^2}\,dz = 2m\pi - \pi/2 - \pi \qquad \text{(A8)}$$

When mode shapes interact with the bottom, the phase accumulated due to complex reflection coefficient R_b is

$$\theta_b = \arctan\left\{\Im(R_b)/\Re(R_b)\right\},$$

or in terms of the real and imaginary parts of the complex bottom impedance Z_b

$$\theta_b = \arctan\left\{\frac{\Im(Z_b)/\rho c(z_b)}{1+\Re(Z_b)/\rho c(z_b)}\right\}.$$

In these cases, if the mode does not interact with the free surface the accumulated phase requirement may be written

$$2\int_{z_l}^{z_u}\sqrt{\omega^2 c^{-2}(z)-k_m^2}\,dz = 2m\pi - \pi/2 - \theta_b \qquad \text{(A9)}$$

Finally, if the mode interacts both with the ocean surface and the bottom, the accumulated phase must satisfy the relation

$$2\int_{z_l}^{z_u}\sqrt{\omega^2 c^{-2}(z)-k_m^2}\,dz = 2m\pi - \pi - \theta_b \qquad \text{(A10)}$$

Equations A7 through A10 are solved interatively for the modal eigenvalue k_m through the use of Brent's method [3] calling a function which returns an error metric proportional to the square of the difference between the right hand and the left hand sides of these equations. When the error metric is minimized, Brent's method returns the eigenvalue estimate. This eigenvalue estimate is refined and the corresponding eigenvector or mode shape is estimated using a FD scheme.

Using Finite Differences

With a good estimate of the modal eigenvalue, one can apply the finite difference (FD) scheme to determine the corresponding modal eigenfunction. The resulting mode shapes can also be used to refine the modal eigenvalue estimate. The depth separated Helmholtz equation

$$\left\{\frac{\partial}{\partial z^2}+k_0^2(z)-k_m^2\right\}\psi = 0$$

with an arbitrary impedance boundray condition at the bottom

$$\left(\frac{\partial}{\partial z}+i\omega\rho/Z\right)\psi = 0$$

(which may be used to represent a radiation condition to infinite depth to limit the problem for deep water,) may be written as a generalized eigenvalue problem using second order finite differences [4]

$$\left(\mathbf{A}-k_m^2\mathbf{I}\right)\Psi = 0$$

where the matrix **A** is a tri-diagonal approximation to the second partial derivative in depth which also includes on the main diagonal the addition of the local term $k_0^2(z)$. Given the WKB estimate of the modal eigenvalue k_m the mode shape itself may be estimated using inverse iteration [5]

$$\left(\mathbf{A} - k_m^2\mathbf{I}\right)\Psi_{i+1} = \Psi_i \qquad \text{(A11)}$$

where the subscript *i* indicates the iteration number. In addition, after a few iterations of equation A11 for the mode shape function, the modal eigenvalue itself may also be refined through the update procedure

$$\left(k_m^2\right)^{i+1} = \left(k_m^2\right)^i + \frac{\Psi_{i+1}^T \Psi_i}{\left|\Psi_{i+1}\right|^2}$$

Modal Attenuation

Modal attenuation can be readily derived from perturbation to the horizontal wavenumber given in Appendix B

$$\Delta k_m = -\frac{\omega^2}{k_m^0}\int_{-\infty}^{0} \frac{\Delta c(z)}{c_0^3(z)} \frac{\psi_m^2(z)}{\rho(z)} dz \qquad \text{(B3)}$$

where $\rho(z)$ is the density profile. The attenuation to be included in the modal eigenvalue is usually expressed in terms of a bottom attenuation Λ in dB/λ. This loss can be re-written in terms of an imaginary component of the sound speed. The definition of loss can be used to determine the imaginary part of the bottom wavenumber ηk_b as follows

$$\begin{aligned} A &= -20\log_{10}\left(\left|e^{ik_b(1+i\eta)\lambda}\right|\right) \\ &= -20\log_{10}\left(\left|e^{-2\pi\eta}\right|\right) \\ &= 54.6\eta \end{aligned}$$

Since we are interested in small perturbations, the imaginary part of the wavenumber is linearly related to the imaginary part of the sound speed, $c_b\zeta$

$$\begin{aligned} k_b(1+i\eta) &= \omega c_b^{-1}(1-i\zeta) \\ \zeta &= -\eta = -A/54.6 \end{aligned}$$

If we treat the imaginary part of the sound speed as the perturbation in equation (B3), we obtain an expression for the imaginary part of the modal eigenvalue

$$\Im(k_m) = \frac{Ak_b^2}{54.6k_m^0}\int_{-\infty}^{-D}\frac{\psi_m^2(z)}{\rho_b(z)}dz \qquad \text{(A12)}$$

where D is the bottom depth and the bottom wavenumber k_b is equal to ω/c_b.

Since the WKB mode approximations described above do not include the mode shape function in the bottom, this needs to be calculated from the mode shape function value at the bottom $\psi_m(-D)$ and the modal eigenvalue k_m. From the latter, the imaginary vertical wavenumber in the bottom may be determined

$$k_{bz} = i\sqrt{k_m^2 - \omega^2 c_b^{-2}},$$

yielding the following expression for the modal eigenfunction in the bottom.

$$\psi_m(z) = \psi_m(-D)e^{-k_{bz}(D-z)} \qquad z < -D$$

This in turn may be squared and inserted into equation (A12), yielding a closed form expression for the bottom attenuation in terms of the known bottom density and sound speed ρ_b and c_b, the desired bottom attenuation A in dB/λ, the frequency ω, the unperturbed modal eigenvalue k_m^0 and the mode shape function at the bottom $\psi_m(-D)$

$$\Im(k_m) = \frac{Ak_b^2\psi_m^2(-D)}{k_m^0\rho_b\sqrt{k_m^2 - k_b^2}}$$

where as before the bottom wavenumber k_b is equal to ω/c_b.

References

[1] Jensen, Kuperman, Porter and Schmidt. Computational Ocean Acoustics, Section 2.5.2

[2] Tolstoy and Clay. Ocean Acoustics, Appendix 1.

[3] Press, Flannery, Teukolsky and Vetterling, Numerical Recipies in C, Section 10.2.

[4] Porter and Reiss, *A numerical method for bottom interacting ocean acoustic normal modes*, JASA 77, pp 1760-1767 (1985)

[5] Press, Flannery, Teukolsky and Vetterling, Numerical Recipies in C, Section 11.7

Appendix B
Expressions for the statistics of modal properties

This appendix documents the derivation of expressions for the statistics of modal properties used in HydroCAM. In particular, perturbation theory is applied to equations for the horizontal wavenumbers, group velocities, and modal slowness variance.

The analysis begins with the depth-separated Helmholtz equation for laterally homogeneous waveguides of constant depth

$$\left\{\frac{\partial^2}{\partial z^2}+\left(\frac{\omega^2}{c(z)^2}-k_m^2\right)\right\}\psi_m(z)=0 \qquad \text{(B1)}$$

where $c(z)$ is the sound speed as a function of depth, and k_m and $\psi_m(z)$ are the horizontal wavenumber and the mode shape function corresponding to the m^{th} mode respectively.

Perturbation of horizontal wavenumber

For horizontal ray tracing on the surface of the world, the perturbations to these wavenumbers as functions of small variations to the sound speed profile may be desired in lieu of a full re-calculation based on full or approximate wave theory. Expanding the sound speed $c(z)$ about some mean sound speed c_0 plus a random perturbation Δc, we write the second term in equation B1

$$k_{(z)}^2=\frac{\omega^2}{\left(c_0(z)+\Delta c(z)\right)^2}\cong\omega^2\left\{c_0^{-2}(z)-2\frac{\Delta c(z)}{c_0^3(z)}+h.o.t.\right\}.$$

Similarly, the square of the modal wavenumber may be expanded about a mean value corresponding to the unperturbed sound speed profile

$$k_m^2\approx\left(k_m^0\right)^2+2k_m^0\Delta k_m$$

so that the terms in equation B1 may be grouped into $O(1)$ and $O(\Delta c/c)$ equations

$$O(1)\qquad\left\{\frac{\partial^2}{\partial z^2}+\left(\frac{\omega^2}{c_0^2(z)}-\left(k_m^0\right)^2\right)\right\}\psi_m(z)=0,$$

and

$$O(\Delta c/c) \quad \left\{ -2\omega^2 \frac{\Delta c(z)}{\underbrace{c_0^3(z)}_{function\_of\_z}} - 2k_m^0 \Delta k_m \right\} \psi_m(z) = 0 \qquad \text{(B2)}$$

Using the orthonormal properties of the mode shape functions

$$\int_{-\infty}^{\infty} \frac{\psi_m(z)\psi_n(z)}{\rho(z)} = \delta_{mn}$$

and the fact that the second term in equation B2 is not a function of depth, one solves for the perturbation to the horizontal wavenumber

$$\Delta k_m = -\frac{\omega^2}{k_m^0} \int_{-\infty}^{0} \frac{\Delta c(z)}{c_0^3(z)} \frac{\psi_m^2(z)}{\rho(z)} dz \qquad \text{(B3)}$$

where $\rho(z)$ is the density profile.

Modal group slowness by depth integration

For the development of subsequent expressions for modal slowness perturbations and variance, a brief derivation of the single frequency approximation for group slowness is given. The partial of equation B1 with respect to angular frequency yields

$$\left(2\frac{\omega}{c(z)^2} - 2\frac{\partial k_m}{\partial \omega} k_m \right) \psi_m(z) + \left\{ \frac{\partial^2}{\partial z^2} + \left(k^2(z) - k_m^2 \right) \right\} \frac{\partial \psi_m(z)}{\partial \omega} = 0 \qquad \text{(B4)}$$

Assuming $\frac{\partial \psi}{\partial \omega}$ is negligible, the first term of equation B4 may be integrated over depth to obtain the modal slowness

$$\frac{\partial k_m}{\partial \omega} = \frac{\omega}{k_m} \int_{-\infty}^{0} \frac{\psi_m^2(z)}{c^2(z)\rho(z)} dz. \qquad \text{(B5)}$$

Modal group slowness for sound speed perturbations

If we wish to evaluate how sound speed fluctuations manifest themselves into perturbations of the modal group slowness, we once again expand the inverse square of the sound speed about the mean

$$c^{-2}(z) \approx c_0^{-2}(z) - 2\frac{\Delta c(z)}{c_0^3(z)} + 3\frac{\Delta c^2(z)}{c_0^4(z)} + h.o.t. \qquad \text{(B6)}$$

and expand the modal group slowness about its unperturbed value

$$\frac{\partial k_m}{\partial \omega} = \frac{\partial k_m^0}{\partial \omega} + \Delta S_g \tag{B7}$$

Insertion of equations B6 and B7 into B4 and collection of $O(\Delta c/c)$ terms yields

$$\underbrace{\Delta S_g k_m^0}_{\text{independent of z}} \psi(z) = -2\omega \underbrace{\frac{\Delta c(z)}{c^3(z)}}_{\text{function of z}} \psi(z)$$

Integrating out the depth dependence by taking the inner product with the mode shape function yields an expression for the modal slowness perturbation based on a weighted depth integral of the sound speed perturbation

$$\Delta S_g = -2\frac{\omega}{k_m^0}\int_{-\infty}^{0} \frac{\Delta c(z)}{c_0^3(z)} \frac{\psi_m^2(z)}{\rho(z)} dz \tag{B8}$$

Equation B8 allows the estimation of the perturbations to the modal group slowness over a variety of sound speed profiles, using the modal wavenumber and mode shape function from a representative location, provided the first order terms in equation B6 dominate.

Modal slowness variance over sound speed perturbations

In order to quantify the travel time variability over horizontal paths due to temporal fluctuations in sound speed, we can derive a second order expression for the modal group slowness and take the formal ensemble average of the square of this expression, keeping terms to second order in $\Delta c/c$. Inserting equation B6 into equation B5 yields the approximation

$$S_g = \frac{\partial k_m}{\partial \omega} \approx \frac{\omega}{k_m^0}\int_{-\infty}^{0} \frac{\psi_m^2(z)}{\rho(z)} \left[c_0^{-2}(z) - 2\frac{\Delta c(z)}{c_0^3(z)} + 3\frac{\Delta c^2(z)}{c_0^4(z)} \right] dz \tag{B9}$$

Taking the ensemble over the square of equation B9 and including only those terms which will not average to zero yields

$$\left\langle S_g^2 \right\rangle = \frac{\omega^2}{k_m^2}\int_{-\infty}^{0} dz_1 \int_{-\infty}^{0} dz_2 \frac{\psi_m^2(z_1)\psi_m^2(z_2)}{\rho(z_1)\rho(z_2)}$$
$$\times \left\langle \left\{ c_0^{-2}(z_1)c_0^{-2}(z_2) + 4\frac{\Delta c(z_1)\Delta c(z_2)}{c_0^3(z_1)c_0^3(z_2)} + 3\frac{\Delta c^2(z_1)}{c_0^4(z_1)c_0^2(z_2)} + 3\frac{\Delta c^2(z_2)}{c_0^4(z_2)c_0^2(z_1)} \right\} \right\rangle \tag{B10}$$

The mean of equation B9 may also be evaluated

$$\langle S_g \rangle = \frac{\omega}{k_m^0} \int_{-\infty}^{0} \frac{\psi_m^2(z)}{\rho(z)} \left[c_0^{-2}(z) + 3 \frac{\langle \Delta c^2(z) \rangle}{c_0^4(z)} \right] dz. \qquad \text{(B11)}$$

To evaluate the slowness variance we subtract the square of equation B11 from equation B10. Using equation B5 to simplify results in an expression for the variance of the local modal group slowness in terms of the vertical statistics of the sound speed fluctuations

$$\sigma_{S_g}^2 = 4 \frac{\omega^2}{\left(k_m^0\right)^2} \int_{-\infty}^{0} dz_1 \int_{-\infty}^{0} dz_2 \frac{\psi_m^2(z_1)\psi_m^2(z_2)}{\rho(z_1)\rho(z_2)} \frac{\langle \Delta c(z_1)\Delta c(z_2) \rangle}{c_0^3(z_1)c_0^3(z_2)} \qquad \text{(B12)}$$

If the statistics of the sound speed fluctuations versus depth are stationary, then equation B12) can be written using the vertical slowness correlation function $R(\Delta z)$ as

$$\sigma_{S_g}^2 = 4 \frac{\omega^2}{\left(k_m^0\right)^2} \int_{-\infty}^{0} dz \frac{\psi_m^2(z)\sigma_{\Delta c}^2(z)}{\rho(z)c_0^3(z)} \int_{-\infty}^{0} d\Delta z \frac{\psi_m^2(z+\Delta z)R(\Delta z)}{\rho(z+\Delta z)c_0^3(z+\Delta z)}. \qquad \text{(B13)}$$

From equation B11, an expression for the slowness bias due to the sound speed fluctuations is

$$S_g - \langle S_g \rangle = -3c_m^0 \int_{-\infty}^{0} \frac{\psi^2(z)}{\rho(z)} \frac{\sigma_{\Delta c}^2(z)}{c_0^4(z)} dz, \qquad \text{(B14)}$$

where c_m^0 is the modal phase velocity ω / k_m^0. This equation implies that the mean slowness is slower than what one would estimate using the mean water column properties alone. In practice, this bias is extremely small and can be neglected.

Appendix C -- Bending Global Rays

This appendix documents the development of a perturbational approach for computing horizontally refracted raypaths on global scales. Typical applications of HydroCAM, most notably network performance studies and analysis of existing datasets, use fixed source and receiver geometries. The traditional approach to solving this problem is to iteratively perturb the ray's initial launch angle until the refracted path from the source passes through the known receiver position. Unfortunately, this approach suffers from stability problems and is very computationally intensive.

An alternate approach is to perturb an initial path connecting a source and receiver using the gradients of the index of refraction along the path. Iteratively "bending" the raypath using this approach may result in a path close to the actual horizontally refracted eigenray. The advantages of this "bending" approach include computational efficiency and robustness (ie, the ray path always connects the source and receiver). Disadvantages are currently under investigation, but of course include the fact that the approach is iterative. The Bender is provided as part of HydroCAM to facilitate these studies. The primary references to this work are a paper by Collins and Kuperman where similar methods were used to overcome ray chaos [1] and a discussion of the use of relaxation techniques in two-point boundary value problems by Press et. al. [2].

Geodesic Ray Equations

The coupled ray equations on a geodesic surface have been derived by Heaney et al [3]

$$\frac{\partial \phi}{\partial s} = \frac{\cos\alpha}{\mu(\phi)} \tag{C1a}$$

$$\frac{\partial \lambda}{\partial s} = \frac{\sin\alpha}{\eta(\phi)\cos\phi} \tag{C1b}$$

$$\frac{\partial \alpha}{\partial s} = \frac{\sin\alpha}{\eta(\phi)}\tan\phi - \left(\frac{\sin\alpha}{\mu(\phi)}\frac{\partial}{\partial\phi} - \frac{\cos\alpha}{\eta(\phi)\cos\phi}\frac{\partial}{\partial\lambda}\right)\ln k_n \tag{C1c}$$

where ϕ, λ and α are the latitude, longitude and ray angle in radians (ray angle measured clockwise from north), and k is the wavenumber which is a function of ϕ, and λ . The local radii of curvature

$$\mu(\phi) = \frac{r_{eq}\left(1-\varepsilon^2\right)}{\left(1-\varepsilon^2\sin^2\phi\right)^{3/2}}$$

$$\eta(\phi) = \frac{r_{eq}}{\left(1 - \varepsilon^2 \sin^2 \phi\right)^{1/2}},$$

are defined in terms of the radius of the earth at the equator r_{eq}, and the eccentricity of the earth ε. Examination of (C1a) shows that the derivatives are taken with respect to the path length s, and that horizontal refraction is contained in the spatial derivatives of the horizontal wavenumber in (C1c). To ease subsequent manipulations, equations C1 may be written in a non-linear state equation form

$$\frac{d}{ds}\begin{bmatrix}\phi\\ \lambda\\ \alpha\end{bmatrix} = \begin{bmatrix} f(\phi,\alpha)\\ g(\phi,\alpha)\\ h(\phi,\lambda,\alpha)\end{bmatrix}. \qquad \text{(C2)}$$

Perturbations from a Notional Trajectory

In the case where the notional trajectory is the geodesic path, the approach to perturbing equations C1 is essentially to assume that all the deviations to the ray trajectory are caused by the non-zero partials of the refractive index $\frac{\partial \ln k}{\partial \phi}$ and $\frac{\partial \ln k}{\partial \lambda}$. Indeed, without these forcing terms the equations C1 simply give the geodesic paths on the surface of the earth, which are the shortest distance between any two points following a trajectory confined to the surface. However it should be noted that the notional trajectory may be any trajectory which connects the source and receiver chosen for reasons of convenience. This may be an attractive alternative when the geodesic between a source and receiver passes through an obstruction such as an island. In this case it is quite possible that the refracted path will not be obstructed by the island, but in order for the perturbation to work, the notional trajectory must have meaningful gradients of the index of refraction along its entire length.

To obtain the perturbations to the notional path, the Taylor series expansions of the non-linear state equation C2 are first obtained

$$\begin{aligned}
\frac{d\phi}{ds} + \frac{d\delta\phi}{ds} &= f(\phi,\alpha) + \delta\phi\frac{\partial f}{\partial \phi} + \delta\alpha\frac{\partial f}{\partial \alpha} + h.o.t.\\
\frac{d\lambda}{ds} + \frac{d\delta\lambda}{ds} &= g(\phi,\alpha) + \delta\phi\frac{\partial g}{\partial \phi} + \delta\alpha\frac{\partial g}{\partial \alpha} + h.o.t.\\
\frac{d\alpha}{ds} + \frac{d\delta\alpha}{ds} &= h(\phi,\lambda,\alpha) + \delta\phi\frac{\partial h}{\partial \phi} + \delta\lambda\frac{\partial h}{\partial \lambda} + \delta\alpha\frac{\partial h}{\partial \alpha} + h.o.t.
\end{aligned} \qquad \text{(C3)}$$

where $[\phi\ \lambda\ \alpha]$ is the aforementioned notional trajectory which in general does not satisfy the ray equations C2. This being so, the resulting inhomogeneous $O(1)$ terms may be collected on the right hand side and terms of order higher than $O(\delta)$ may be discarded, resulting in the forced linear state equation for the trajectory perturbations

$$\begin{bmatrix} -\frac{d}{ds}+\frac{\partial f}{\partial \phi} & 0 & \frac{\partial f}{\partial \alpha} \\ \frac{\partial g}{\partial \phi} & -\frac{d}{ds} & \frac{\partial g}{\partial \alpha} \\ \frac{\partial h}{\partial \phi} & \frac{\partial h}{\partial \lambda} & -\frac{d}{ds}+\frac{\partial h}{\partial \alpha} \end{bmatrix} \begin{bmatrix} \delta\phi \\ \delta\lambda \\ \delta\alpha \end{bmatrix} = \frac{d}{ds}\begin{bmatrix} \phi \\ \lambda \\ \alpha \end{bmatrix} - \begin{bmatrix} f(\phi,\alpha) \\ g(\phi,\alpha) \\ h(\phi,\lambda,\alpha) \end{bmatrix}. \qquad \text{(C4)}$$

Finite Difference Solution to Path Perturbations

Rather than integrating the ODE C4 along the notional trajectory, it is our objective to satisfy the ODE everywhere along the notional trajectory, subject to certain boundary conditions. The approach is to discretize the notional trajectory along intervals of Δs and then approximate equation C4 by a first order backward finite difference scheme. Under this scheme equation C4 is recast at a particular position along the notional trajectory s as follows

$$\begin{bmatrix} \frac{1}{\Delta s}+\frac{\partial f}{\partial \phi}/2 & 0 & \frac{\partial f}{\partial \alpha}/2 & -\frac{1}{\Delta s}+\frac{\partial f}{\partial \phi}/2 & 0 & \frac{\partial f}{\partial \alpha}/2 \\ \frac{\partial g}{\partial \phi}/2 & \frac{1}{\Delta s} & \frac{\partial g}{\partial \alpha}/2 & \frac{\partial g}{\partial \phi}/2 & -\frac{1}{\Delta s} & \frac{\partial g}{\partial \alpha}/2 \\ \frac{\partial h}{\partial \phi}/2 & \frac{\partial h}{\partial \lambda}/2 & \frac{1}{\Delta s}+\frac{\partial h}{\partial \alpha}/2 & \frac{\partial h}{\partial \phi}/2 & \frac{\partial h}{\partial \lambda}/2 & -\frac{1}{\Delta s}+\frac{\partial h}{\partial \alpha}/2 \end{bmatrix} \begin{bmatrix} \partial\phi(s-\Delta s) \\ \partial\lambda(s-\Delta s) \\ \partial\alpha(s-\Delta s) \\ \partial\phi(s) \\ \partial\lambda(s) \\ \partial\alpha(s) \end{bmatrix}$$

$$= \begin{bmatrix} \left(-\phi(s-\Delta s)+\phi(s)\right)/\Delta s \\ \left(-\lambda(s-\Delta s)+\lambda(s)\right)/\Delta s \\ \left(-\alpha(s-\Delta s)+\alpha(s)\right)/\Delta s \end{bmatrix} - \begin{bmatrix} \left(f(\phi(s-\Delta s),\alpha(s-\Delta s))+f(\phi(s),\alpha(s))\right)/2 \\ \left(g(\phi(s-\Delta s),\alpha(s-\Delta s))+g(\phi(s),\alpha(s))\right)/2 \\ \left(h(\phi(s-\Delta s),\lambda(s-\Delta s),\alpha(s-\Delta s))+h(\phi(s),\lambda(s),\alpha(s))\right)/2 \end{bmatrix} \qquad \text{(C5)}$$

Using the backwards finite difference scheme in equation (C5), the perturbations to the notional trajectory may be determined by solving a block diagonal system of equations. If there are N discrete positions along the notional trajectory, then this block diagonal system of equations has three more columns than it has rows: it is under-determined by a factor of three, since only three finite difference equations result from the first two positions along the notional trajectory (a total of six unknowns.) However several boundary conditions are required in order for the perturbed trajectories to be useful in the framework of fixed source and receiver positions. These boundary conditions are that the perturbed latitude and longitude $\delta\phi$ and $\delta\lambda$ must be zero at $s=0$ and $s=L$, where L is the unperturbed path length. When these boundary conditions are introduced the system of equations has one extra row: it is now over-determined by a factor of one, so that the perturbations to the notional trajectory must actually be determined through least-square solution of the block diagonal system of equations.

The partial derivatives of the non-linear functions in the state equation C2 are given here for completeness. First the derivatives of f are

$$\frac{\partial f}{\partial \phi} = -\frac{3\cos\alpha}{\mu}\left(\frac{\varepsilon^2 \sin\phi\cos\phi}{1-\varepsilon^2\sin^2\phi}\right)$$

and

$$\frac{\partial f}{\partial \alpha} = -\frac{\sin\alpha}{\mu}.$$

The derivatives of g are given by

$$\frac{\partial g}{\partial \phi} = \frac{\sin\alpha\sin\phi}{\eta\cos^2\phi} - \frac{\sin\alpha}{\eta\cos\phi}\left(\frac{\varepsilon^2\sin\phi\cos\phi}{1-\varepsilon^2\sin^2\phi}\right)$$

and

$$\frac{\partial g}{\partial \alpha} = \frac{\cos\alpha}{\eta\cos\phi}$$

Finally, the derivatives of h are

$$\frac{\partial h}{\partial \phi} = \frac{\sin\alpha}{\eta\cos^2\phi} - \frac{\sin\alpha}{\mu}\frac{\partial^2 \ln k}{\partial^2\phi} + \frac{\cos\alpha}{\eta\cos\phi}\frac{\partial^2 \ln k}{\partial\phi\partial\lambda} + \frac{\cos\alpha\sin\phi}{\eta\cos^2\phi}\frac{\partial \ln k}{\partial\lambda}$$
$$-\left(\frac{\sin\alpha\tan\phi}{\eta} + \frac{\cos\alpha}{\eta\cos\phi}\frac{\partial \ln k}{\partial\lambda}\right)\left(\frac{\varepsilon^2\sin\phi\cos\phi}{1-\varepsilon^2\sin^2\phi}\right) + 3\frac{\sin\alpha}{\mu}\frac{\partial \ln k}{\partial\phi}\left(\frac{\varepsilon^2\sin\phi\cos\phi}{1-\varepsilon^2\sin^2\phi}\right)$$

$$\frac{\partial h}{\partial \lambda} = -\frac{\sin\alpha}{\mu}\frac{\partial^2 \ln k}{\partial\phi\partial\lambda} + \frac{\cos\alpha}{\eta\cos\phi}\frac{\partial^2 \ln k}{\partial\lambda^2},$$

and

$$\frac{\partial h}{\partial \alpha} = \frac{\cos\alpha\tan\phi}{\eta} - \frac{\cos\alpha}{\mu}\frac{\partial \ln k}{\partial\phi} - \frac{\sin\alpha}{\eta\cos\phi}\frac{\partial \ln k}{\partial\lambda}.$$

References

[1] M. D. Collins and W. A. Kuperman, *Overcoming ray chaos*, JASA **95**, pp 3167-3170 (1994)

[2] W. H. Press, B. P. Flannery, S. A. Teukolsky and W. T. Vetterling, Numerical Recipes in C, Cambridge University Press, Cambridge 1988, p. 609-621

[3] K. D. Heaney, W. A. Kuperman and B. E. MacDonald, *Perth-Bermuda sound propagation (1960): Adiabatic mode interpretation*, JASA **90**, pp 2586-2594 (1991)

Appendix D -- Derivation of the AOU Equations

This appendix documents the equations being used for determining the location Area of Uncertainty (AOU) in the current version of the Hydroacoustic Coverage Assessment Model (HydroCAM). The general problem and the underlying assumptions are presented. The problem statement is followed by brief description of Maximum Likelihood Estimation. The equations for calculating the AOU are then derived.

Assumptions

The problem is to predict the performance of a source location algorithm. The inputs to the algorithm are a set of arrival time measurements, $\{t_i : i = 1,2,...,N\}$, from N spatially distributed sensors. The output of the algorithm is an estimate $\hat{\mathbf{s}}$ of the unknown non-random state vector $\mathbf{s}$,

$$\mathbf{s}^T = [\phi \quad \lambda \quad t_o] \tag{1}$$

which contains the source latitude ϕ, longitude λ and origin time t_o. The arrival time measurements are assumed to be independent Gaussian random variables. For unbiased estimates of $\mathbf{s}$, the boundary of confidence regions for the estimate are ellipsoidal. The metric for algorithm performance is the Area Of Uncertainty, defined here as the area in square km of the bounding ellipse for a specified confidence region.

Maximum Likelihood Estimation

This section follows the derivations presented in [1]. Let $f(\mathbf{s},\mathbf{r}_i)$ be a model for predicting the travel time between a source at $\mathbf{s}$ and a receiver at $\mathbf{r}_i$. The predicted arrival time at $\mathbf{r}_i$ is then given by

$$\hat{t}_i = f(\mathbf{s},\mathbf{r}_i) + t_o = h_i(\mathbf{s}) \tag{2}$$

If the model is linear, then (2) reduces to

$$\hat{t}_i = \mathbf{H}_i^T \ \mathbf{s}. \tag{3}$$

The model for the arrival time measurement is then

$$t_i = \hat{t}_i + v_i \tag{4}$$

where v_i is a zero mean Gaussian random variable with known variance σ_i^2. In this case, the conditional probability of measuring t_i given the source and receiver locations is

$$p(t_i|\mathbf{s}) = \frac{1}{\sigma_i\sqrt{2\pi}}\exp\left[-\frac{1}{2\sigma_i^2}(t_i - \hat{t}_i)^2\right]. \quad (5)$$

Using equation (2), and the assumption that the measurements are independent, the joint probability of all measurements can be written as

$$p(t_1, t_2, \ldots t_N|\mathbf{s}) = \prod_{i=1}^{N}\frac{1}{\sigma_i\sqrt{2\pi}}\exp\left[-\frac{1}{2\sigma_i^2}(t_i - h_i(\mathbf{s}))^2\right]. \quad (6)$$

The maximum likelihood estimate $\hat{\mathbf{s}}$ is the value of $\mathbf{s}$ that most likely caused a given collection of arrival times to occur, i.e. the value of $\mathbf{s}$ that maximizes (6). Equivalently, we can find the value of $\mathbf{s}$ that satisfies

$$\underset{\mathbf{s}}{Min}\sum_{i=1}^{N}\frac{1}{\sigma_i^2}(t_i - h_i(\mathbf{s}))^2. \quad (7)$$

Linear ML Estimate

If h is linear, then substituting (3) into (7) yields

$$\underset{\mathbf{s}}{Min}\sum_{i=1}^{N}\frac{1}{\sigma_i^2}(t_i - H_i^T\cdot\mathbf{s})^2. \quad (8)$$

By taking the gradient of (8) with respect to $\mathbf{s}$ and setting the result to zero

$$\sum_{i=1}^{N}\frac{1}{\sigma_i^2}H_i(t_i - H_i^T\cdot\hat{\mathbf{s}}) = 0. \quad (9)$$

Solving this equation for the linear MLE estimate produces

$$\hat{\mathbf{s}} = \mathbf{J}^{-1}\sum_{i=1}^{N}\frac{1}{\sigma_i^2}H_i t_i, \quad (10)$$

where $\mathbf{J}$ is the Fisher information matrix

$$\mathbf{J} = \sum_{i=1}^{N} \frac{1}{\sigma_i^2} H_i H_i^T . \tag{11}$$

The expected value of the estimate is

$$E\{\hat{\mathbf{s}}\} = \mathbf{J}^{-1} \sum_{i=1}^{N} \frac{1}{\sigma_i^2} H_i E\{t_i\}. \tag{12}$$

Substituting equation (3) into (12) results in

$$E\{\hat{\mathbf{s}}\} = \mathbf{J}^{-1} \sum_{i=1}^{N} \frac{1}{\sigma_i^2} H_i H_i^T \cdot \mathbf{s} = \mathbf{J}^{-1}\mathbf{J} \cdot \mathbf{s} = \mathbf{s}, \tag{13}$$

which shows that the linear MLE in equation (10) is unbiased. Similarly, the covariance of the estimate can be shown to be

$$\mathbf{R} = E\left\{(\hat{\mathbf{s}} - \mathbf{s})(\hat{\mathbf{s}} - \mathbf{s})^T\right\} = \mathbf{J}^{-1}. \tag{14}$$

In the Area of Uncertainty section below, it will be shown how to derive the AOU from the covariance matrix.

Approximate Non-Linear ML Estimate

For our problem, h is non-linear, so we expand it around a trial solution $\mathbf{s}_0$

$$h_i(\mathbf{s}) = h_i(\mathbf{s}_0) + \nabla_{\mathbf{s}}^T h_i(\mathbf{s}_0) \cdot (\mathbf{s} - \mathbf{s}_0) + H.O.T \tag{15}$$

By ignoring the higher order terms, (15) can be rewritten as

$$\Delta t_i = h_i(\mathbf{s}) - h_i(\mathbf{s}_0) \approx \nabla_{\mathbf{s}}^T h_i(\mathbf{s}_0) \cdot \Delta\mathbf{s}. \tag{16}$$

The estimation problem can now be reformulated as a linear estimate of $\Delta\mathbf{s}$. If H is redefined as

$$H_i = \nabla_{\mathbf{s}} h_i(\mathbf{s}_0) \tag{17}$$

then the ML estimate corresponding to (10) becomes

$$\hat{\mathbf{s}} - \mathbf{s}_0 = \mathbf{J}^{-1} \sum_{i=1}^{N} \frac{1}{\sigma_i^2} H_i \left(t_i - h_i(\mathbf{s}_0)\right), \tag{18}$$

and the Fisher information matrix is now given by

$$\mathbf{J} = \sum_{i=1}^{N} \frac{1}{\sigma_i^2} \left(\nabla_{\mathbf{s}} h_i\right)\left(\nabla_{\mathbf{s}}^T h_i\right). \tag{19}$$

Derivation of AOU Equations

In this section, the equations for the error ellipse and the Area of Uncertainty will be derived. First, we will present two models for the travel time needed in equation (2). Then, we will derive the equations for the covariance matrix of the estimation error using equation (18). Finally, the equations for the error ellipse and AOU will be shown based on the covariance matrix.

Travel Time Models

Recall that the arrival time model can be written as

$$\hat{t}_i = f(\mathbf{s}, \mathbf{r}_i) + t_o = h_i(\mathbf{s}) \tag{20}$$

and that to determine the location performance, we need to find the gradient of (20) with respect to **s**. In the network performance module of HydroCAM, there are two options available for computing this gradient. In the first case, the gradient is numerically evaluated using finite differences on the travel times predicted by the ray path model (integrating the group slowness along any ray path). The second option is derived from a simple analytic model of the travel time

$$f(\mathbf{s}, \mathbf{r}_i) = \frac{\mathrm{Re}}{c}\theta_i \tag{21}$$

where Re is the radius of the spherical earth, c is an average sound speed, and θ_i is the included angle between the source at **s** and the receiver at $\mathbf{r}_i$. Figure 1 shows the geometry under consideration. The included angle is related to the source and receiver positions by

$$\cos\theta_i = \hat{\mathbf{r}}_s \cdot \hat{\mathbf{r}}_i = \cos\phi\cos\phi_i\cos(\lambda - \lambda_i) + \sin\phi\sin\phi_i \tag{22}$$

$$\hat{\mathbf{r}} = \begin{bmatrix} \cos\phi\cos\lambda \\ \cos\phi\sin\lambda \\ \sin\phi \end{bmatrix}$$

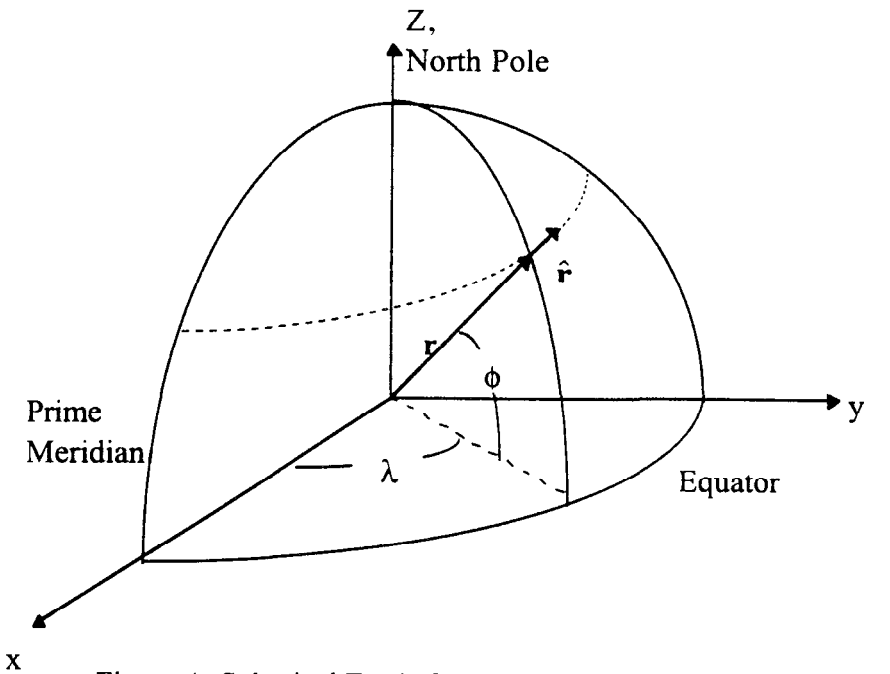

Figure 1: Spherical Earth Geometry

Covariance Matrix

To determine the covariance matrix using (14) and (19), each of the partial derivatives in

$$\nabla_s\left(h_i(\mathbf{s})\right) = \begin{bmatrix} \frac{\partial h(\mathbf{s})}{\partial\phi} \\ \frac{\partial h(\mathbf{s})}{\partial\lambda} \\ \frac{\partial h(\mathbf{s})}{\partial t_o} \end{bmatrix} = \begin{bmatrix} \frac{\partial f(\mathbf{s})}{\partial\phi} \\ \frac{\partial f(\mathbf{s})}{\partial\lambda} \\ 1 \end{bmatrix} \tag{22}$$

must be computed. Using equation (21) and letting $\cos\theta_i = u$ results in

$$\nabla_s\left(h_i(\mathbf{s})\right) = \begin{bmatrix} \frac{-\mathrm{Re}}{c\sin(\theta_i)}\frac{\partial u}{\partial\phi} \\ \frac{-\mathrm{Re}}{c\sin(\theta_i)}\frac{\partial u}{\partial\lambda} \\ 1 \end{bmatrix} \tag{23}$$

Evaluating the derivatives in (23) using equation (22) yields

$$\nabla_s\left(h_i(\mathbf{s})\right)=\begin{bmatrix}\dfrac{\mathrm{Re}}{c\sin(\theta_i)}\left(\cos\phi_i\sin\phi\cos(\lambda-\lambda_i)-\cos\phi\sin\phi_i\right)\\ \dfrac{\mathrm{Re}}{c\sin(\theta_i)}\left(\cos\phi_i\cos\phi\sin(\lambda-\lambda_i)\right)\\ 1\end{bmatrix}=\begin{bmatrix}A_i\\ B_i\\ C_i\end{bmatrix}. \quad (24)$$

Finally, from equations (19) and (24), the Fisher information matrix is computed using

$$\mathbf{J}=\sum_{i=1}^{N}\mathbf{J}_i \quad (25)$$

where the individual contribution of each sensor to the matrix is

$$\mathbf{J}_i=\frac{1}{\sigma_i^2}\begin{bmatrix}A_i^2 & A_iB_i & A_iC_i\\ A_iB & B_i^2 & B_iC_i\\ A_iC_i & B_iC_i & C_i^2\end{bmatrix} \quad (26)$$

Area Of Uncertainty

At this point in the analysis, we have an estimate of the source location, and the statistics of the estimation error (i.e. The error is unbiased and has a covariance matrix **R**). Since our approach to solving the non-linear estimation problem resulted in a linear estimation equation, and the input noise is Gaussian, the errors will be jointly Gaussian. Let **e** be the error in the estimate,

$$\mathbf{e}^T=(\hat{\mathbf{s}}-\mathbf{s})^T=\begin{bmatrix}\Delta\phi & \Delta\lambda & \Delta t_o\end{bmatrix} \quad (27)$$

then the distribution of the error is given by

$$p(\mathbf{e})=\frac{1}{(2\pi)^{3/2}|\mathbf{R}|^{1/2}}\exp\left\{-\frac{1}{2}\mathbf{e}^T\mathbf{R}^{-1}\mathbf{e}\right\} \quad (28)$$

where **R** is the 3 x 3 covariance matrix of the errors

$$\mathbf{R}=\begin{bmatrix}\sigma_\phi^2 & \sigma_{\phi\lambda} & \sigma_{\phi t_o}\\ \sigma_{\phi\lambda} & \sigma_\lambda^2 & \sigma_{\lambda t_o}\\ \sigma_{\phi t_o} & \sigma_{\lambda t_o} & \sigma_{t_o}^2\end{bmatrix} \quad (29)$$

What we wish to determine is the probability of the true source geographic location independent of the origin time. In other words, we need the marginal distribution of the latitude and longitude errors. Reference [3] shows that any k-dimensional marginal density function obtained by integrating out N-k random from an N jointly Gaussian random variables will also be Gaussian. In addition, it is shown that the covariance matrix of the remaining k variables is equal to the appropriate k x k submatrix of the N x N covariance matrix. For our case, this means that the density function of the spatial location error is given by

$$p(\Delta\phi,\Delta\lambda) = \frac{1}{(2\pi)|\mathbf{R}|^{1/2}} \exp\left\{-\frac{1}{2}[\Delta\phi \quad \Delta\lambda]\mathbf{R}^{-1}\begin{bmatrix}\Delta\phi \\ \Delta\lambda\end{bmatrix}\right\} \tag{30}$$

where **R** is now the 2 x 2 covariance matrix of the latitude and longitude errors

$$\mathbf{R} = \begin{bmatrix}\sigma_\phi^2 & \sigma_{\phi\lambda} \\ \sigma_{\phi\lambda} & \sigma_\lambda^2\end{bmatrix}. \tag{31}$$

Equation (30) shows that equal-probability contours are defined by

$$[\Delta\phi \quad \Delta\lambda]\mathbf{R}^{-1}\begin{bmatrix}\Delta\phi \\ \\ \Delta\lambda\end{bmatrix} = C^2 \tag{32}$$

which is the equation of an ellipse. The probability that a point lies outside this ellipse can be obtained by substituting (32) into (30) and integrating from C to ∞ [2, p 78.], which results in

$$1 - P = \exp\left(-\frac{C^2}{2}\right), \tag{33}$$

where P is the probability that a point lies *inside* the ellipse. In addition, the area of the concentration ellipse in (32) is

$$A = |\mathbf{R}|^{1/2}\pi C^2 \tag{34}$$

Since the elements of **R** are in units of radians, and we desired an AOU in square kilometers, (34) need to be modified. However, the mapping between lat/lon and x/y in km depends on latitude, so we need to transform **R** before applying equation (34). The arc length in the east-west (x) direction and north-south (y) direction between two points separated in angle by $\Delta\phi,\Delta\lambda$ on a sphere is approximately

$$x = \mathrm{Re} \cdot \cos(\phi)\Delta\lambda$$
$$y = \mathrm{Re} \cdot \Delta\phi.$$

So we can transform the covariance matrix into the appropriate units using

$$\mathbf{R}_{xy} = \begin{bmatrix} \sigma_x^2 & \sigma_{xy} \\ \sigma_{xy} & \sigma_y^2 \end{bmatrix}. \tag{35}$$

where

$$\sigma_x^2 = R_e^2(\cos^2\phi)\sigma_\lambda^2 \tag{35a}$$
$$\sigma_{xy} = R_e^2(\cos\phi)\sigma_{\phi\lambda} \tag{35b}$$
$$\sigma_y^2 = R_e^2\sigma_\phi^2 \tag{35c}$$

This section has derived all of the equations necessary to calculate a concentration ellipse (32,33) and the associated AOU (34) from the error covariance matrix **R**. However, these equations are inconvenient for displaying ellipses in a variety of formats. HydroCAM diagonalizes the covariance matrix, and with $C = 1$, calculates the major and minor axes of the error ellipse, the angle of the error ellipse and the AOU. These "normalized performance parameters" are then saved to a set of data files for manipulation by the display software. A description of the specific equations used in HydroCAM for display of the error ellipse is provided in the main body of the HydroCAM Users Guide.

References

[1] Perl, Robert. Dependence of Localization Performance on Sensor Geometry and Measurement Accuracy. BBN Technical Report 4614, Arlington VA, July 1981.

[2] Van Trees, Harry L. Detection and Estimation Theory, Part I. John Wiley and Sons, 1968.

[3] Peebles, Peyton Z. Probability, Random Variables, and Random Signal Principles. McGraw Hill, 1987.

Appendix E -- Data File Formats

This appendix documents the formats of the following data files used in HydroCAM:

- Source Files
- Scenario Files
- Receiver Files
- Network Files
- Path Files
- Grid Files

Source File

Source files contain the pressure time-series at a set of depths in the format specified in LLNL Report UCRL-ID-122595. These files should be given a unique filename, with the extension *.source,* and placed in the *config/source* subdirectory. The files must contain the number of time samples and the number of depths on the first line of the file.

Scenario File

All scenario files should be located in the *config/scenario* subdirectory. There are four types of scenario files: star, grid, point and list. All are ASCII files.

The star scenario file has the *scen* extension. Since a star scenario may be run by turning the eigenray option off and setting the angle parameters on the ***Setup GlobeRay*** form, this scenario is typically not used. Star scenario files may contain comments after the data on each row as shown in the following example (has the following *Star1.scen*)

```
1                       !Scenario Type (1=star, 2=grid, 3=point, 4=list)
0.0, 360.0, 1.0         !Launch Angle Min, Max and Increment (deg)
0.0, 20000.0, 50.0      !Range Min, Max and Increment (km)
```

Example star scenario file with launch angles at 1 degree increments

Grid scenario files also have the *scen* extension. These files may contain comments after the data on each row, or at the end of the file as shown in the following example (*World1.scen):*

```
2                       !Scenario Type (1=star, 2=grid, 3=point, 4=list)
60                      !Grid Resolution (minutes)
-79.5 -179.5 79.5 179.5 ! Min Lat, Min Lon, Max Lat , Max Lon (deg)
```

Example grid scenario file covering most of the world at 1 degree resolution

Point scenario files have the *src* extension. These files may contain comments after the data on each row, or at the end of the file as shown in the following example (*HIFT.src):*

```
3                          !Scenario Type (1=star, 2=grid, 3=point, 4=list)
-53.366666667,74.5         !Source Lat (N) and Lon (E)
30.0                       !Range Increment (not used)
Nominal HIFT Source Coordinates
```

The list scenario file contains latitude in the first column and longitude in the second column. The coordinates are specified in decimal degrees from -90 to 90 latitude and -180 to 180 longitude.

Receiver Files

Receiver files describe the location and characteristics of receiving stations. These ASCII files are located in the *config/receiver* directory and have the extension *rec.* Receiver files are normally generated automatically using the **Receiver** form. The format of the receiver files is illustrated by the example *Asc1.rec:*

```
Ascension 1
SH
-7.800000 -14.600000 840.00000
00EXAMPLE
00EXAMPLE
00EXAMPLE
1.0
```

The first line in the file contains the full name of the receiver. This name is used for annotation purposes only. The so-called receiver abbreviation (the filename without the extension) is used by the network files and most of the software to refer to the receiver. The second line contains the receiver type. Valid options are SH (simple hydroacoustic), AH (array hydroacoustic), SS (simple seismic), AS (array seismic), and IA (infrasonic array). The third line in the file contains the latitude, longitude and depth (in meters) of the receiver. The next three lines give the filenames (without extensions) of the ambient noise, directionality and system loss files for the receiver. The format of these files is provided below. The last line in the receiver file contains the "picking error" in seconds.

Ambient Noise File (.an) -- New files can be manually created in the *config/receiver* directory. These files can be also be created using the *Create AN* button. The file contains a table of the ambient noise as a function of direction and frequency. The example file provided with HydroCAM illustrates the format. Do NOT include

comments in these files. The numbers in the table need to be delimited by spaces *not* commas.

Listing of config/receiver/00EXAMPLE.an

```
7                       ! Number of Frequencies
1 2 5 10 20 50 100      ! Frequencies in Hz
-180 180 180            ! Azimuth Start, Stop, Increment (deg TN)
100 110 70              ! AN at first frequency vs direction
85 90 70                ! AN at second frequency vs direction
80 85 70                ! AN next frequency vs direction
75 80 70                ! AN next frequency vs direction
70 75 70                ! AN next frequency vs direction
70 75 70                ! AN next frequency vs direction
70 75 70                ! AN last frequency vs direction
```

Directionality File (.direct) – This file contains a weighting factor applied to the sonar equation as a function of azimuth and frequency. See the *Receiver Characterization* section of this report for a more detailed description of the uses of this file. An example is provided with HydroCAM. Do NOT include comments in these files. The numbers in the table need to be delimited by spaces *not* commas.

Listing of config/receiver/00EXAMPLE.dir

```
7                   ! Number of Frequencies
1 2 5 10 20 50 100  ! Frequencies in Hz
-180 180 180        ! Azimuth Start, Stop, Increment (deg TN)
0 0 0               ! Az weighting at first frequency vs direction
0 0 0               ! Az weighting at second frequency vs direction
0 0 0               ! Az weighting at next frequency vs direction
0 0 0               ! Az weighting at next frequency vs direction
0 0 0               ! Az weighting at next frequency vs direction
0 0 0               ! Az weighting at next frequency vs direction
0 0 0               ! Az weighting at last frequency vs direction
```

System Loss File (.sloss) -- This file is used to account for all losses occurring in the sensor, receiver, and processing systems that are not accounted for elsewhere. A typical use is to include the island seismic station loss in this file. Four columns are provided to contain four different types of losses. The total of these four columns is used for the loss factor at each frequency. Do NOT include comments in these files. The numbers in the table need to be delimited by spaces *not* commas.

Listing of config/receiver/00EXAMPLE.sloss

```
7                                   ! Number of frequencies
1.00   0.1   0.0   0.0   0.0       ! Frequency and 4 loss data pts
2.00   0.2   0.0   0.0   0.0
5.00   0.3   0.0   0.0   0.0
10.00  0.4   0.0   0.0   0.0
20.00  0.5   0.0   0.0   0.0
50.00  0.6   0.0   0.0   0.0
100.00 0.7   0.0   0.0   0.0
```

Network Files

Network files are located in the *config/network* subdirectory. They are ASCII files with the extension *.net*. They contain a list of receiver abbreviations, one receiver per line of the file.

Path Files

Path files are created by GlobeRay, and read by a number of MATLAB functions. They can be located in any directory. There are two types of path files: the path description file and the path data file. The path description file contains geographic information on the path. The path data file contains data for a single variable along the path (such as travel time).

The path description file always has the extension *.path*. The file contains one data record for each path. The data record is in the following format

Variable	*Description*	*Type*
np	number of points in the path	4-byte integer
mode	mode number of the phase/group speed grid used to generate the path	4-byte integer
angle0	path launch angle in degrees, measured from true north	float
data	for each point in the path, there are four floating point numbers: latitude, longitude, distance and angle	float

The *latitude* and *longitude* values are in degrees; *distance* is in kilometers, and *angle* is in degrees from true north. Each path in the file uses *np*4*4+12* bytes.

The path data file has an extension that depends on the type of data. Examples include *TL* for transmission loss, *TT* for travel time, *ST* for travel time standard deviation, *bathy*

for bathymetry. There is always a corresponding path description file which has the same base filename. Each path in the path data file consists of the number of points in the path (4-byte integer) followed by the data for each point (float).

Grid Files

Grid files are used by a number of programs in HydroCAM. They are created by GlobeRay, MakeGridDB and the MATLAB function *write_GridDB.m*. They are used by HydroNET and the MATLAB function *read_GridDB.m*. Grid files are an integral part of the *GridDB* object class, and much of the interface software is contained in *GridDB.cc*.

Grid files consist of a header followed by a number of data blocks that contain the data on the grid. The format of the 48 byte header is

Header Variable	*Description*	*Type*
Nlats	number of latitudes (rows) in the grid	4-byte integer
Nlons	number of longitudes (columns) in the grid	4-byte integer
latBase	latitude of the center of the southernmost grid cell	double
lonBase	longitude of the center of the westernmost grid cell	double
latInc	latitude resolution (degrees)	double
lonInc	longitude resolution (degrees)	double
ngrids	number of grids in the grid file	4-byte integer
wrap_flag	indicates whether the 1st column should be considered next to the last column (wraparound in longitude)	4-byte integer

The data block consists of *Nlats*Nlons* single-precision floating point numbers. They are written from the south-west corner of the grid. All points in the first row (latitude) are followed by all points in the next latitude. If multiple grids are contained in the file, they are provided in sequence.

Appendix F -- Description of Object Classes

This appendix describes the following object classes used in HydroCAM:

- Grid Databases (GridDB)
- SuperGrids, a collection of grids (SGridDB)
- Receiving Stations (StationClass)
- Monitoring Networks (Network)

A general description of the purpose of each class is followed by summary tables of the member functions. This information is intended as a functional overview; please use the header file for actual programming.

GridDB Class

The GridDB class is used to store and manipulate gridded geographic information. In HydroCAM, GridDB is used for both environmental database information (such as phase speed and group speed), and for outputs of the propagation model (transmission loss and travel time). For environmental information, most grids are actually SuperGrids (see the description of this class below).

Constructors

GridDB( )	Makes a generic GridDB structure of size 0
GridDB(filename)	Reads the grid database selected by filename.
GridDB(filename, grid_number)	Reads the grid database selected by filename, skipping grid_number into the file (there may be multiple grids in a grid database file).

Input and Output

read(filename)	Reads a grid database selected by filename
read(filename, grid_number)	Same as constructor
write(filename)	Writes a grid database file

Accessors

num_lats()	Returns the number of latitude points in the grid
num_lons()	Returns the number of longitude points in the grid
lat_base()	Returns the base (southernmost) latitude
lon_base()	Returns the base (westernmost) longitude
lat_increment()	Returns the latitude resolution
lon_increment()	Returns the longitude resolution
operator(lat, lon)	Returns the value at the specified lat, lon without

	interpolation
index(lat, lon)	Returns the index values for the specified lat, lon
before(lat, lon)	Returns the index values for the point before the specified lat, lon
inside(lat, lon)	Returns whether the lat, lon is inside the grid
linear(lat, lon)	Returns the bilinearly interpolated value at lat,lon
gradient(lat, lon,dlat,dlon)	Returns the bilinearly interpolated latitude derivative (dlat) and longitude derivative (dlon)
replaceNaN(new_value)	Replace all NaN values in the grid with new_value
replace(value, new_value)	Replace all grid points equal to value with new_value
resolution()	Returns the latitude and longitude resolutions
setGradient()	Used before calls to gradient(). Changes values in the index() function, so must be called before index() is called.
UnsetGradient()	These two functions must be used when using gradient(): setGradient() index() gradient() UnsetGradient()

Operators

The following operators work between GridDB objects and between a GridDB object and a float: +, -. The * operator only works between a GridDB object and a float. The = operator works with two GridDB objects. The << operator pretty prints information about the GridDB object.

SuperGrid Class (SGridDB)

This class is a container class of GridDB objects. It loads GridDB objects into storage and selects the best GridDB for use. The *best grid* is defined as the grid that contains the requested point and has the best resolution at that point. The advantage of this class is that statements such as *Bathy.linear(lat,lon)* allow users to simultaneously search a large number of bathymetry grids at different locations and resolutions, and linearly interpolate the best value. Note that the constructors for this class all use the environment variable SGRIDPATH to search for grid files.

Constructors

SGridDB(listfile)
SGridDB(listfile, grid_number)
SGridDB(listfile, suffix)
SGridDB(prepend, listfile, suffix)

listfile is the name of a file containing the filenames of the individual GridDB data files that are to be part of the SuperGrid. The constructors allow several options for selecting the filename by using the suffix and prefix options. *grid_number* is the same as described in GridDB section above. The *prepend* is a character string added to the beginning of each filename in the listfile. The *suffix* is added to the end of each filename in the listfile.

Consider the following example for a supergrid of transmission loss data used in the network performance model HydroNET:

SGRIDPATH = /home/hydro/grid_files:/home/master/grid_files
prepend = run1
suffix = .TLgrid

Assume the first station in the network is Wak. The grids that would be searched are /home/hydro/grid_files/run1Wak.TLgrid and /home/master/grid_files/run1Wak.TLgrid. The search is terminated as soon as one is found, so the order of directories in SGRIDPATH is important.

Accessors

num_grids()	Returns the number of grids included in the supergrid.
operator(index)	Returns the GridDB object at the requested index
get_resolution(lat, lon)	Returns the best resolution for the requested point

The remaining accessors are identical to the GridDB accessors of the same name, except that the operation will apply to the highest resolution grid available in the supergrid.

index()
before()
inside()
linear()
gradient()
replaceNaN()
replace()
operator (lat, lon)
unsetGradient()
setGradient()

StationClass:

StationClass is used to store information about the station, including position, directionality, losses and ambient noise. Functions for interpolating the directionality, losses and ambient noise are also provided.

Constructor Station()

Input Functions are load(prepend, filename) and load(filename). These functions read the receiver configuration file (see the file descriptions in Appendix E). The ambient noise, directionality and loss files are also loaded into memory.

Accessors include get_lat(), get_lon() and get_picking_error(), which return the appropriate variables. A number of calculation functions are also provided. All frequency interpolation is logarithmic. All other interpolation is linear.

an_interpolate(frequency, az)	Interpolates the ambient noise table
an_interpolate(frequency, grid_database)	2-D interpolation at *frequency* using all angle values in the GridDB *grid_database.* Creates a new GridDB with the results
dir_interpolate(frequency, az)	Same as an_interpolate, except the directionality table is used
dir_interpolate(frequency, grid_database)	Same as an_interpolate, except using directionality table
sloss_interpolate(frequency)	Logarithmic interpolation of system losses at *frequency*

Network class:

A network is a collection of station classes. Networks are constructed by providing a network filename that contains all of the stations in the network.

Constructors are Network(filename) and Network(prepend, filename, suffix). These functions read the network file specified by *filename* (which must include the complete path to the network file), and load all station files contained in the network. The second option uses *prepend* and *suffix* to find the station files.

Two **accessors** are provided for this class. The first, num_stations(), returns the number of stations in the network. The second, operator(index), returns the Station from the container at position *index* in the network list.

Technical Information Department • **Lawrence Livermore National Laboratory**
University of California • Livermore, California 94551